DISSERTATION

EVALUATING RISK FOR CURRENT AND FUTURE *BROMUS TECTORUM* INVASION AND LARGE WILDFIRES AT MULTIPLE SPATIAL SCALES IN COLORADO AND WYOMING, USA

Submitted by

Amanda M. West

Graduate Degree Program in Ecology

In partial fulfillment of the requirements

For the Degree of Doctor of Philosophy

Colorado State University

Fort Collins, Colorado

Summer 2015

Doctoral Committee:

Advisor: Cynthia S. Brown
Co-Advisor: Sunil Kumar

Paul H. Evangelista
Ruth A. Hufbauer

ABSTRACT

EVALUATING RISK FOR CURRENT AND FUTURE *BROMUS TECTORUM* INVASION AND LARGE WILDFIRES AT MULTIPLE SPATIAL SCALES IN COLORADO AND WYOMING, USA

The Western United States is experiencing rapid ecologic change. These changes are driven largely by anthropogenic factors including introduction of alien invasive species, wildfire ignition and suppression, climate change, and feedbacks between these occurrences. Average temperatures in some areas of the Western U.S. increased as much as 1.1 °C between 2000 and 2006. The advancement of spring also provides evidence for climate change in the region; earlier snowmelt and runoff has been documented in recent decades for areas of the Intermountain West. These rapid changes will certainly affect the distribution of the alien invasive *B. tectorum* and large wildfires in Colorado and Wyoming as well as their associated feedbacks and cascading ecosystem effects. Prompted and inspired by natural resource manager concerns, this research evaluates these ecological phenomena at three spatial scales: Rocky Mountain National Park, Colorado; a wildfire disturbance in Medicine Bow National Forest, Wyoming; and the area encompassed by these two states. The products from this research are maps that can be incorporated into decision support systems for land management and vulnerability assessments for climate change preparedness.

An evaluation of the current and future suitable habitat for *B. tectorum* in Rocky Mountain National Park was conducted at a 90 m^2 spatial resolution using a MaxEnt model fit with climatic, vegetation cover, and anthropogenic covariates (i.e. distance to roads as a surrogate for propagule pressure). One of the important considerations of this research was spatial scale; 250 m^2 and 1 km^2 resolution climate surfaces cannot capture climate refugia in a small area such as Rocky Mountain National Park (1,076 km^2) with high topographic heterogeneity (2,300

m to 4,345 m elevation). Based on model results, the suitable habitat for *B. tectorum* in the Park increases more than 150 km^2 through the year 2050.

Four multi-temporal and multiscale species distribution models were developed for *B. tectorum* in the Squirrel Creek Wildfire post-burn area of Medicine Bow National Forest using eight spectral indices derived from five months of 30 m^2 Landsat 8 imagery corresponding to changes in species phenology and time of field data collection. These models were improved using an iterative approach in which a threshold for abundance (i.e. ≥40% foliar cover) was established from an independent dataset, and produced highly accurate maps of current *B. tectorum* distribution in Squirrel Creek burn with independent AUC values of 0.95 to 0.97. The most plausible model based on field observations showed the distribution of *B. tectorum* has increased 30% from pre-disturbance observations in the area. This model was incorporated in a habitat suitability model for *B. tectorum* in the same area using topographic covariates with inclusion of propagule dispersal limitations to provide an estimate of future potential distribution.

Three historic (years 1991 – 2000) environmental suitability models for large wildfires (i.e. > 400 ha) in Colorado and Wyoming were developed at a 1 km^2 spatial resolution and tested using an independent dataset of large wildfire occurrence in the same area from the subsequent decade (years 2001 – 2010). The historic models classified points of known fire occurrence exceptionally well using decadal climate averages corresponding to the temporal resolution of wildfire occurrence and topographic covariates. When applied to an independent dataset, the test sensitivity was 0.91 for the best model (i.e. MaxEnt). We then applied the model to future climate space for the 2020s (years 2010-2039) and 2050s (years 2040-2069) using two future climate ensembles (i.e. two representative concentration pathways; RCP 4.5 and RCP 8.5 with ensemble average projections from 15 global circulation models) to rank areas for large wildfire risk in the future.

ACKNOWLEDGEMENTS

I would like to begin by thanking the Graduate Degree Program in Ecology for accepting me, a returning student two years out of my Masters of Science Program. My committee, Dr. Cynthia Brown, Dr. Sunil Kumar, Dr. Paul Evangelista, and Dr. Ruth Hufbauer gave me the reins on my dissertation while providing invaluable guidance, and I thank them for their support throughout the constantly evolving research that culminated in my dissertation. Dr. Catherine Jarnevich was constantly extending her knowledge and experience to me, and her mentorship kept me motivated. Thanks to Jim Bromberg for providing data and insight for Chapter 2; Aaron Swallow, Lee Knox, and the entire staff at the Laramie, Wyoming USFS office for participating in Chapter 3; and Dr. William Romme for advise in Chapter 4. I extend thanks to Nick Young, Stephen Chignell, Matt Luizza, Tewodros Wakie, Ryan Anderson, Peter Gibbons, Elizabeth Reiling, Brian Woodward, Jack Van Vleet, and Richard Fordham for their positive attitude during long days camping and hiking for field data collection and for providing unique insights on everything from ecology to linguistics that challenged my existing knowledge. Special thanks to the USGS Fort Collins Science Center, Invasive Species Branch for allowing me to use computing resources in the RAM room. I am grateful for support from the National Needs Fellowship program of National Institute of Food and Agriculture, U.S. Department of Agriculture (Award No.- 2010-03280), the Department of Bioagricultural Sciences and Pest Management, the Natural Resource Ecology Laboratory, and The Rocky Mountain Club Foundation. Thanks to the NASA DEVELOP program for providing me with experience using remote sensing for applied ecological forecasting and increasing my confidence serving as a leader. Finally, I would be remiss if I didn't extend thanks to my mother and late father for always encouraging me to follow my dreams and trust what follows. Any use of trade, product, or firm names is for descriptive purposes only and does not imply endorsement by the U.S. Government.

TABLE OF CONTENTS

CHAPTER 1. BACKGROUND

History and Ecology of *Bromus tectorum* in the Western United States

Invasive plants are non-native species that negatively impact ecosystem structure and/or function. Traits common to invasive species that promote their success include asexual reproduction, rapid growth from seedling to sexual maturity, adaptation to environmental stress (phenotypic plasticity), high tolerance to environmental heterogeneity, and long-lived seed banks (Sakai et al. 2001). *Bromus tectorum* L. (common names downy brome or cheatgrass) is an invasive annual grass that possesses all of these characteristics except a long-lived seed bank (seeds remain viable in the soil around five years; (Mack 1981). *B. tectorum* is native to regions of Europe, northern Africa, and southwest Asia, and was first introduced into the Intermountain West in the 19th century (Mack and Pyke 1983, Bradford and Lauenroth 2006, Zouhar et al. 2008). Specifically in sagebrush steppe communities across the Western U.S. (hereafter the West), this non-native was considered naturalized in the 1940s (Stewart and Hull 1949, Zouhar et al. 2008).

The winter annual life history of *B. tectorum* is not common amongst grass species in the Intermountain West. It may germinate in autumn and overwinter as a semi-dormant seedling or germinate in spring and complete its life cycle as a spring annual, depending on temperature and water availability (Mack 1981, Bradford and Lauenroth 2006). If there is sufficient precipitation in late summer to autumn, *B. tectorum* will behave as a winter annual, germinating in autumn and overwintering as a semi-dormant seedling (Mack and Pyke 1983, Brown and Rowe 2004). Spring germinating seeds of *B. tectorum* reach reproductive maturity in just over a month given appropriate environmental conditions (Mack and Pyke 1983). These two variations in *B. tectorum* demography allow this invasive plant the opportunity to outcompete native grasses and shrubs, especially the fall germinating population because the seedlings are

already established in the spring and begin growing rapidly upon snow melt (Mack and Pyke 1983, Brown and Rowe 2004).

Land Managers' Concerns Associated with *B. tectorum* Invasion

Despite being considered naturalized in some plant communities in the West, *B. tectorum* continues to be problematic for land managers. Negative potential impacts of *B. tectorum* invasion include effects on ecosystem structure and function. *B. tectorum* may be implicated in altered nitrogen cycling and soil water content, interspecific competition with native plant species, altering wildlife forage and habitat quality, and increasing fire frequency and intensity (Mack 1981, Brown and Rowe 2004). Management of *B. tectorum* is thus of high importance to both natural areas and agroecosystems in the United States, where approximately 22.5 million hectares were affected by this alien invasive in 2005 (Duncan et al. 2004).

History and Ecology of Large Wildfires in the West

For the past 1,000 years, the reconstructed history of wildfires in the West follows climate trends and human development (e.g., suppression and ignition). During the "Medieval Warm Period", (an elevated period of aridity with peaks between ca. 900 to 1300) there is evidence of megadrought conditions in the West (Cook et al. 2004, 2015). Based on dendrochronological analysis of fire scars, Trouet et al. (Trouet et al. 2010) found much of the West was still impacted by this extreme drought in the 1400s. This was followed by a decline in fire frequency in the late 16th century corresponding to declining temperatures of the "Little Ice Age" (ca. 1500 to 1800; Trouet et al. 2010).

Frequent, low-severity wildfires prior to the 20th century played important ecological roles in community structure, diversity, productivity, biogeochemical processes, hydrology, and wildlife habitat in low to mid-elevation forests of the West (Brown and Shepperd 2001, Kaufmann et al. 2007). However, beginning in the late 19th century, European settlement in the West brought extensive land clearing (e.g., using fire; the American Indians were implementing this prior to

European settlement and logging) and livestock grazing that suppressed these natural regimes. In the year 1891, the Forest Reserve Act was established and forest fires were increasingly controlled, with the Clarke-McNary Act in 1924 effectively creating a national fire exclusion policy (Stephens 2005). This exclusion policy increased fuel loads in the ponderosa and mixed-conifer forests but was likely suited to Rocky Mountain lodgepole pine forests that are adapted to high-severity crown fires with low frequency (Stephens 2005). Average annual area burned in the West continued to decrease through the 1960s (Brown et al. 2004). Then, in the mid-1980s the incidence of large wildfires (>400 ha) began rapidly increasing (Westerling et al. 2006). Additionally, wildfires began burning for a longer period of time, from an average of one week in the 1970s to five weeks in the 1980s (Westerling et al. 2006). The federal fire policy of 1995 recognized wildfire as a critical ecosystem process; efforts have been made in recent decades to use wildfires in forest management and restoration (e.g., in 2002 the US National Fire Plan resulted in 1 million ha of thinning and prescribed fire across federal land; Schoennagel et al. 2004). The extent of USFS area burned increased significantly across the West from 1940 to 2000 with the exception of California (Stephens 2005).

Land management concerns associated with cheatgrass – wildfire feedback

Wildland fire (among other disturbances including human-induced) can promote invasion by non-native invasive plants (Brooks et al. 2004). After a fire, new sunlight and soil resources may become available to seedling establishment in an unoccupied niche. Two inorganic forms of nitrogen, ammonium (NH_4^+; product of combustion) and nitrate (NO_3^-; forms from the ammonium via nitrification) typically increase in soils following fires (Certini 2005). Nitrate typically leaches out in the soils, however the increased ammonium is readily available to plants as it is adsorbed to soil particles (much of this ammonium will eventually transform back to nitrate; Certini 2005). In one study, *B. tectorum* grown in burned soil had higher growth rates (seedlings had more leaves and were taller), N uptake and more enriched N than individuals grown in unburned soil (Johnson et al. 2010).

Wildfires are abiotic ecological processes that may be characterized as a function across ecological gradients. Invasive species may alter this function, affecting extent, frequency, intensity, or even the seasonality of fire (Freeman et al. 2007). Fires fueled by *B. tectorum* have historically cost the Great Basin as much as $10 million per year in control (Knapp 1996). In areas where *B. tectorum* is established and following the winter annual lifecycle, fire frequency and intensity may be expected to increase because the alien invasive grass creates a new abundance of fine fuel (i.e. standing dry biomass and litter; also referred to as the fuel packing ratio, or the amount of fuel per unit volume of space; Brooks et al. 2004) during a time of the year that corresponds to fire season (i.e. early summer through autumn). This fine fuel also increases the fuel surface-to-volume ratio, which may increase horizontal fuel continuity (Brooks et al. 2004) There has been evidence that *B. tectorum* greatly alters the natural fire cycle in sagebrush ecosystems; 60 to 500 year intervals between fires has become a three to five year interval in some *B. tectorum* dominated ecosystems (Knapp 1996, Chambers and Roundy 2007). Fire intensity (i.e. the rate at which a fire produces thermal energy) may be affected by fuel packing ratio and/or the moisture content of live and dead fuel, factors that are altered in *B. tectorum* invaded ecosystems. Air temperature, humidity, wind speed, and topography are additional factors that may determine fire intensity at a given site (Certini 2005). Blach et al. (2013) concluded increased fire frequency, size, and duration were associated with *B. tectorum* in the Great Basin ecoregion. Rangelands dominated by *B. tectorum* in these systems were nearly four times more likely to burn than native land cover during the 2000s (Balch et al. 2013). Areas of the Rocky Mountain National Park that have been previously burned had four to five-times greater cover and mean patch area of *B. tectorum* than unburned areas (Banks and Baker 2011).

***B. tectorum*, large wildfire, and climate change**

Beginning with large scale industrialization in the mid-1800s, the human contribution to greenhouse gases in the atmosphere accelerated rapidly, trapping heat in the earth's

atmosphere and altering the climate. Climate change is happening rapidly in the West; some areas increased as much as 1.1 °C between 2000 and 2006 (Hoerling and Eischeid 2007). Since the 1980s there have been significant snowpack declines along the entire Rocky Mountain range due to warmer spring temperatures (Pederson et al. 2013). The current advancement of spring in many areas will certainly have implications for germination and reproductive success of *B. tectorum* and could give this exotic an even greater advantage over slower-growing native grasses.

Rapid climate change may facilitate invasive species such as *B. tectorum* with high phenotypic plasticity, rapid growth from seedling to sexual maturity (Mack 1981), and the potential to shift phenological development to maximize growth and reproduction (Zelikova et al. 2013). Any or all of these qualities may escalate the competitive advantage this grass has over native grasses under future novel climates. Clements and DiTommaso (2011) outlined plant traits that confer an advantage in novel climates, and some of these are consistent with Sakai et al. (2001): (1) high growth rate, (2) wide climatic or environmental tolerance, (3) short generation time, (4) prolific or consistent reproduction, (5) modified seed size, (6) effective dispersal, (7) uniparental reproduction capacity, (8) no specialized germination requirements, (9) high competitive ability, and (10) effective defenses against natural enemies. *B. tectorum* exemplifies all these traits except (8), as it has an after-ripening requirement before germination can occur (Mack 1981).

Climate also affects wildfire regimes. Wildfires have been historically suppressed, resulting in infrequent, larger and more severe fires, in the western US. This has been compounded in the last decade by severe regional drought. The United States General Accounting Office reported annual wildland fire-suppression costs increased from $1.3 billion for the years 1996 through 2000 to $3.1 billion for the years 2001 through 2005 (it must be noted that this increase is at least in part due to an increase in development at the wildland-urban interface). Wildfires even enhance drought through the absorption of solar radiation by smoke particles, as seen in a

simulation of radiative forcing and atmospheric response in the mid-latitudes of the U.S. (Liu 2005).

Species distribution and habitat suitability models as tools for assessing current risk and forecasting potential risk for invasive species and wildfires

The field of macroecology is a rapidly emerging subdiscipline that addresses societal concerns of environmental problems at regional to continental scales (Heffernan et al. 2014). Methodological approaches in macroecology involve large quantities of data at multiple scales and advanced statistical analysis (Levy et al. 2014). Species distribution models and habitat suitability models have become widely used in macroecology. These models assume that we can predict the entire (or potential) spatial distribution of an ecological phenomenon by relating sites of known presence (and absence if available) to predictor variables known for these and all other sites of interest (Hijmans and Elith 2013). In 1869, Ernst Haeckel defined the term 'ecology' as "the study of the natural environment including the relations of organisms to one another and their surroundings" (Odum and Barrett 2005). These relations are the foundation of species distribution models and habitat suitability models. Furthermore, understanding pattern and scale is of great importance in ecology (Elton 1927). Species distribution models are best distinguished from habitat suitability models by their use; the former typically assesses the current distribution of an ecological phenomenon such as a species on the landscape, while the latter follows Grinnellian niche theory, attempting to quantify the suitable habitat given constraints in the local environment that allow the population to grow (Hirzel and Le Lay 2008). There are many diverse applications of these models, increasing their use in both theoretical and applied ecology. Niche theory, metapopulation theory, and source-sink theory are examples of ecological theories often evaluated using these models, and they are also used to formulate hypothesis concerning biogeography, ecology, and evolution of flora and fauna (Guisan and Thuiller 2005, Franklin 2009). The growing popularity of these models has led to their continued methodological scrutiny, refinement, and improvement.

Two commonly used methods to develop species distribution models or habitat suitability models are regression and machine learning. Examples of regression methods include generalized linear models (GLM) and multivariate adaptive regression splines (MARS) (Franklin 2009). Examples of machine learning methods include Boosted Regression Trees, Random Forests, and MaxEnt. Generalized Linear Model (GLM) is a generalized ordinary linear regression approach that specifies a relationship between the mean of a random variable and a function of the linear combination of predictors (McCullagh and Nelder 1989, Hijmans and Elith 2013). Multivariate Adaptive Regression Splines (MARS) is a non-parametric regression technique that automatically models non-linearities and interactions between variables (Friedman 1991, Friedman and Roosen 1995). The recursive partitioning of MARS makes it capable of fitting complex, non-linear relationships between species and predictors. Boosted Regression Trees (BRT) is a stochastic additive regression model. It combines regression trees, which relate a response to a set of predictors using recursive binary splits, and boosting which is an adaptive combination of a wide array of simple models to increase predictive performance (De'ath 2007, Elith and Leathwick 2008, Elith et al. 2008). Random Forest (RF) is an ensemble decision tree method that utilizes a bagging approach, combining a multitude of trees and averaging to produce more accurate classifications (De'ath et al. 2000, Breiman 2001). Random Forest has high classification accuracy and the ability to model complex interactions among predictors, using an array of functions including regressions, classifications, survival analyses, and unsupervised learning. MaxEnt determines patterns in data given constraints placed on the system, and then selects the most likely configuration of the system based on maximizing Shannon's entropy (Phillips et al. 2006, Merow et al. 2013). The MaxEnt approach is non-parametric, therefore it works well with small sample sizes (Guisan and Thuiller 2005, Phillips and Dudík 2008).

Caveats in Modeling; model selection, scale, and environmental covariates

Model selection, spatial and temporal scales, and environmental covariates are all important considerations when employing species distribution models or habitat suitability models. The RF, BRT, MARS, and GLM models can all be fit with presence-absence data for the ecological phenomenon being evaluated; BRT models are particularly useful when analyzing covariate interactions (Elith et al. 2006). Regression methods including GLM and MARS are robust with presence-background (or psueoabsence) data; however BRT and RF models can also be fit with this type of data and MaxEnt is a presence-only model. If there is interest in extrapolating to new, unsampled space, regression methods work well (Elith et al. 2006). In any of these methods, one inherent bias that is important to consider is that records of an observed phenomenon (i.e. a presence) may only provide a subset of sites that are actually occupied within the area of interest.

The spatial scale of a model is dependent on the size of the study area and how much detail is necessary to capture the environmental heterogeneity that influences where the ecological phenomenon being modeled occurs. For example, a temperature surface with a spatial scale of 1 km^2 means that there is one value for temperature per 1 km grid cell. This scale could be appropriate for a continental-scale model but is unlikely to capture the influence of temperature on an ecological phenomenon in a wildlife refuge. Spatial autocorrelation should also be considered in any species distribution or habitat suitability model; if presences or absences are "clumped" together, there may be more than one record for an environmental grid cell (Elith and Leathwick 2009). There are many ways to correct for this, including Moran's *I* (Dormann et al. 2013). Temporal scale is also important to consider in modeling; the time of occurrence data collection should match the relative time of environmental data being considered to produce a more robust model (Elith and Leathwick 2009).

Environmental covariates can come in the form of climate data, remotely sensed data, and anthropogenic land feature data among others. Prior ecological knowledge of the phenomenon being modeled is essential for collecting important environmental covariates. Climate data include variables such as annual, seasonal, or monthly temperature, precipitation, and growing degree day averages. For future potential climate, there are climate projections from climate modeling centers that focus on various emissions scenarios (IPCC 2013). Topographic data are typically derived from a remotely sensed digital elevation model (DEM). Elevation plays a role in microclimate, wind speed, and solar radiation, among other environmental variables (Rosenberg 1983), and therefore may serve as a proxy for these constraints on habitat suitability. A DEM can be used to produce other topographic indices that serve as proxies for soil and water qualities on the landscape including slope, aspect, and compound topographic index (i.e. steady state wetness index; a function of both the slope and the upstream contributing area per unit width orthogonal to the flow direction) among others. Slope and wetness individually accounted for one-half of the variability in organic matter content, pH, extractable P, and silt and sand content across a 5.4-ha toposequence in Colorado (Gessler et al. 1995). Topographic covariates are commonly used for delineating the habitat of species or functional groups on the landscape (Franklin 2009). The Shuttle Radar Topography Mission (SRTM) was flown by the National Aeronautic and Space Administration (NASA) in 2000, and provides publically available DEMs for the entire globe at 90m pixel spatial resolution. Beginning in late 2014, NASA began releasing DEMs for the entire globe at 30m (1 arc-second) spatial resolution.

In addition to DEMs, remote sensing provides other unique ways to detect ecological phenomenon. Spectral reflectance, transmittance, and absorption of plant leaves for ultraviolet, visible, and near infrared (IR) frequencies have been recognized as tools to distinguish vegetation on the since the 1960s (Gates et al. 1965, Myers and Allen 1968, Gausman et al. 1969). Chlorophyll absorbs energy in the blue and red wavelength bands centered around 0.45

and 0.67 μm therefore healthy vegetation appears green, and unhealthy vegetation appears yellow as this absorption decreases. In the near IR portion of the spectrum (i.e. 0.7 to 1.3 μm), a healthy plant leaf reflects up to 50 percent of solar energy, with the total amount reflected greatly dependent on leaf structure. Thus, the near IR band may be used to distinguish specific plant species on the landscape based on leaf structure. For wavelength values greater than 1.3 μm, leaf reflectance is inversely related to total water content of the leaf (Lillesand et al. 2008). Spectral vegetation indices are dimensionless measurements developed from mathematical ratios of these frequencies and require multispectral imagery of the earth's surface. One of the first and most common vegetation indices used is the normalized difference vegetation index (NDVI = near infrared band – red band / near infrared band + red band) developed by Rouse et al. (1974). Since that time, many more useful vegetation indices have been developed to aide in mapping vegetation on the landscape. Similar to NDVI, the Normalized Burn Ratio (Key and Benson 2005) can be used to map fires on the landscape.

The Landsat 8 satellite that was launched in 2013 provides multispectral, moderate spatial resolution imagery of earth's surface at a temporal resolution of 16 days (an 8-day offset from the Landsat 7 satellite), making it an ideal tool for monitoring ecological phenomena on the landscape. The Operational Land Imager (OLI) on the Landsat 8 satellite provides images with nine spectral bands with a spatial resolution of 30 m^2 for bands 1 through 7 and 9, and 15 m^2 for band 8 (i.e. panchromatic band). The Landsat program has been operated by the US Federal Government since 1972, and images are archived and freely available from the United States Geological Survey (USGS) Earth Resources Observation and Science (EROS) center.

Applications

Guisan et al. (2013) noted that although the last decade has seen a rise in the use of species distribution models and habitat suitability models in peer-reviewed literature, few of these studies include the perspective of practitioners and decision makers on their utility. The first two

Chapters of this dissertation address this challenge; the first was guided and inspired by the work of a land managers in Rocky Mountain National Park. The second was prompted by a Rangeland Management Specialist with the U.S. Forest Service in Medicine Bow National Forest, Wyoming, and became an iterative modeling process that considered and included valuable insights and data gained from a group of concerned land managers ranging from fire ecologists to wildlife biologists. The final chapter of this dissertation was not directly influenced by a practitioner, however work on the first two Chapters resulted in the development of hypotheses concerning wildfires that could be tested using the same methods, and the maps produced will provide a useful tool for future risk assessments. Finally, as demonstrated in the discussion and supplementary material, these models can provide the basis for developing new hypotheses concerning ecological phenomena.

CHAPTER 2. USING HIGH RESOLUTION FUTURE CLIMATE SCENARIOS FOR FORECASTING INVASION IN NATIONAL PARKS[1]

Introduction

Bromus tectorum L. is an invasive winter annual grass that was introduced into the United States from Eurasia in the late 19th century. While the current distribution of *B. tectorum* extends throughout the United States, it is particularly abundant in the Intermountain West (Mack 1981), and it is listed as a Class C noxious weed in the state of Colorado ("United States Department of Agriculture PLANTS database" 2014). Prior research has linked *B. tectorum* abundance and distribution to climate (Bradford and Lauenroth 2006, Bradley 2009), roads and trails (Bromberg et al. 2011, Banks and Baker 2011), elevation (Bromberg et al. 2011, Banks and Baker 2011), vegetation community type (Bromberg et al. 2011), and soils when moisture is limiting (Miller et al. 2006, Bradford and Lauenroth 2006).

The winter annual life history of *B. tectorum* is not common amongst grass species in the Intermountain West. It may complete its life cycle as a winter or spring annual depending on temperature and water availability (Mack 1981, "United States Department of Agriculture PLANTS database" 2014). Autumn germinating individuals overwinter as semi-dormant seedlings; therefore these plants may begin growing earlier in the spring than native warm-season grass seedlings. Plant traits that harbor an advantage in novel climates include (1) high growth rate, (2) wide climatic or environmental tolerance, (3) short generation time, (4) prolific or consistent reproduction, (5) modified seed size, (6) effective dispersal, (7) uniparental reproduction capacity, (8) no specialized germination requirements, (9) high competitive ability,

[1] *A version of this chapter was published in PLoS ONE: West AM, Kumar S, Wakie T, Brown CS, Stohlgren TJ, Laituri M, and Bromberg J (2015). Using high-resolution future climate scenarios to forecast B. tectorum invasion in Rocky Mountain National Park. PLoS ONE 10 (2): e0117839. doi:10.1371/journal.pone.0117893.*

and (10) effective defenses against natural enemies (Clements and DiTommaso 2011). Seven of these traits are exemplified by *Bromus tectorum* (it has an after-ripening requirement that stimulates germination; (Mack 1981)). Furthermore, evidence from studies across a broad range of ecosystems suggests a significant shift upward (in elevation) and poleward (in latitude) for some plant species distribution in response to climate change (Davis and Shaw 2001, Lenoir et al. 2008), including *B. tectorum,* which has been documented recently at increasing elevations (Bromberg et al. 2011, Banks and Baker 2011). Rapid climate change may facilitate invasive species such as *B. tectorum* with high phenotypic plasticity and rapid growth from seedling to sexual maturity, increasing its competitive advantage over native species (Mack 1981).

Species distribution models (SDMs) may enhance our understanding of the environmental variables that most influence the bioclimatic niche of a species, a subset of its fundamental ecological niche defined by associations between aspects of climate and known species occurrences (Araújo and Peterson 2012). The fundamental ecological niche of a species is defined as the multivariate space occupied by the species, including the environmental conditions associated with population maintenance (Hutchinson GE 1957). Through the inclusion of future climate variables in SDMs, we may visualize the potential future geographic distribution of a species (Jarnevich and Stohlgren 2008).

The maximum entropy model or MaxEnt (Phillips et al. 2006), is a machine learning SDM that determines the probability distribution of a species over geographic space by estimating this distribution under the maximum entropy principle (i.e., exponential distribution given linear combination of features; equivalent to the Gibbs distribution). This SDM is of particular value when examining an introduced species such as *B. tectorum* because it requires only species presence data, whereas other SDMs such as logistic regression require presence and absence data. Models that include absence locations do not necessarily indicate unsuitable habitat,

rather that the species has not had time or resources for broad dispersal (Jiménez-Valverde et al. 2011).

There are many reasons that MaxEnt was chosen for our study. MaxEnt is a non-parametric model and can automatically include interactions among both continuous (e.g., climate) and categorical (e.g., vegetation community type) variables (Phillips and Dudík 2008), is effective with small sample sizes (Hernandez et al. 2006, Pearson 2007, Wisz et al. 2008, Kumar and Stohlgren 2009), and has been shown to outperform or at least preform as well as many other modeling algorithms for SDMs of terrestrial plants, birds, bats, reptiles, and diseases (Elith et al. 2006, Evangelista et al. 2008a, Kearney et al. 2010, Flory et al. 2012). In addition, inclusion of static and dynamic variables other than climate, such as vegetation community type and distance to roads may enhance the predictive capabilities of SDMs (Guisan and Thuiller 2005, Stanton et al. 2012). Similar to other species distribution models, MaxEnt can also be applied to future climate modeling (Hijmans and Graham 2006, Kearney et al. 2010). Process-based mechanistic niche models such as CLIMEX also provide powerful tools for evaluating the potential effects of climate change on species distributions (Shabani et al. 2012, 2014, Taylor et al. 2012); however these SDMs may not be ideal for use in a National Park. Correlative models such as MaxEnt can be fit to existing occurrence data whereas process-based models typically require detailed experimental data that may not be available for an introduced species in a National Park (Dormann et al. 2012). Furthermore, the finest resolution of the climate surfaces in CLIMEX are 1km (Kriticos et al. 2012), which may not be appropriate for modeling climate effects on species distribution in National Parks.

When managing for invasive species at the landscape scale, regional weather patterns important to fecundity may not be captured in coarse-resolution data (Hamann and Wang 2006, Ashcroft et al. 2009, Delong 2010, Austin and Van Niel 2011). Capturing climate refugia for species in areas with widely varying elevation such as Rocky Mountain National Park may be

improved by using fine-scale data (Lenoir et al. 2008, Randin et al. 2009, Gillingham et al. 2012b, Franklin et al. 2013). ClimateWNA software provides climate data for point locations, time series, and climate surfaces for Western North America (Wang et al. 2012). This software was developed using downscaling algorithms (delta approach; for methods see (Wang et al. 2012)) where baseline climate data (PRISM and ANUSPLIN grids), historical data (CRU TS 2.1), and future projected data (Coupled Model Intercomparison Project; IPCC 2007) are interpolated as the difference from a common reference period, with their accuracy tested against local weather station data. Furthermore, partial derivative functions of temperature change along elevation gradients are incorporated in these methods, making them ideal for areas such as Rocky Mountain National Park (Wang et al. 2012).

Species distribution models are powerful tools in evaluating the bioclimatic niche of a species; however the assumption of niche conservatism should always be considered when projecting these models into future potential environmental space (Pearman et al. 2008). To address this concern, ordination methods may be used to estimate the maximum variance of climatic predictors and climatic niche overlap between current and future potential distributions (Broennimann et al. 2012). Thus, we may examine the ordinal climatic niche space of a species in a given area currently, overlay it with the ordinal climatic niche space of the same species given the future climate projections, and evaluate the overlap and shift of this niche space. These niche comparisons may elucidate the potential distributional progression of a species and are useful tools to augment SDMs.

Based on preliminary analysis of current *B. tectorum* distribution in Rocky Mountain National Park (hereafter, the Park) and projected climate change in the Park, the primary hypothesis driving this study was that this alien invasive grass may continue to be problematic in current disturbed areas of the Park well into the future, and expand its bioclimatic niche as the climate changes in the Park. Our objectives were to: (1) evaluate the current bioclimatic niche including

climatic variables that have a significant influence on *B. tectorum* occurrence in the Park using MaxEnt and high-resolution climatic data generated from ClimateWNA, (2) model the potential bioclimatic niche of *B. tectorum* in the Park for the year 2050 based on climate change, and (3) create a high-resolution map of *B. tectorum* habitat in the Park both now and in the future for use by Park managers. We also sought to better understand the usefulness of ordination methods to evaluate niche dynamics in ordinal space.

Methods

Study Area

Rocky Mountain National Park covers about 1,076 km^2 in northern Colorado, USA, at approximate latitudes 40°10'N to 40°32'N. The elevation varies greatly in the Park, from 2,300 m to 4,345 m at the summit of the highest peak (Longs Peak) and the Continental divide separates the Park with 60% on the east slope and 40% on the west slope. At Estes Park climate station (station #052759 at 2364 m elevation; ("Western Regional Climate Center" n.d.), mean annual temperature from 1981-2010 was of 6.9˚C, and mean annual precipitation was 41.8 cm. Montane, subalpine, and alpine ecosystems blanket the Park, yielding habitat to a wide variety of flora. Rocky Mountain National Park lists 28 alien plant species as common to abundant including *B. tectorum* ("The National Park Service Rocky Mountain National Park Website" n.d.). The United States National Park Service defines an alien species as "those that occur in a given place as a result of direct or indirect, deliberate, or accidental actions by humans" ("The National Park Service Rocky Mountain National Park Website" n.d.). We received a scientific research and collecting permit from Rocky Mountain National Park to proceed with this study (ROMO-2013-SCI-0038).

Species Occurrence Data

Occurrence data for *B. tectorum* were combined from four prior field surveys in the Park conducted in 1996, 1999, 2007, and 2008 (n=211; (Bromberg et al. 2011)). These surveys were

conducted using a modified-Whittaker plot design (Stohlgren et al. 1995). We assumed these data were from populations that have not currently filled the entire bioclimatic niche due to dispersal limitations (Gallien et al. 2012). Additional *B. tectorum* occurrence data within a 100,000 m perimeter of Park boundaries were evaluated for inclusion in the study; however it was concluded that no new ecosystem types would be represented by these locations.

Environmental Variables

We used current data (climate normals 1981-2010) encompassing 21 annual and 48 seasonal bioclimatic (continuous) variables at a 90 m resolution generated using ClimateWNA v. 4.72 program (Wang et al. 2012), distance to roads and trails (continuous), and vegetation community type (categorical) variables (Appendix 2.1).

The 90-m^2 spatial resolution was chosen for this study after an evaluation of climate data at 4 km^2 ("PRISM"; www.prism.oregonstate.edu) and 1 km^2 ("WorldClim"; worldclim.org) determined finer climate refugia for the Park may not be captured at these spatial scales (Figure 2.1).

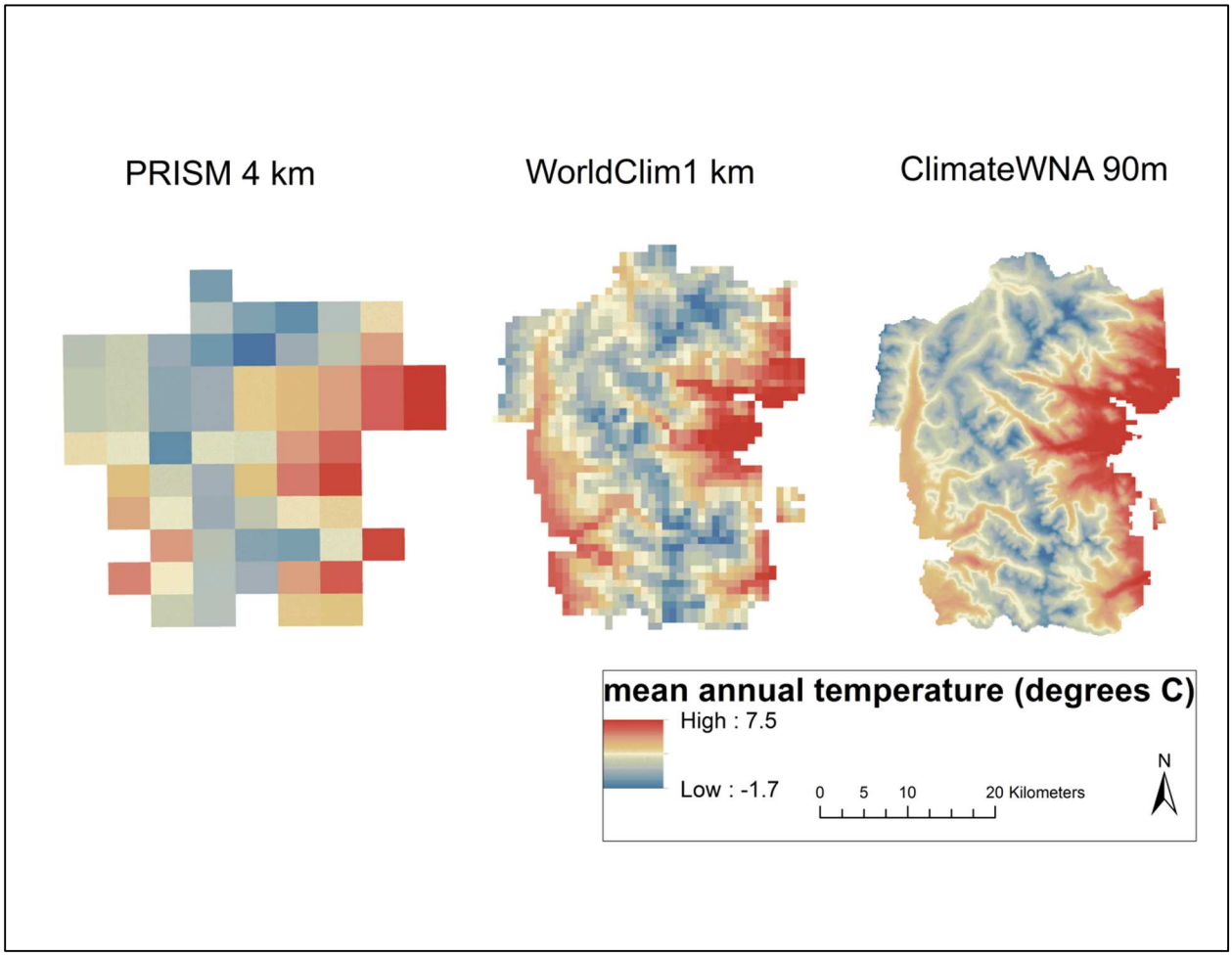

Figure 2.1. Comparison of mean annual temperature (MAT) at three spatial resolutions (4 km, 1 km, and 90 m) for climate normals 1981-2010 in Rocky Mountain National Park, Colorado. Data Sources: PRISM Climate Group (www.prism.oregonstate.edu) WorldClim (www.worldclim.org) and ClimateWNA (http://climatewna.com/).

The 90-m spatial resolution resulted in 133,849 (90 x 90 m) grid cells, each with a unique value for the 71 variables. Distance to roads and trails was included as a surrogate for *B. tectorum* propagule pressure; the seeds of *B. tectorum* readily attach to vehicle tires, hiking boots, and animal fur (Bromberg et al. 2011, Banks and Baker 2011). Elevation data ("CGIAR_CSI Geoportal" n.d.), a proxy for climate, was not included in model development, but was used to

extract all data from ClimateWNA, and evaluated post-modeling to gain insight concerning the potential elevational limits of *B. tectorum* in the Park.

Future climate scenarios (year 2050) from six global circulation models (GCMs) were extracted at a 90 m resolution from ClimateWNA. These included two runs of CCCMA (Canadian Centre for Climate Modeling and Analysis), MIROC-H (Centre for Climate Research, Japan), MRI (Meteorological Research Institute, Japan), BCCR (Bjerknes Centre for Climate Research, and GFDL (United States National and Atmospheric Administration Geophysical Fluid Dynamics Laboratory). Global circulation models incorporate energy flux measurements between the sun, atmosphere, and earth's surface in algorithms that compute surface conditions. For all GCMs used in this model, the A2 climate change scenario was selected as this scenario follows observed trends in atmospheric carbon dioxide concentrations in the mid-2000s (Raupach et al. 2007). All variables considered were projected in Universal Transverse Mercator (UTM) coordinates in NAD83 datum (to match the *B. tectorum* occurrence data) using geographic information system format (ArcGIS v.10; ESRI, Redlands, CA, USA). Although there is uncertainty associated with any future climate scenario, these data provide the most reasonable predictions given our current understanding of future conditions.

Statistical Analysis and Spatial Modeling

We used R v.3.0.1 statistical software (R Core Team 2012) to calculate Pearson correlations (Hmisc package; Frank Harrell) among the 69 climatic variables. All correlation values (r) were statistically significant ($p < 0.001$). When two or more variables were highly correlated ($|r| \geq 0.70$), variables with the lower biologic relevance to *B. tectorum* was dropped (Dormann et al. 2013). Highly correlated variables do not add new information to SDMs, and their exclusion is the first step in determining the most parsimonious model. The distance to roads and trails and vegetation community type variables were not included in the Pearson correlation analysis (the former was retained to represent propagule pressure; the latter was a categorical variable). The

correlation analysis resulted in nine variables for inclusion in the initial SDM: mean annual temperature, continentality (temperature difference between mean warmest month temperature and mean coldest month temperature, °C), summer chilling degree-days, beginning of frost-free period, mean summer precipitation, spring heating degree days, winter reference evaporation, distance to roads, and vegetation community type.

These nine variables were included in MaxEnt along with the *B. tectorum* occurrence data. An initial SDM was run in MaxEnt (one run; raw output setting) to acquire lambda values used in ENMTools v.1.3 (Warren et al. 2010) to calculate Akaike's Information Criterion (AIC; Anderson and Burnham 2002) for a model fit with all nine variables, eight, seven, six, five, four, three, two, and one of the variables, respectively (Table S2). This method selects the fitted approximating model that is estimated to be closest to the unknown truth on average (i.e. the most parsimonious model). The model that was most parsimonious in our case (lowest AIC value) had six variables: mean annual temperature, continentality, beginning of frost-free period, mean summer precipitation, spring heating degree days, and distance to roads and trails.

These six variables were then incorporated into MaxEnt along with the *B. tectorum* occurrence data. The same six variables were included as projection layers for the year 2050 for all six GCMs. MaxEnt requires the user to specify a background for the study area from which the algorithm will select random points that are assumed as 'pseudo-absences'. We set MaxEnt to select 10,000 random background points from the entire Park. The *B. tectorum* occurrences used in this study were collected using stratified random sampling in the Park, and personal communication with Park staff verified that these invaded areas were the only ones reported for the Park at the time these occurrences were sampled, justifying this background point selection method. MaxEnt allows the user to change default settings based on study objectives (Phillips and Dudík 2008, Merow et al. 2013). We changed the following settings: (1) created response curves to evaluate *B. tectorum* response to individual variables, (2) conducted jackknife

procedure to measure variable importance, (3) selected a random seed, (4) set random test percentage at 10 to evaluate model performance and reduce bias (90% of the data trained the model), (5) set replicates at 100 so that model results would not be dependent on a single sample and to ensure variability, (6) replicated run-type was set as subsample, (7) chose that plot data be written, (8) set maximum iterations to 5,000 allowing the model adequate time for convergence (prevents over- or under- prediction of correlations), (9) selected that background predictions be written, and (10) conducted 'fade by clamping' to ensure consistency in probabilities for the future climate projections.

MaxEnt produced seven continuous surface ASCII files; one for current probabilities of occurrence and one for each year 2050 GCM (i.e. six future climate scenarios). These ASCIIs contained relative probabilities of *B. tectorum* presence predicted for each 90-m pixel of the study area. Using ArcGIS v.10, the seven ASCII files were converted to binary maps in raster format, where 1= suitable habitat and 0= unsuitable habitat. This classification was based on the 10^{th} percentile training presence logistic threshold (= 0.32) produced by the MaxEnt model. Finally, the six year 2050 GCM rasters were combined and reclassified into non-habitat, decreasing, increasing, and stable habitat for *B. tectorum* in the Park using an ensemble approach (Araújo and New 2007).

Model evaluation

To evaluate the final MaxEnt model with six variables compared to random expectations we calculated a partial AUC (area under receiver operating characteristic curve) ratio (pAUC) following (Peterson et al. 2008). A pAUC value of 1 indicates the model preformed no better than random; values >1 indicate the model performed better than random. Partial AUC considers only the portion of the AUC curve that corresponds to model predictions rather than commission error rate (i.e. ratio of incorrectly predicted absence data to all absence data), which is not applicable for presence-only SDMs. For the pAUC analysis, 80% of the *B. tectorum*

occurrence data (n = 169) were randomly selected to train a MaxEnt model using 10-fold cross validation . The remaining 20% of the data (n = 42) were used to test the logistic predictions of this model. The modeled suitability values of each testing point are used to calculate pAUC, and we ran 1000 iterations with 50% of the points resampled with replacement for each bootstrap.

To prepare data for a principle components analysis (PCA), 10,000 random points were selected from the entire study area of the Park, and current and future (year 2050; ensemble from averaging six GCMs) values for the five non-correlated climatic variables were extracted for these points in ArcMap v.10. Using R v.3.0.1, a PCA analysis was conducted for these variables to reduce dimensionality; multivariate attributes were reduced to two values (each variable was regarded as constituting a different dimension, in a p-dimensional hyperspace). The *niche.overlap*, *occ.prep*, and *niche.dynamic* functions in R were utilized and code was modified from (Broennimann et al. 2012). This method converted the *B. tectorum* presence points (n = 211) to density values via kernel smoothing. The density values were then ordered along PCA axes of the current environmental grid (10,000 random background points) and then the future (2050) environmental grid (same 10,000 random background points). The current and 2050 models were overlaid to determine the extent of *B. tectorum* niche overlap in ordinal space, between current and future climates. This PCA does not substantiate the results of the MaxEnt model; rather it provides another tool to evaluate the potential future niche of a species in ordinal space (i.e., the fundamental niche) rather than geographic space.

Results

Variable correlation and parsimony analysis

Out of 69 climatic variables, seven were found to be uncorrelated using Pearson correlation ($|r| \leq 0.70$): mean annual temperature, continentality (temperature difference between mean warmest month temperature and mean coldest month temperature, ˚C), summer chilling degree-days, beginning of frost-free period, mean summer precipitation, spring heating degree

days, and winter reference evaporation. The AIC analysis indicated a model with five of these seven climatic variables (mean annual temperature, continentality, beginning of frost-free period, mean summer precipitation and spring heating degree days) and the distance to roads and trails variable would be most parsimonious. Thus, these six variables were used in the final MaxEnt model.

Final MaxEnt model with six variables

The average pAUC value for the best model was 1.77 (± 0.0005), indicating the MaxEnt algorithm performed exceptionally well in discriminating areas as suitable *B. tectorum* habitat. Mean annual temperature had the greatest contribution to the model (43.7%), followed by spring degree days below 18˚C (19.5%; Table 2.1).

Table 2.1. Variables and their relative contribution in the final MaxEnt model.

Variable	Percent Contribution[2]	Permutation Importance
Mean annual temperature	43.7	17.2
Spring degree days below 18˚C	19.5	5.1
Distance to roads	13.5	34.1
Beginning of frost-free period	13.5	6.4
Mean summer precipitation	6.3	23.7
Continentality	3.5	13.4

Distance to roads and beginning of frost-free period contributed equally to the model (13.5%), and mean summer precipitation contributed 6.3%. Continentality only contributed 3.5% to the model; however we felt confident in its inclusion because of the low AIC value associated with the six variable model compared to a model with more or fewer variables. Model response to the top predictor variable (i.e. mean annual temperature) indicated the probability of *B. tectorum*

[2] *Percent contribution is calculated as the increase in regularized gain added to the contribution of the corresponding variable for each of the 5000 iterations of the model (subtracted if the change to the absolute value of lambda is negative).*

presence in a given cell is greater than 50% when mean annual temperature is between 5.5 and 7.5˚C. Likewise, spring degree days below 18˚C between 1000 and 1200 yielded at least 50% logistic probability, as well as beginning of frost-free period Julian date between 145 and 165, and distance to roads less than 1000 m. Mean summer (May – Sept.) precipitation and continentality showed the most conservative thresholds for *B. tectorum* response. Mean summer precipitation greater than 250 mm and less than 300 and continentality greater than 21˚C but less than 22˚C yielded greater than 50% logistic probability, and while their significance in the model was lower than the other four variables these narrow thresholds merit further investigation. Jackknife output confirmed the importance of mean annual temperature, spring degree days below 18˚C, and beginning of frost free period to the final model (i.e., higher training gain and test AUC value; Figures 2.2 a, b).

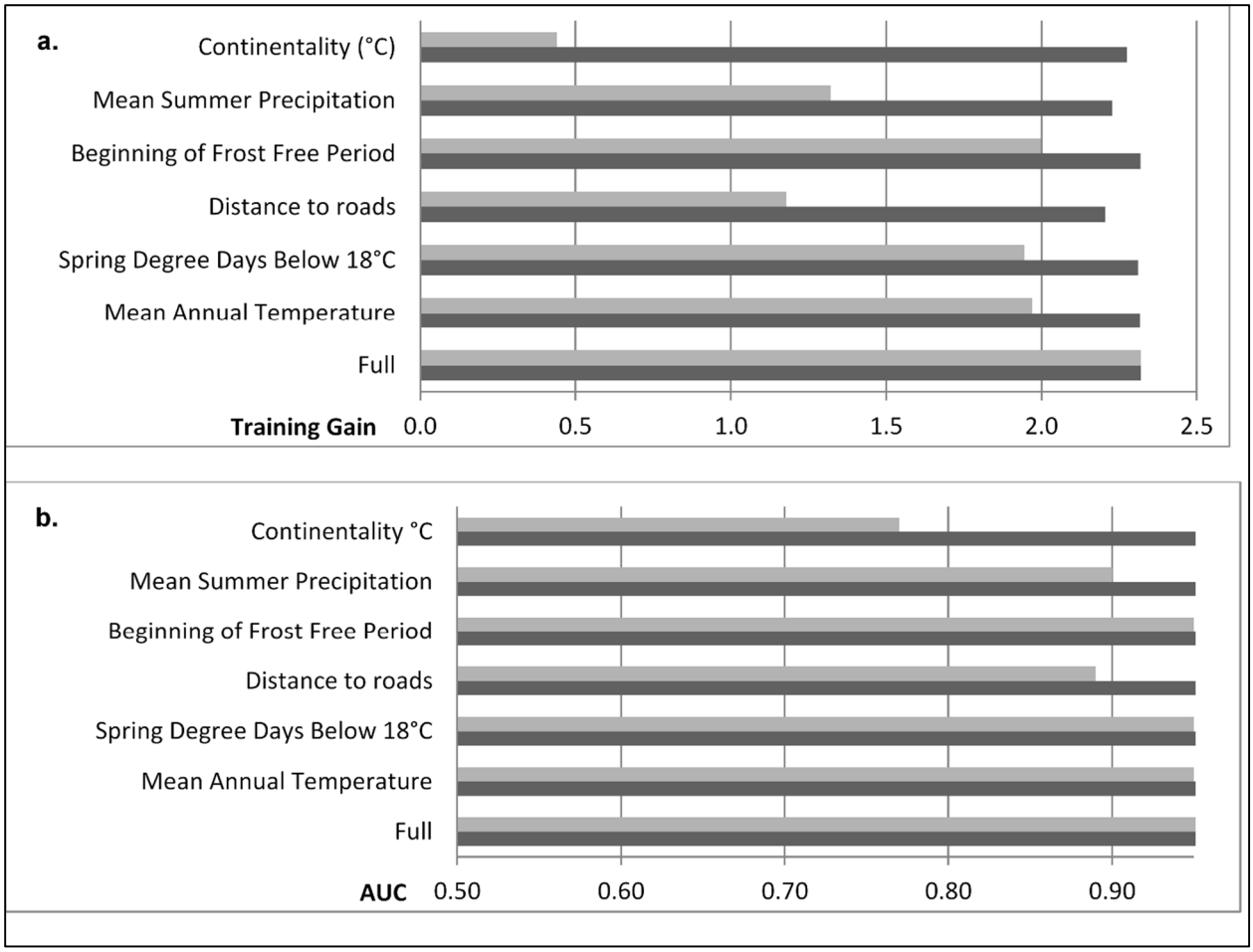

Figure 2.2. Variable contribution to (a) training gain and (b) AUC (area under curve). Light gray bars indicate how well the model performs with only that variable versus a full model, which are the dark gray bars. Values shown are averaged over 100 replicate MaxEnt model runs.

Current and future potential suitable habitat of B. tectorum in the Park

The current suitable habitat for *B. tectorum* in the Park is 62.2 km^2, and in the future (year 2050) our ensemble model indicated 219.4 km^2 of the Park as suitable habitat (Figures 2.3a, b).

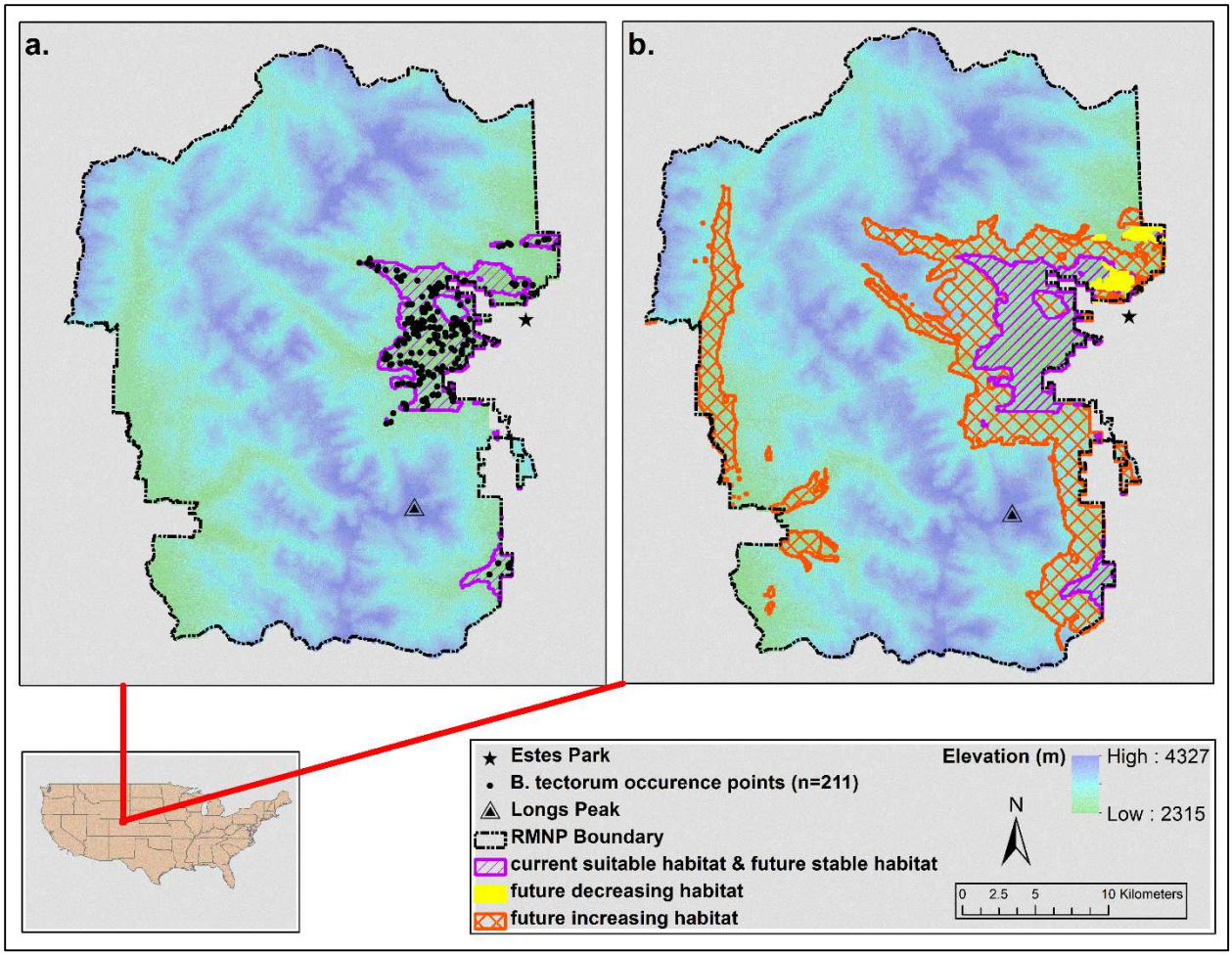

Figure 2.3. *Bromus tectorum* current suitable habitat in Rocky Mountain National Park and (a) increasing, decreasing, stable, and unsuitable habitat for the year 2050 (b) based on MaxEnt model outputs. Elevation has been included for reference. Coordinate system NAD 1983 UTM Zone 13 N.

In the future model, 5.5% of the Park currently suitable remains stable habitat for *B. tectorum* (59.1 km^2) while 0.3% decreases in suitability (3.1 km^2). An additional 14.9% of the Park becomes suitable habitat (160.3 km^2) compared to current conditions. Although elevation (a proxy for climate) was not included in the model, we overlaid the final model results on a digital elevation model of the Park to evaluate the potential elevational limits of *B. tectorum* given future climates. Currently, *B. tectorum* has been found up to 2,800 m elevation in the Park, and the current suitable habitat MaxEnt results agree with this. The future ensemble model indicates *B. tectorum* may reach nearly 3,300 m in elevation by the year 2050.

Principle components analysis

Relative occupancy for the current realized and year 2050 projected realized niches of *B. tectorum* in the Park are shown along each axis of the PCA model (Figure 2.4).

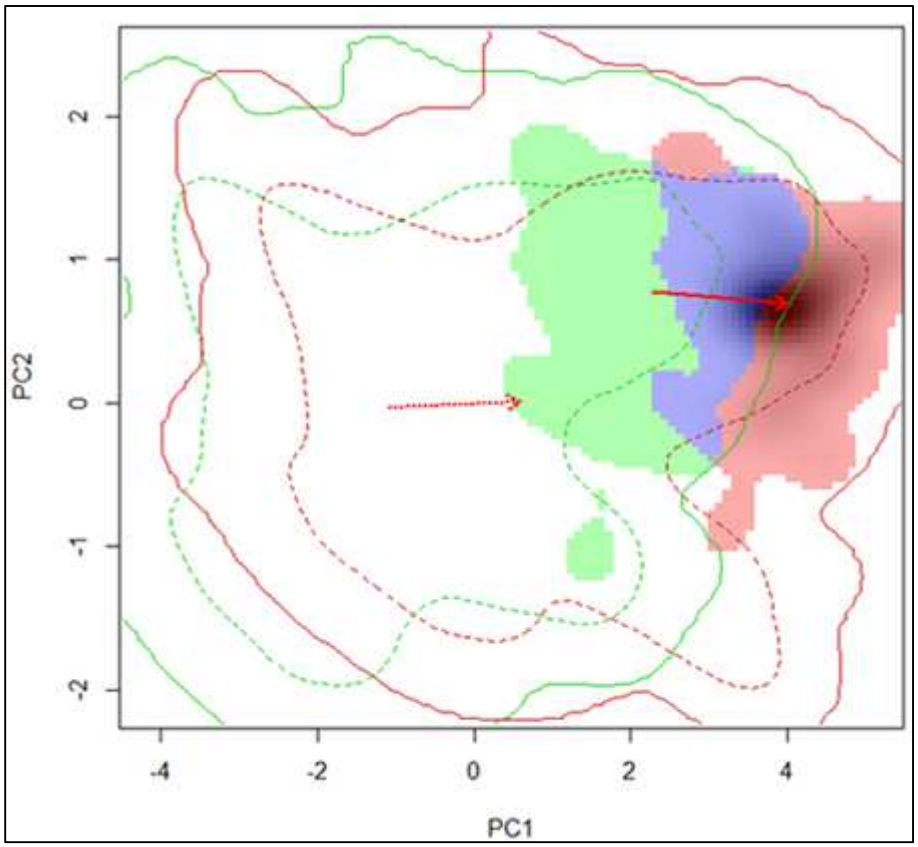

Figure 2.4. PCA of niche overlap (blue) for *B. tectorum* in Rocky Mountain National Park based on current (green) and future (red) climate space. Averages for five climatic variables from six global circulation models (GCMs) were included in this analysis: mean annual temperature, spring degree days below 18˚C, beginning of frost-free period, mean summer (May-Sept.) precipitation, and continentality (see methods for description of GCMs).

The PCA indicated both niche conservation (*D* = 0.22 or 22% overlap between current climate niche space and future ordinal niche space) and a shifting niche for *B. tectorum* in the Park between current and future conditions. Thus, 22% of the ordinal climatic niche of this species may remain in the Park under future climates, and 78% of this niche space may shift.

Discussion

In this study we used MaxEnt model to integrate species occurrences and high-resolution (i.e. 90 m) current and future climatic and other environmental data layers to develop current and future potential habitat distribution maps for *B. tectorum*. Compared to current conditions, in the year 2050 an additional 14.9% of the Park will be suitable habitat for *B. tectorum* (160.3 km^2). Interestingly, the final MaxEnt model indicated some areas of the Park that are currently suitable may no longer be suitable *B. tectorum* habitat in the future. Therefore, it is likely one of the most significant climatic variables may surpass an upper or lower value threshold for *B. tectorum* survival given its probability of presence. For example, the strongest predictor in the MaxEnt model, mean annual temperature may exceed the upper threshold of 7.5˚C under future potential conditions in some areas of the Park. The distribution of both C3 and C4 grasses has been explained in previous studies primarily by mean annual temperature (Paruelo and Lauenroth 1996, Bremond et al. 2012). *Bromus tectorum* is a C3 grass, a group whose relative abundance tends to decrease with increasing mean annual temperature (Paruelo and Lauenroth 1996). The raw ClimateWNA data indicated that mean annual temperature will increase for most of the Park in all six GCMs. Our model forecasts suitable habitat for *B. tectorum* at increasing elevations in the Park for the year 2050, suggesting this alien grass may respond to increasing mean annual temperatures by moving upward in elevation to maintain its niche space. This model showed suitable habitat for *B. tectorum* up to 3,300 m elevation, indicating this invasive grass may become problematic in subalpine ecosystems of the Park. *Bromus tectorum* has already been found at 3,000 m elevation in the Himalayan mountains (Upadhyaya 1986).

The significance of all six variables that were selected through our parsimony analysis to *B. tectorum* ecology indicates the importance of careful scrutiny and correlation analysis of available environmental data for a study site of interest *a priori*, as other authors have indicated

(Kumar et al. 2009, Sheppard 2013). In particular, mean annual temperature, spring degree days below 18°C, beginning of frost-free period and distance to roads and trails have relevant ecological importance to the distribution of this alien invasive grass species. While prior research has indicated vegetation community type is important in determining habitat suitability for *B. tectorum*, we were not concerned when this variable was dropped based on AICc values; this variable is not static given future potential climates and disturbances such as fire and pine beetle outbreaks in the Park. The logistic probability response indicated 1000 and 1200 spring degree days below 18°C (also known as heating degree days) increases the likelihood of *B. tectorum* presence, and this finding is supported by (Ball et al. 2004), whose study across Western US States including Colorado supported the hypothesis that seed development for this alien grass can be related to cumulative growing degree days at a given geographic location. Furthermore, the current advancement of spring (warmer average temperatures earlier in the year) in the study area will certainly have implications for green-up and reproductive success of *B. tectorum.* Since the 1980s, there have been significant snowpack declines along the entire Rocky Mountain range due to warmer spring temperatures (Pederson et al. 2013), which may give this alien an even greater advantage over slower-growing native grasses(Compagnoni and Adler 2014).

Beginning of frost-free period and distance to roads/trails variables contributed equally to the MaxEnt model and should be considered as indicators of *B. tectorum* distribution in the Park. Beginning of frost-free period is important when considering release from temperatures that may damage plant tissue. The inclusion of distance to roads in the final model was consistent with prior research of *B. tectorum* distribution in the Park (Bromberg et al. 2011); the seeds of *B. tectorum* easily attach to vehicle tires and hiking shoes, making roads a key mechanism in its dispersal.

A bioclimatic model at ~4 km spatial resolution was developed for the Great Basin ecoregion of the US that indicated summer, annual, and spring precipitation and winter temperatures were the best predictors of *B. tectorum* distribution(Bradley 2009). Coarser resolution SDMs (e.g., greater than 1 km^2) are useful for large areas such as the Great Basin, but are likely to have greater inherent prediction error in smaller study areas and areas with higher elevational range and topographic heterogeneity such as Rocky Mountain National Park (Gillingham et al. 2012a). The *B. tectorum* occurrence locations used in this study were spread across a broad elevation gradient, making a finer-scaled SDM important (Randin et al. 2009). The 90 m resolution grid cells used in our model combined with climate data that included local weather station data were more likely to capture small areas of climate refugia for *B. tectorum* than coarse-scale models that are often used in SDMs.

Our PCA results indicated that some of the ordinal niche space of *B. tectorum* may be conserved in the Park, however a larger portion of this space will shift under future climate conditions. Given the increased within-population genetic variation of *B. tectorum* in North American populations and the high phenotypic plasticity of this alien invasive grass (Novak et al. 1993, Ellstrand and Schierenbeck 2006, Leger et al. 2009), the future potential shift of its bioclimatic niche space merits constant monitoring for new populations in the Park. One study cited that although *B. tectorum* already occurs in Canada, it has the potential to expand this range due to “weedy” genotypes (Clements and DiTommaso 2011). A more recent study indicated *B. tectorum* has the potential to shift phenological development to maximize growth and reproduction (Zelikova et al. 2013). Although quantifying evolutionary adaptations has yet to be realized in SDMs, supplementing these models with PCA may fill the gap in uncertainties associated with niche conservation.

Existing research indicates that climate and soil disturbance are main drivers for successful *B. tectorum* invasion (D’Antonio and Vitousek 1992, Bradford and Lauenroth 2006). Future

research modeling *B. tectorum* distribution in the Park may incorporate measurements such as soil disturbance that may result in bare ground or loss of competing vegetation, as well as slope and aspect to provide an even stronger case for monitoring particular areas within the Park. *Bromus tectorum* grows in a broad range of soil types; however it is intolerant of shade (Mack 1981). A niche model incorporating variables such as slope and light exposure as proxies for shade may provide further inference to *B. tectorum* distribution in the Park (Austin and Van Niel 2011).

The SDM methods outlined in this study provide useful tools for land managers to plan for future potential climates across space and time. An ensemble of six different global circulation models takes into consideration the varying sensitivities to model input among extrapolated climates, thus reducing uncertainty in our projections. This method combined with fine-resolution data from ClimateWNA and the inclusion of annual climate, seasonal climate, and distance to roads/trails produced the most robust estimates of current and future habitat for *B. tectorum* in the Park. These maps can improve the efficiency and lower the cost of future surveys. Our methodology can be adopted to generate high resolution species distribution maps under current and future climate scenarios for small study areas and other species, such as the 27 additional invasive species in Rocky Mountain National Park. Land managers can incorporate the maps created from these models into integrated pest management regimes, and further tailor them based on what is already known about an area, keeping in mind that the models must be used in an iterative manner to improve their accuracy. Finally, maps such as these may be displayed to the public to increase awareness of climate change implications in National Parks and beyond.

Appendices

Appendix 2.1. Environmental variables (n = 71) evaluated for inclusion in the model[1].

Variable description and units of measurement
Annual Variables
Mean annual temperature (°C)
Mean warmest month temperature (°C)
Mean coldest month temperature (°C)
Continentality (°C; difference between MWMT and MCMT)
Mean annual precipitation (mm)
Mean summer (May to Sept.) precipitation (mm)
Annual heat: moisture index (MAT+10)/(MAP/1000)
Summer heat:moisture index ((MWMT)/(MSP/1000))
Degree days below 0°C
Degree days above 5°C
Degree days below 18°C
Degree days above 18°C
Number of frost-free days
Frost-free period (FFP)
Julian date on which FFP begins
Julian date on which FFP ends
Precipitation as snow (mm) between Aug and July
Extreme minimum temperature over 30 years
Extreme maximum temperature over 30 years
Hargreaves reference evaporation
Hargreaves climatic moisture deficit

Seasonal Variables
Winter (Dec.(prev. yr) - Feb.) mean temperature (°C)
Spring (Mar. - May) mean temperature (°C)
Summer (Jun. - Aug.) mean temperature (°C)
Autumn (Sep. - Nov.) mean temperature (°C)
Winter mean maximum temperature (°C)
Spring (Mar. - May) mean maximum temperature (°C)
Summer (Jun. - Aug.) mean maximum temperature (°C)
Autumn (Sep. - Nov.) mean maximum temperature (°C)
Winter (Dec.(prev. yr) - Feb.) mean minimum temperature (°C)
Spring (Mar. - May) mean minimum temperature (°C)
Summer (Jun. - Aug.) mean minimum temperature (°C)
Autumn (Sep. - Nov.) mean minimum temperature (°C)
Winter (Dec.(prev. yr) - Feb.) precipitation (mm)
Spring (Mar. - May) precipitation (mm)
Summer (Jun. - Aug.) precipitation (mm)
Autumn (Sep. - Nov.) precipitation (mm)
Winter (Dec.(prev. yr) - Feb.) degree days below 0°C
Spring (Mar. - May) degree days below 0°C
Summer (Jun. - Aug.) degree days below 0°C
Autumn (Sep. - Nov.) degree days below 0°C
Winter (Dec.(prev. yr) - Feb.) degree days above 5°C
Spring (Mar. - May) degree days above 5°C
Summer (Jun. - Aug.) degree days above 5°C
Autumn (Sep. - Nov.) degree days above 5°C

Winter (Dec.(prev. yr) - Feb.) degree days below 18°C
Spring (Mar. - May) degree days below 18°C
Summer (Jun. - Aug.) degree days below 18°C
Autumn (Sep. - Nov.) degree days below 18°C
Winter (Dec.(prev. yr) - Feb.) degree days above 18°C
Spring (Mar. - May) degree days above 18°C
Summer (Jun. - Aug.) degree days above 18°C
Autumn (Sep. - Nov.) degree days above 18°C
Winter (Dec.(prev. yr) - Feb.) number of frost-free days
Spring (Mar. - May) number of frost-free days
Summer (Jun. - Aug.) number of frost-free days
Autumn (Sep. - Nov.) number of frost-free days
Winter (Dec.(prev. yr) - Feb.) precipitation as snow
Spring (Mar. - May) precipitation as snow
Summer (Jun. - Aug.) precipitation as snow
Autumn (Sep. - Nov.) precipitation as snow
Winter (Dec.(prev. yr) - Feb.) Hargreaves reference evaporation
Spring (Mar. - May) Hargreaves reference evaporation
Summer (Jun. - Aug.) Hargreaves reference evaporation
Autumn (Sep. - Nov.) Hargreaves reference evaporation
Winter (Dec.(prev. yr) - Feb.) Hargreaves climatic moisture deficit
Spring (Mar. - May) Hargreaves climatic moisture deficit
Summer (Jun. - Aug.) Hargreaves climatic moisture deficit
Autumn (Sep. - Nov.) Hargreaves climatic moisture deficit
Other Variables

Distance to roads (m)
Vegetation Community Type (categorical)

[1]Source: ClimateWNA (Wang et al. 2012).

Appendix 2.2. Akaike's Information Criterion (AICc) values for a MaxEnt model with differing numbers of variables.

Number of Variables in MaxEnt Model	AICc score
9	3975.36
8	3934.77
7	3933.65
6	3918.85
5	3936.18
4	3944.69
3	3984.79
2	4081.40
1	4084.35

CHAPTER 3. INCORPORATING MULTI-TEMPORAL SPECTRAL INDICES IN AN ITERATIVE SPECIES DISTRIBUTION MODEL FOR AN INVASIVE SPECIES IN A POST-WILDFIRE LANDSCAPE[3]

Introduction

The western United States has experienced an increasing trend in large wildfire frequency in the last 30 years (Westerling et al. 2006, Dennison et al. 2014). Wildland fires are naturally occurring, managed, and prescribed across vast landscapes in the West. However, the introduction of invasive species such as *Bromus tectorum* (cheatgrass) has the potential to alter any of these fire regimes. Wildfires are abiotic ecological processes that may be characterized as a function across ecological gradients. Invasive species such as cheatgrass alter this function, affecting extent, frequency, intensity, or even the seasonality of fire (Freeman et al. 2007). Following disturbance, new sunlight and soil resources become available to seedling establishment in an unoccupied niche (Stohlgren and Binkley 1999). This may be exemplified in sagebrush steppe and ponderosa pine communities of Wyoming. Two inorganic forms of nitrogen, ammonium (NH_4^+; product of combustion) and nitrate (NO_3^-; forms from the ammonium via nitrification) may increase post-fire in soils (Certini 2005). Nitrate typically leaches out in the soils; however the increased ammonium is readily available to plants as it is adsorbed to soil particles, and rapidly growing species such as cheatgrass may take advantage of these resources. In one study, cheatgrass grown in burned soil had higher growth rates, N uptake and more enriched N than individuals grown in unburned soil (Johnson et al. 2010).

In areas where cheatgrass is established and following the winter annual lifecycle, fire frequency and ground fire intensity may be expected to increase because the alien invasive grass creates a new abundance of fine fuel (i.e. standing dry biomass and litter; also referred to

[3] Coauthors: Paul Evangelista, Catherine Jarnevich, Sunil Kumar, Aaron Swallow, Matt Luizza, and Stephen Chignell

as the fuel packing ratio, or the amount of fuel per unit volume of space (Brooks et al. 2004)) during a time of the year that corresponds to wildfire season. This fine fuel also increases the fuel surface-to-volume ratio, which may increase horizontal fuel continuity (Brooks et al. 2004). Litter per acre produced by cheatgrass has been reported from 118 to 293 pounds (Uresk et al. 1979).There has been evidence that *B. tectorum* greatly alters the natural fire cycle in sagebrush ecosystems; 60 to 500 year intervals between fires has become a three to five year interval in some *B. tectorum* dominated ecosystems (Knapp 1996, Chambers and Roundy 2007). Using Moderate Resolution Imaging Spectroradiometer (MODIS) imagery for 2000–2009, Balch et al., 2013 concluded increased fire frequency, size, and duration were associated with cheatgrass cover in the Great Basin ecoregion. Cheatgrass dominated rangelands in these systems were nearly four times more likely to burn than native land cover during the 2000s.

Not only has cheatgrass has been implicated in altering fire regimes, nitrogen cycling, and soil water content, the invasion of this species is also associated with interspecific competition with native grass and forb species, degrading range site productivity, depleting wildlife forage, and diminishing habitat quality. Management of *B. tectorum* is of high importance to both natural areas and agro-ecosystems in the United States, where approximately 22.5 million hectares were affected by this alien invasive in 2005 (Duncan et al. 2004).

Remote Sensing provides a unique tool for detection of invasive plants (*for a review see* Bradley, 2013). Spectral reflectance, transmittance, and absorption of plant leaves for ultraviolet, visible, and near infrared (IR) frequencies have been recognized as useful tools to distinguish vegetation on the landscape since the 1960s (Gates et al. 1965, Myers and Allen 1968, Gausman et al. 1969). Chlorophyll absorbs energy in the blue and red wavelength bands centered around 0.45 and 0.67 μm; therefore, healthy vegetation appears green, and unhealthy vegetation appears yellow as this absorption decreases. In the near IR portion of the spectrum (i.e. 0.7 to 1.3 μm), a healthy plant leaf reflects up to 50 percent of solar energy, with the total

amount reflected greatly dependent on leaf structure. Thus, the near IR band may be used to distinguish specific plant species on the landscape based on leaf structure. For wavelength values greater than 1.3 μm, leaf reflectance is inversely related to total water content of the leaf (Lillesand et al. 2008). Spectral vegetation indices are dimensionless measurements developed from mathematical ratios of these frequencies and require multispectral imagery of the earth's surface. One of the first and most common vegetation indices used is the normalized difference vegetation index (NDVI; Rouse et al., 1974). Since that time, many more useful vegetation indices have been developed to assist in mapping vegetation on the landscape. The Landsat 8 satellite that was launched in 2013 provides multispectral, moderate spatial resolution imagery of the earth's surface at a temporal resolution of 16 days (an 8-day offset from the Landsat 7 satellite), making it an ideal tool for monitoring vegetation on the landscape. The Operational Land Imager (OLI) on the Landsat 8 satellite provides images with nine spectral bands with a spatial resolution of 30 m for bands 1 through 7 and 9, and 15 m for band 8 (i.e. panchromatic band).

Spectral indices provide powerful tools for assessing the current distribution of plant species on the landscape; however, management goals for invasive species may also often center on delineating their suitable habitat for risk assessment. Following Grinnellian niche theory, we can attempt to quantify the suitable habitat for a species on the landscape given constraints in the local environment that allows the population to grow (Hirzel and Le Lay 2008). Topographic covariates are commonly used for delineating the habitat of species or functional groups on the landscape (Franklin 2009). Although climate and soils play a major role in suitable habitat for plant species, these data are rarely available at the fine to moderate spatial scale (e.g. 30 m pixel of a Landsat image) needed for spatial analysis of habitat suitability in regional areas such as a National Forest. Elevation plays a role in macroclimate, wind speed, and solar radiation, among other environmental variables (Rosenberg 1983), and therefore may serve as a proxy for

these constraints on habitat suitability. Digital elevation models can be used to produce other topographic indices that serve as proxies for soil and moisture properties on the landscape including slope, aspect, and compound topographic index among others.

Fires fueled by cheatgrass have historically cost the Great Basin as much as $10 million per year in control (Knapp 1996), therefore it is easily understood that risk assessments of cheatgrass cover are a high priority to land managers. These approaches often begin with a quantification of the entire area invaded to determine management objectives and potential cost of treatment methods, and are complimented by maps of potential suitable habitat based on biogeographical information (Pearson 2007). A cheatgrass population may be spectrally distinct at three stages in its annual lifecycle; the “boot stage” or formation of grass spikelets; the “purple to red stage” and the “brown stage” to senescence. This attribute makes multi-temporal spectral analysis of remotely sensed imagery a powerful tool for estimating cheatgrass cover on the landscape, and several methods have been evaluated. One study reported a 77% overall accuracy using multi-temporal stacking with linear spectral unmixing of Landsat 7 imagery to detect cheatgrass, and a 66% overall accuracy in detection using the difference in NDVI between two Landsat 7 images (i.e. June 26 – April 23) (Singh and Glenn 2009). Another study analyzed cover of cheatgrass from two Landsat 7 ETM+ images using tobit regression, with the final model using MNDVI (i.e. modified NDVI for quadratic modeling; 1- ∆NDVI), late season green band, and elevation as covariates, and reported r = 0.71 with 9% RMSE (Peterson 2005). Phenological indices derived from 1km MODIS satellite imagery were important among a suite of predictors for cheatgrass presence in an ensemble model (Stohlgren et al., 2010), and MODIS was used to relate cheatgrass cover to fire in the Great Basin (Balch et al. 2013). Research has also indicated elevation to be a primary determinant of cheatgrass abundance (Bradley and Mustard 2006, Bromberg et al. 2011, Sherrill and Romme 2012).

Land managers need time- and cost- effective approaches to evaluate risk of invasive species, particularly following disturbance. Our primary objective in this study was to create a highly accurate map of cheatgrass cover in a post-wildfire landscape that could be used by land managers in an environmental impact statement and for targeted aerial herbicide spraying in an area with high topographic heterogeneity. We sought to develop a method using freeling available data to predict the distribution of invasive species accurately in a way that could be easily replicated by land managers across time and space. We also sought to evaluate the added confidence in species distribution model output when a threshold for percent cover is established through a novel iterative approach. Finally, we investigated cheatgrass habitat suitability using topographic covariates and dispersal limitations to evaluate future invasion risk.

Methods

Study Site

Medicine Bow National Forest comprises 561,729 ha of public land in Wyoming, USA. The elevation in this area ranges from approximately 1,005 m to 3,948 m, lending to a broad range of habitat types with dominant lodgepole pine (*Pinus contorta*) forests. Subalpine fir (*Abies lasiocarpa*) and Engelmann spruce (*Picea engelmannii*) may also be found at the highest elevations and a mixture of trees including aspen (*Populus tremuloides*), Douglas fir (*Pseudotsuga menziesii*) and ponderosa pine (*P. ponderosa*) are more common at the mid-elevations. Sagebrush steppe comprised of *Artemesia sp.*, and grasslands dominate the mid- to lower- elevations, and riparian habitats with willows (*Salix sp.*), narrowleaf cottonwood (*Populus angustifolia*), and wetland forbs at the lowest elevations. Mammals in Medicine Bow National Forest serve important ecologic and economic (i.e. game species) roles, including elk (*Cervus canadensis*), mule deer (*Odocoileus hemionus*), pronghorn (*Antilocapra americana*), and moose (*Alces alces*).

The Squirrel Creek wildfire (41.12°N latitude, -106.069°W longitude) began on June 30th, 2012 and was contained within 10 days (http://inciweb.nwcg.gov/incident/2970/; accessed 1/7/2015). This fire burned 4,450 ha of forested and un-forested areas typical of the Medicine Bow National Forest in an area managed primarily for deer and elk crucial winter range, and to a lesser degree dispersed recreation. Burn severity was categorized as low to moderate. The dominant fuels of the Squirrel Creek wildfire were timber (litter and understory), grass, timber grass understory, timber litter, and light logging slash. Cheatgrass populations prior to the burn were estimated to cover 10% of the total Squirrel Creek wildfire area (personal communication).

Initial Field Data Collection

Beginning in May 2014 and ending July 2014, we conducted field surveys in the Squirrel Creek Wildfire post-burn. To ensure we captured the high degree of heterogeneity in topography across the study area without biasing sampling toward roads and trails, we sampled 7.32 m plots (Stohlgren et al., 2010) randomly stratified (Hirzel and Guisan 2002) across North-South transects, spaced 1,000 m apart (n = 184 plots). We recorded cover (as a percent of the total plot from 0 to 100) for five distinct categories in each plot: cheatgrass, other forbs and grasses, shrub and woody, rock, and bare ground. In this study we only considered cheatgrass cover. The decision to place transects 1,000 m apart was based on study area and sampling time constraints, which typifies sampling efforts across a broad range of agencies. To minimize spatial autocorrelation, all samples were taken at a distance greater than 30 m from the next closest sample (i.e. corresponds with the 30 m^2 pixel resolution of a Landsat image).

Data processing

Cheatgrass may germinate at any time of the year. Therefore, in order to avoid confounding spectral absorption and reflection with other ground cover, we compiled Landsat 8 OLI imagery for five months of the growth cycle (i.e. Path 35 Row 31; May – Sept. 2014, which also corresponds to time of field data collection). All images had less than 10% cloud cover for both

study areas. Eight spectral indices were derived from combinations of the blue, green, red, near IR, short-wave infrared 1 and 2 bands in ENVI v.5.1 (Exelis Visual Information Solutions, Boulder, Colorado; Table 3.1).

Table 3.1. Indices derived from Landsat 8 imagery.

Index	Equation
Normalized Difference Vegetation Index (NDVI)	NDVI = ρNIR – ρRed/ ρNIR – ρRed
Soil-Adjusted Vegetation Index (SAVI)	[(ρNIR – ρRed) x (1 + L) / (ρNIR + ρRed+L)]
Enhanced Vegetation Index (EVI)	[(ρNIR – ρRed) / (ρNIR + C1∗ ρRed − C2 ∗ ρBlue + L)[14]
Normalized Difference Water Index (NDWI)	ρGreen – ρNIR / ρGreen + ρRed
Modified Normalized Difference Water Index (MNDWI)	MNDWI = ρGreen – ρSWIR1 / ρGreen + ρSWIR1
Tasseled cap soil brightness (TCAP bright)	weighted composite of six bands into one orthogonal band[5]
Tasseled cap vegetation greenness (TCAP green)	weighted composite of six bands into one orthogonal band[2]
Tasseled cap soil/vegetation wetness (TCAP wet)	weighted composite of six bands into one orthogonal band[2]

We downloaded a 30 m digital elevation model (DEM) collected from the NASA Shuttle Radar Topography Mission (SRTM) that included the Squirrel Creek Wildfire from EarthExplorer (http://earthexplorer.usgs.gov/). From this DEM, we developed seven continuous topographic surfaces in ArcMap v.10.2 (ESRI, Redlands, CA, USA; Table 3.2).

[4] *C1 = atmospheric resistance red correction coefficient, C2 = atmospheric resistance red correction coefficient, L = canopy background brightness correction factor (L = 1)*
[5] *Coefficients from Baig et al. (2014).*

Table 3.2. Indices derived from digital elevation model (DEM).

Index	Equation/description
Elevation	Derived directly from DEM
Slope	Derived from DEM[16]
Aspect	Derived from DEM[1]
SDS	Second derivate of slope[27]
COS	Cosine transformation of aspect[2]
SIN	Sine transformation of aspect[2]
Compound topographic index (CTI)	CTI = (As / (tan (beta)) where As = area value calculated as (flow accumulation + 1) * (pixel area in m2) and beta is the slope expressed in radians)[2]
Heat Load Index (HLI)	Derived through "folding" the aspect so the highest values are SW and lowest values are NE; accounts for steepness of slope[2]
TRASP	Linear transformation of circular aspect; value of 0 for land oriented in a N-NE direction (typically coolest and wettest orientation); value of 1 for S-SW direction (hotter, dryer slopes)[2]

Preliminary Species Distribution Modeling

To develop preliminary current species distribution models for cheatgrass in the Squirrel Creek Wildfire, we executed regression and machine-learning statistical models using the multi-temporal, multispectral indices from Landsat 8 OLI imagery and cheatgrass presence and

[6] *Topographic covariates derived using ArcMap v. 10.2.*
[7] *Geomorphology and Gradient Metrics Toolbox for ArcGIS (Evans et al. 2014).*

absence data in the USGS Software for Assisted Habitat Modeling (SAHM; Morisette et al. 2013). The SAHM program is an open source modeling platform that expedites pre-processing and execution of species distribution models and habitat suitability models. First, we used the Project, Aggregate, Resample, and Clip tool (PARC) module within SAHM to ensure consistency between all remotely sensed and topographic indices. The Covariate Correlation and Model Selection module was then applied to evaluate cross-correlation among all variables and address the issue of multicollinearity (Dormann et al. 2013). When two variables had a Pearson, Spearman, or Kendall correlation coefficient, $|r| \geq 0.70$, only one of the pair was selected for model development, based on percent deviances explained from a univariate GAM with the predictor, relative importance of each variable, and expert knowledge of cheatgrass phenology in the study area. We retained seven variables for model development: May TCAP wet, May SAVI, July TCAP wet, July TCAP bright, August MNDWI, August TCAP wet, and August NDVI.

Using this subset of variables, we fit four species distribution models in SAHM for the Squirrel Creek Wildfire: Boosted Regression Trees (BRT), Random Forest (RF), Generalized Linear Model (GLM), and Multivariate Adaptive Regression Spline (MARS). BRT is a stochastic additive regression model. It combines regression trees, which relate a response (i.e. cheatgrass presence and absence) to a set of predictors (i.e. remotely sensed indices) by recursive binary splits, and boosting which is an adaptive combination of a wide array of simple models to increase predictive performance (De'ath 2007, Elith and Leathwick 2008, Elith et al. 2008). RF is an ensemble decision tree method (similar to BRT) that utilizes a bagging approach, combining a multitude of trees and averaging to produce more accurate classifications (De'ath et al. 2000, Breiman 2001). RF is known to have high classification accuracy and the ability to model complex interactions among predictors, using an array of functions including regressions, classifications, survival analyses, and unsupervised learning.

Generalized Linear Model (GLM) is a generalized ordinary linear regression approach that specifies a relationship between the mean of a random variable and a function of the linear combination of predictors (McCullagh and Nelder 1989, Hijmans and Elith 2013). MARS is a non-parametric regression technique that automatically models non-linearity and interactions among variables (Friedman 1991, Friedman and Roosen 1995). The recursive partitioning of MARS makes it capable of fitting complex, non-linear relationships between species and predictors. The GLM, MARS, and RF models were left at default settings. The BRT model was optimized through testing learning rate values between 0.0005 and 0.01 and tree complexity values between one and five (Elith and Leathwick 2008). For model fitting, we partitioned the cheatgrass occurrence data into training and test subset and employed ten-fold cross validation, in which a different 90% of the data were used to train the models and 10% of the data were used to test the models for each of ten runs. It is important to note here that we had two primary objectives in developing the preliminary models; (1) to prioritize areas for additional sampling to test model results, and (2) as a basis for developing a threshold for percent cheatgrass cover necessary for detection at the $30m^2$ spatial resolution of Landsat 8 imagery. The Landsat 8 scenes available at the time of preliminary model development were for May, July and August months.

Threshold Development

The four preliminary models (i.e. BRT, RF, GLM, and MARS) were based on presence and absence rather than percent cover measurements recorded from the sampling plots. To determine a threshold for percent cover necessary to distinguish the spectral reflection and absorption of cheatgrass from other vegetation, we first extracted values from the probability surface produced by the RF preliminary model in Squirrel Creek Wildfire at locations where the independent test data were collected (n = 81). Next, we used a simple linear regression to evaluate how well this model predicted percent cheatgrass cover from these locations.

Final Species Distribution Modeling

We ran the four SDMs (i.e. BRT, RF, GLM, and MARS) with cheatgrass presence defined as plots with cover greater than or equal to the threshold. In these models, absence was defined as any cover below the threshold. At this time, we also added June and September indices derived from Landsat 8 OLI imagery (i.e. these images were not available during preliminary model development). After covariate correlation analysis we retained 11 variables: May NDWI, June TCAP bright, June TCAP green, July TCAP green, July TCAP wet, July TCAP bright, August TCAP wet, August MNDWI, August NDWI, September TCAP bright, and September MNDWI. Once again, we calculated a simple linear regression using the independent test data and predicted probability values to evaluate how well the model predicted cheatgrass cover, and how much model fit improved using the threshold.

Secondary Field Data Collection and Independent Test of the Final Models

To test the final models, we collected an independent set of random points in the Squirrel Creek Wildfire. One of the outputs from SAHM is a geospatial probability surface for each model (i.e. a grid with cell values between 0 and 1, where 0 = no probability of species occurrence and 1 = 100% probability of species occurrence). We discretized the probability surfaces for each of the four final models (i.e. BRT, RF, GLM, and MARS) using the threshold where sensitivity equals specificity to assign a binary value of cheatgrass present or cheatgrass absent, and then combined them into a frequency histogram ensemble (i.e. shows the number of models forecasting cheatgrass presence at any pixel on the map) using raster calculator in ArcMap v.10.2 (Crall et al., 2013; Stohlgren et al., 2010). We generated random points within this ensemble raster based on the multivariate environmental similarity surface (MESS) maps produced by SAHM. The MESS maps indicate areas where the models are forecasting into novel conditions (i.e. those not observed in the training data, thus sampling these areas will add new information to the models). Additionally, we added random points in areas where only one

or two of the models agreed on cheatgrass presence. We surveyed these random points using the same 7.32 m plots used in the transect surveys in September 2014 (n = 81).

Habitat Suitability Modeling Analysis

To evaluate habitat suitability for cheatgrass in the Squirrel Creek Wildfire we incorporated topographic covariates in the models as predictors rather than remotely sensed indices used for mapping distribution. These included elevation, slope, aspect, second derivative of slope (SDS), cosine (COS), and sine (SIN) transformations of aspect, compound topographic index (CTI), heat load index (HLI), and a linear transformation of aspect (TRASP; Table 3.2). Six of these variables were retained after covariate correlation analysis: elevation, slope, second derivative of slope, COS, CTI, and HLI. These variables were used to fit the four SDMs (i.e. BRT, RF, GLM, and MARS) in SAHM. Risk of invasion for species such as cheatgrass intuitively depends on propagule pressure and seed dispersal. To account for this, we developed a geospatial buffer in ArcMap v.10.2 around the final RF model of current cheatgrass distribution based on the maximum distance that cheatgrass seeds may disperse via wind in areas following fire (i.e. 2.13 m; Monty et al. 2013). We then overlaid the ensemble map with the dispersal layer and delineated locations where dispersal was probable and the ensemble map had a value > 0 to quantify the area at highest risk for cheatgrass invasion in the Squirrel Creek Wildfire in the near future.

Evaluation of model performance

To evaluate model performance, we used four accuracy measures: test area under the receiver operating characteristic curve (AUC), sensitivity, specificity, and true skill statistic. Test area under the receiver operating characteristic curve (AUC; Swets, 1988) is a commonly used metric in evaluation of species distribution models fit to true presence and absence data. This metric measures the ability of model predictions to discriminate between observed presence and absence for the test data (i.e. the data held aside in the ten-fold cross validation split),

regardless of the absolute value of the predictions (Fielding and Bell 1997, Elith and Graham 2009). An AUC value of 0.5 shows that model predictions are not better than random; less than 0.5 are worse than random; 0.5–0.7 indicates poor performance; 0.7–0.9 reasonable/moderate performance; and .0.9, high performance (Peterson et al. 2011). Sensitivity measures the percentage of presences correctly classified. Specificity measures the percentage of absences correctly classified. The true skill statistic (TSS = sensitivity + specificity – 1) places more weight on model sensitivity than specificity, with values ranging between -1 and 1 (Allouche et al. 2006). Values above zero indicate better model performance than chance alone. This accuracy measure is less sensitive to changes in prevalence (ratio of presence to absence data) within the model than other commonly used accuracy measures such as Cohen's Kappa (Allouche et al. 2006).

Results

Evaluation of the four preliminary cheatgrass distribution models (i.e. BRT, RF, GLM, and MARS) developed with transect data (i.e. cheatgrass presence and absence, where ≥1% cheatgrass cover is present) revealed moderate performance across models (Table 3.3).

Table 3.3. Evaluation of preliminary cheatgrass distribution model performance.

	Preliminary Models			
Model[8]	AUC[9] (±SD)	Sensitivity (±SD)	Specificity (±SD)	TSS[10] (±SD)
BRT	0.76 ± 0.10	0.68 ± 0.11	0.69 ± 0.13	0.37 ± 0.14
RF	0.81 ± 0.09	0.80 ± 0.07	0.63 ± 0.18	0.44 ± 0.18
GLM	0.74 ± 0.08	0.72 ± 0.11	0.71 ± 0.11	0.43 ± 0.15
MARS	0.76 ± 0.10	0.80 ± 0.14	0.70 ± 0.09	0.50 ± 0.15

Cross-validation AUC values ranged between 0.76 and 0.81 for the four models. The simple linear regression we developed using probability values from RF and cheatgrass cover from the

[8] *Models included Boosted Regression Tree (BRT), Random Forest (RF), Generalized Linear Model (GLM), and Multivariate Adaptive Regression Spline (MARS).*
[9] *AUC represents the area under the receiver operating characteristic curve.*
[10] *TSS represents True Skill Statistic.*

independent data indicated that the model would be improved by setting a threshold (R^2 = 0.36; Figure 3.1).

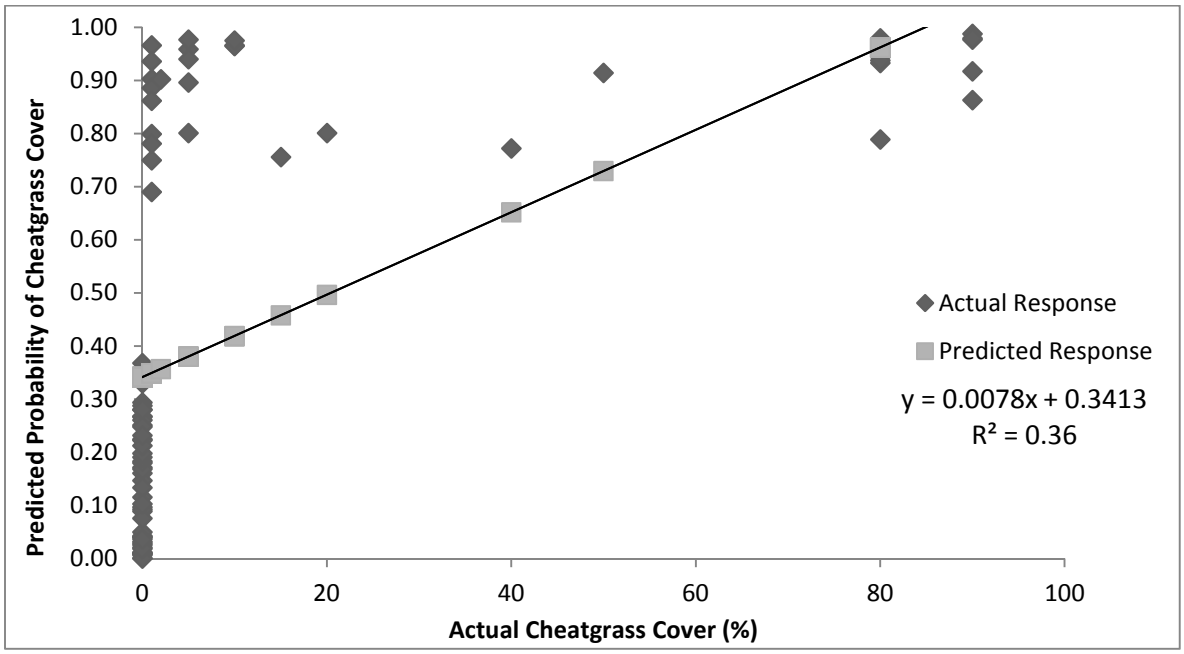

Figure 3.1. Simple regression analysis of test data applied to the preliminary Random Forest Model (i.e. model developed using field plots with ≥ 1% cheatgrass cover).

We chose a 40% threshold for cheatgrass cover to be considered a "presence" based on the simple regression model in concert with the minimum amount assumed detectable by the Landsat 8 OLI sensor and with the management objectives (personal communication).

Evaluation of the four final cheatgrass distribution models (i.e. BRT, RF, GLM, and MARS) developed with transect data (i.e. cheatgrass presence and absence, where ≥40% cheatgrass cover is present) revealed moderate performance across models (Table 3.4).

Table 3.4. Evaluation of final cheatgrass distribution model performance.

	Final Models with Threshold			
Model[11]	AUC[12]	Sensitivity	Specificity	TSS[13]
BRT	0.87 ± 0.11	0.79 ± 0.18	0.81 ± 0.14	0.60 ± 0.29
RF	0.86 ± 0.12	0.54 ± 0.24	0.92 ± 0.10	0.46 ± 0.27
GLM	0.88 ± 0.09	0.76 ± 0.21	0.79 ± 0.11	0.55 ± 0.27
MARS	0.87 ± 0.10	0.72 ± 0.15	0.82 ± 0.16	0.54 ± 0.26

Cross-validation AUC values ranged between 0.86 and 0.88 for the four models. The simple linear regression we developed using probability values from RF and cheatgrass cover from the independent data indicated that the model was greatly improved from setting a 40% threshold as we expected (R^2 = 0.92; Figure 3.2).

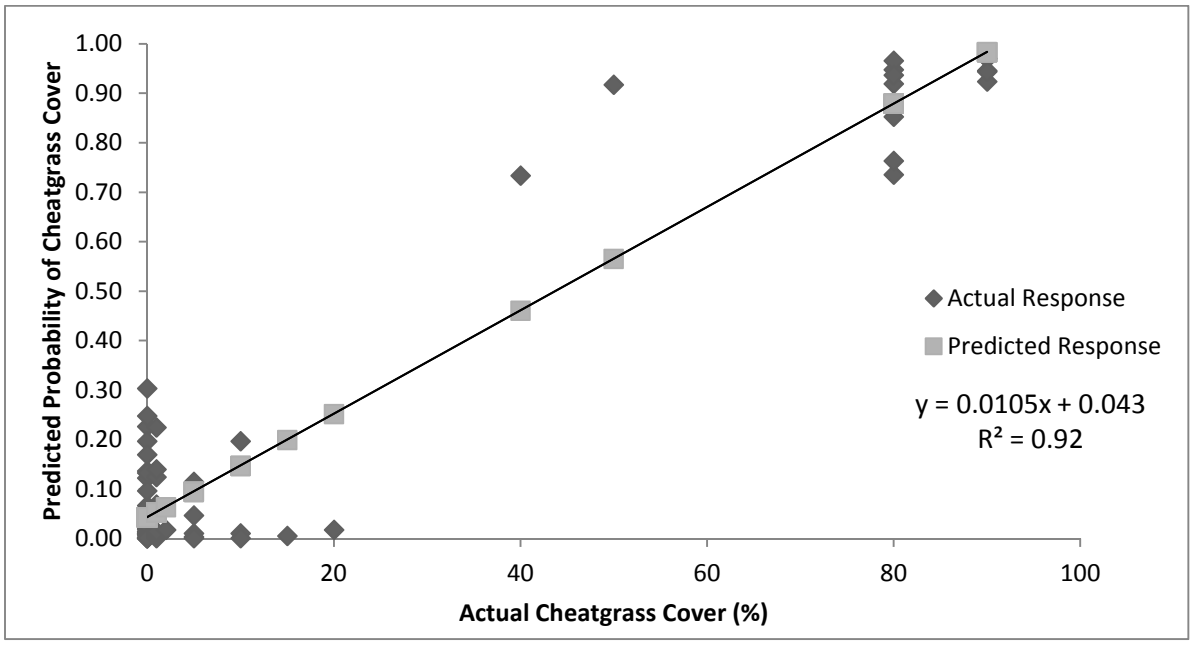

Figure 3.2. Simple regression analysis of test data applied to the final Random Forest Model (i.e. model developed using field plots with ≥ 40% cheatgrass cover).

[11] *Models included Boosted Regression Tree (BRT), Random Forest (RF), Generalized Linear Model (GLM), and Multivariate Adaptive Regression Spline (MARS).*
[12] *AUC represents the area under the receiver operating characteristic curve.*
[13] *TSS represents True Skill Statistic.*

When the four models were applied to the independent test dataset, the AUC values indicated excellent performance, ranging between 0.95 and 0.97 (Table 3.5).

Table 3.5. Evaluation of final cheatgrass distribution model performance based on independent test data.

	Final Models Applied to Independent Data			
Model[14]	AUC[15]	Sensitivity	Specificity	TSS[16]
BRT	0.95	0.87	0.84	0.7
RF	0.95	0.93	0.88	0.81
GLM	0.95	0.87	0.86	0.73
MARS	0.97	0.93	0.91	0.85

In the Squirrel Creek Wildfire, 18.16 km^2 are currently invaded by cheatgrass based on the threshold to discretize the predicted probabilities where sensitivity equals specificity (i.e. 0.49) for the best model, RF (Figure 3.3).

[14] *Models included Boosted Regression Tree (BRT), Random Forest (RF), Generalized Linear Model (GLM), and Multivariate Adaptive Regression Spline (MARS).*
[15] *AUC represents the area under the receiver operating characteristic curve.*
[16] *TSS represents True Skill Statistic.*

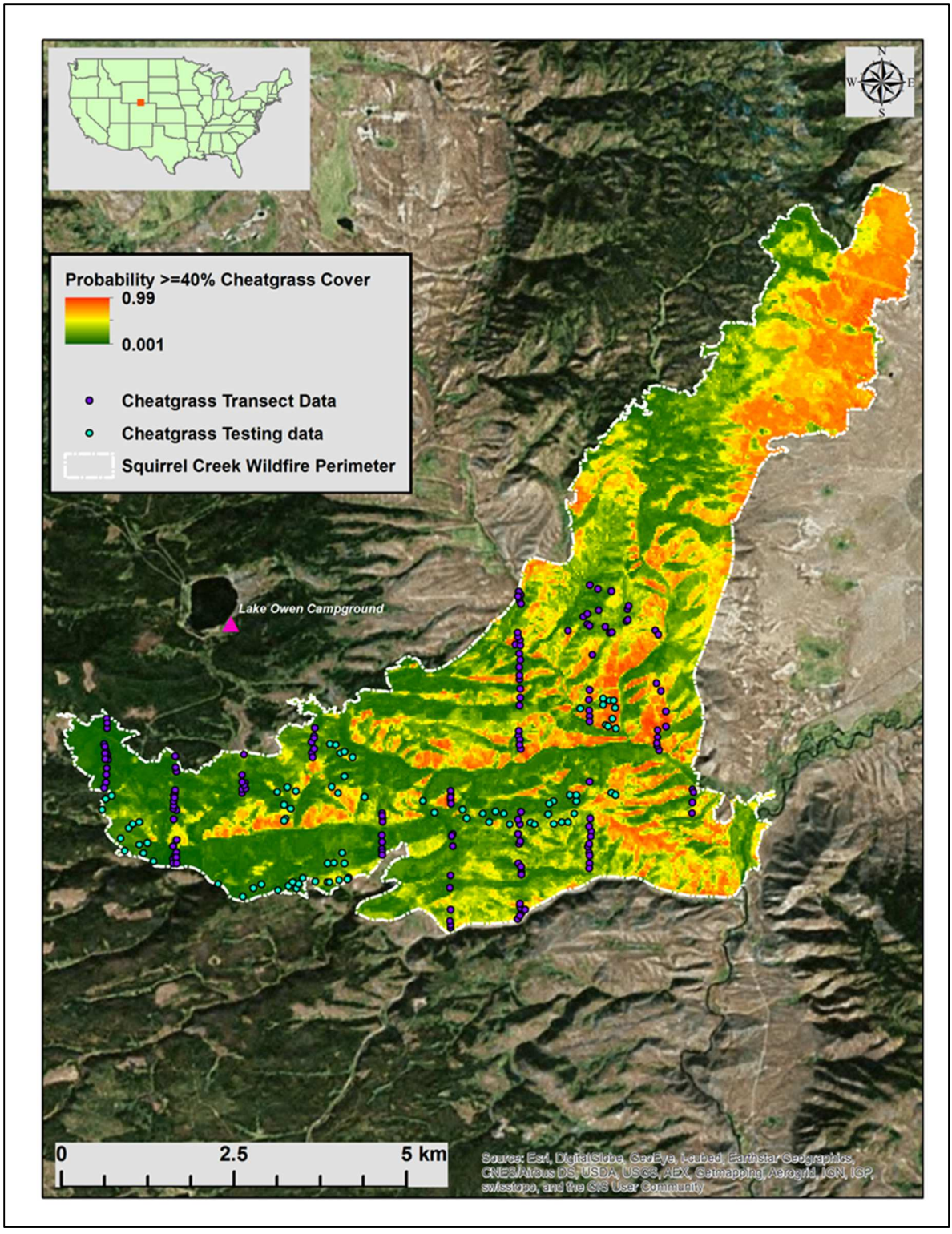

Figure 3.3. Probability of cheatgrass cover ≥ 40% in the Squirrel Creek Wildfire post-burn area based on transect data (purple dots). Test data (blue dots) were collected for model evaluation. Note the northern section of the study area was not sampled due to inaccessibility.

We chose RF as the best model based on evaluation statistics and ecoplausability (i.e. the final output probability map that makes the most ecological sense based on field observation).

September TCAP bright was the most important variable across models. The RF model retained all predictors (Table 3.6).

Table 3.6. Relative importance of final predictors in final Random Forest model for cheatgrass in the Squirrel Creek Wildfire.

Variable	Mean Decrease Accuracy[17]	Mean Decrease Gini[18]
September TCAP bright	31.47	8.31
June TCAP bright	19.16	4.87
June TCAP green	15.36	3.81
August TCAP wet	13.60	3.42
September MNDWI	12.30	2.92
July TCAP green	10.94	2.65
May NDWI	10.90	3.55
July wet	8.66	2.85
July bright	8.02	2.74
August MNDWI	7.40	2.40
August NDWI	7.27	2.70

The BRT model retained September TCAP bright (87.5% relative influence) and June TCAP bright (12.5% relative influence), agreeing with the top two predictors in the RF model. The GLM model retained September TCAP bright, August TCAP wet, September MNDWI, and August NDWI (listed in order of decreasing relative importance). The MARS model retained September TCAP bright, June TCAP bright, September MNDWI, and July TCAP wet (listed in order of decreasing relative importance).

[17] *Mean decrease in accuracy is a measure of how much inclusion of this predictor in the model reduces classification error.*

[18] *Mean decrease in Gini is a sum of the decreases for each individual variable over all trees in the forest (Breiman 2001). For descriptions of variables refer to Table 3.1.*

Based on topography, areas with at least 40% current cheatgrass cover, and potential seed dispersal via wind, the total suitable habitat for cheatgrass in the Squirrel Creek Wildfire for the near future is 42.72 km^2 (Figure 3.4).

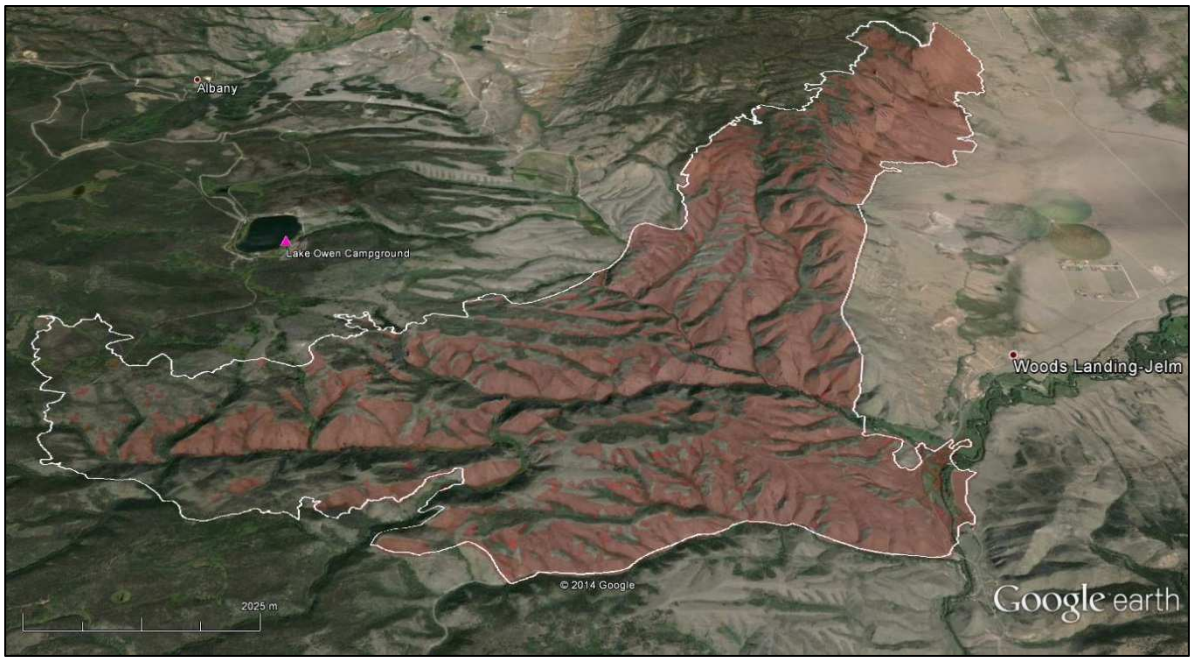

Figure 3.4. Suitable habitat for cheatgrass in the Squirrel Creek wildfire post-burn area, Wyoming based on current distribution, topography, and potential for wind-dispersal of seeds. Ensemble model results (red) is overlaid on a Landsat image (9/12/2014) in Google Earth.

We overlaid ensemble model results in Google Earth to assess how well the model distinguished areas with dense forest cover (i.e. cheatgrass does not grow in a monoculture in areas with dense tree canopy; Upadhyaya 1986), and we were satisfied with the results. We also evaluated a soils layer provided by the US Forest Service to include in the habitat suitability model; however, there was no correlation between soil texture and cheatgrass presence or absence. There were three taxonomic classes where cheatgrass was recorded present; gravelly sandy loam to very gravelly sandy loam and very cobbly loam. The topographic covariates we incorporated in model development stand as proxies for water collection and soil attributes on

the landscape (Moore et al. 1993, Yang et al. 2006). The two most important topographic covariates across models were elevation and COS (cosine transformation of aspect).

Discussion

Spectral indices that incorporate different combinations of bands 2-7 from Landsat 8 over the entire growing season for cheatgrass produced four highly accurate species distribution models in a post-wildfire landscape, and the RF model stood out among these models as the best fit based on our familiarity with the study area and evaluation metrics. Further, all four models suggest these methods work well when relatively small amounts of data are available (i.e. n = 44 with presence defined as ≥ 40% cheatgrass cover). The evaluation statistics for the models applied to a new independent test dataset and new monthly indices confirm not only that these models are robust when fit to remotely sensed indices matching time of field data collection, but also that they may be improved through an iterative approach as new location data and predictor variables become available.

Species occurrence is observably distinct from species cover or abundance on the landscape (Brown 2007). In the case of invasive species, eradication can be an unattainable management target (Rejmánek and Pitcairn 2002), therefore setting a threshold for cover is common practice to maximize treatment efficacy and minimize off-target effects (i.e. herbicide treatment; (Mealor et al. 2013). The threshold we developed in this study not only ensures that the spectral reflection and absorption of cheatgrass is distinguished from surrounding vegetation and land cover, it also adheres to a potential management regime (e.g., areas with greater than 40% cheatgrass cover prioritized for control).

Using Landsat 8 images that corresponded to the dates of field survey collection increases our confidence in the results for the Squirrel Creek Wildfire. As an annual invasive species which is highly dependent on seasonal moisture availability, cheatgrass populations may experience strong year-to-year fluctuations in abundance. Fortunately, the 16-day temporal resolution of

Landsat imagery and quick availability (i.e. images are typically available at EarthExplorer 24 hours post-collection) makes coupling these data with the time of field data collection highly efficient. In addition to the independent data assessments, personal observations also contributed to our confidence in the models. The northernmost section of the Squirrel Creek Wildfire was largely inaccessible due to time constraints; however, personal field observations during the time of year that corresponds to the "red stage" of cheatgrass, when it is easily distinguishable from other vegetation on the landscape, indicated cheatgrass presence in areas predicted by the model.

The variables that contributed most to the Random Forest model are evidence that combinations of Landsat 8 TM bands other than NDVI are important when evaluating the distribution of cheatgrass in post-disturbance areas; particularly indices that account for soil background. These included soil brightness (TCAP bright), vegetation greenness (TCAP green), and soil/vegetation wetness (TCAP wet) which are weighted composites of six Landsat bands into three orthogonal bands (Crist and Cicone 1984). Modified Normalized Difference Water Index (MNDWI) was introduced by Xu (2006) to improve the accuracy of Normalized Difference Water Index (NDWI) in built-up land areas and suppress soil and vegetation noise.

Cheatgrass is listed as a noxious weed in Albany County, WY, where the Squirrel Creek Wildfire occurred. The current distribution map we developed from the Random Forest model creates a robust tool for land managers to develop management plans for cheatgrass in this area. The probability surface from this model is georeferenced, therefore in the case of targeted aerial herbicide spraying a land manager may enter this information into a helicopter global positioning system (GPS). Additionally, the potential habitat suitability model provides a forecast of areas that may be monitored for cheatgrass invasion in future seasons. In the habitat suitability model, we assumed wind to be the primary mode of cheatgrass seed dispersal in the Squirrel Creek Wildfire. However, cheatgrass seeds have long awns that stick to animal fur, hiking boots, and

tires which are other potential mechanisms for long-distance dispersal that were not considered in our risk model (Banks and Baker, 2011; Mack, 1981).

The habitat suitability model agreed with prior studies correlating cheatgrass occurrence to elevation (Bromberg et al. 2011, Banks and Baker 2011, Sherrill and Romme 2012). We find it interesting that COS (cosine transformation of aspect) was also important across all four models. To our knowledge, this variable has not been correlated with cheatgrass distribution in existing research. The COS values range from -1 (at due south) to 1 (at due north) and account for interactions with slope (Stage 1976, Evans et al. 2014). We discovered habitat suitability for cheatgrass decreases with increasing COS values; these values ranged between -0.8 (i.e. 90% probability of cheatgrass occurrence) and 0.5 (i.e. 30% probability of cheatgrass occurrence) in the Squirrel Creek Wildfire.

Cheatgrass was documented as covering 10% of the Squirrel Creek Wildfire prior to the fire. However, with the current abundance of this invasive species and potential risk, up to 40% of the total post-disturbance area is suitable habitat for cheatgrass. This risk may have both societal and cascading ecosystem effects. There are several ranching families in the area that recognize cheatgrass as an aggressive plant that poses not only a threat to important grazing land for cattle, but a potential link to mule deer decline they have observed in recent years (personal communication). When there are large cheatgrass monocultures such as the ones observed in the Squirrel Creek Wildfire, elk rely more on dead forage with lower nutritional quality (Kohl et al. 2012) and mule deer might behave similarly. Other wildlife populations may experience habitat loss due to the conversion of these habitats from perennial- to annual – dominated communities, including greater sage grouse, Gunnison sage grouse, pygmy rabbits, and rodents (Duncan et al. 2004, Pyke 2011). Finally, leaving cheatgrass unmanaged in either study area is likely to increase risk of future fire, as cheatgrass dominated areas create a more continuous fuel source than sagebrush cover (Brooks et al. 2004). In a field study 90 km south

of the Squirrel Creek Wildfire, previously burned areas of Rocky Mountain National Park, Colorado had four to five- times greater cover and mean patch area of cheatgrass than unburned areas (Banks and Baker 2011). Leafy spurge (*Euphorbia esula*), various thistles (*Carduus* and *Cirsium sp.*), knapweed (*Centaurea sp.*), and toadflax (*Linaria sp.*) are examples of other exotic species of concern in the Medicine Bow National Forest that may be evaluated using this methodology. The methods we employed are easily transferable to other landscapes and species, and the remotely sensed data and modeling tools we used are feely available, making this a powerful tool in environmental impact assessments and developing future management plans.

Conclusions

Multi-temporal spectral indices from freely available Landsat 8 imagery are powerful tools in evaluating cheatgrass cover in post-wildfire landscapes. Employing spectral indices beyond the commonly used NDVI such as TCAP brightness, greenness, and wetness, and MNDWI can aid in distinguishing foliar cover from soil background in these areas. As evidenced by our study, applying an iterative approach when employing these indices in species distribution models strengthens their power, especially when a threshold for foliar cover is established. The RF and BRT models preformed especially well in this study compared to the MARS and GLM models, and the current distribution map of cheatgrass cover ≥ 40% produced from the RF model closely followed our observations in the Squirrel Creek Wildfire. Topographic indices and dispersal limitations can be used to augment spectral indices and create habitat suitability models for invasive plant species such as cheatgrass. The maps produced from these models are georeferenced and provide valuable tools for natural resource management.

CHAPTER 4. DECADAL CLIMATE AVERAGES AND TOPOGRAPHIC ROUGHNESS FORECAST LARGE WILDFIRES IN COLORADO AND WYOMING, USA[19]

Introduction

Taken in aggregate, the western United States (hereafter the West), has experienced an increasing trend in large wildfire frequency in the last 30 years (Westerling et al. 2006, Dennison et al. 2014). Globally, an increase in large wildfires has been observed in recent decades, resulting in major environmental, economic, and human losses (Pechony and Shindell, 2010; UNFAO 2010). Understanding the drivers and potential distribution of large wildfire risk in the future is imperative to ecosystem management and human development.

The reconstructed history of wildfires in the West is complex; their frequency follows climate trends and human development (e.g., suppression and ignition). For the past 6000 years, fire regimes in subalpine forests of Colorado have been indirectly impacted by changing vegetation and climate (Higuera et al. 2014). Often referred to as the "Medieval Warm Period", an elevated period of aridity with peaks between ca. 900 to 1300 parallels the megadrought epoch in the West with frequent wildfires (Cook et al. 2004, 2015). Based on dendrochronological analysis of fire scars in the interior West, Trouet et al. (2010) found that in the 1400s, much of the West remained impacted by extreme drought, and that overall fire activity remained high during this time period. There was a decline in fire frequency in the West in the late 16th century that corresponds to declining temperatures of the "Little Ice Age" (ca. 1500 to 1800; (Trouet et al. 2010)). These periods of declining temperatures result in fuel accumulation increases (Schoennagel et al. 2004, Littell et al. 2009).

Low to mid-elevation ponderosa pine (*Pinus ponderosa*) and mixed conifer subalpine forests in the West experienced frequent, low-severity wildfires prior to the 20th century that played

[19] Coauthors: Sunil Kumar and Catherine Jarnevich

important ecological roles in community structure, diversity, productivity, biogeochemical processes, hydrology, and wildlife habitat (Brown and Shepperd 2001, Kaufmann et al. 2007). Additionally, American Indians used fire to clear land. By the late 19th century, European settlement in the West brought more extensive land clearing through fire, logging, and livestock grazing that altered existing wildfire regimes, particularly in the low to mid-elevation forests. In the year 1891, the United States Federal Forest Service (USFS) was established and forest fires were increasingly suppressed, with the Clarke-McNary Act in 1924 effectively creating a national fire exclusion policy (Stephens 2005). This exclusion policy increased fuel loads in the ponderosa and mixed-conifer forests, but was likely suited to lodgepole pine forests that are adapted to high-severity crown fires with low frequency (Stephens 2005). Average annual area burned in the West continued to decrease through the 1960s (Brown et al. 2004), but incidence large wildfires (>400 ha) began rapidly increasing in the mid-1980s (Westerling et al. 2006). Additionally, burn time began increasing from an average of one week in the 1970s to five weeks in the 1980s. Efforts have been made in more recent decades to use wildfires in forest management and restoration (i.e. the federal fire policy of 1995 recognized wildfire as a critical ecosystem process and in 2002 the USA National Fire Plan resulted in 1 million ha of thinning and prescribed fire across federal land; Schoennagel et al., 2004). The extent of USFS area burned increased significantly across the West from 1940 to 2000 with the exception of California (Stephens 2005).

The impacts from historical wildfire management in the West were compounded in the last decade by severe regional drought. Trends in increasing large wildfire occurrence in the West from the years 1984-2011 correspond to trends in increasing drought severity (Dennison et al. 2014). Wildfires even enhance drought through the absorption of solar radiation by smoke particles, as seen in a simulation of radiative forcing and atmospheric response in the mid-latitudes of the USA (Liu 2005). Annual wildland fire-suppression costs for the years 2004 –

2014 increased by approximately 1.9 times the costs for the previous decade (i.e. $16,877,035,000 USD for 2004 – 2014 and $8,918,124,000 for 1993 – 2003, respectively) and equaled more than the combined total cost for the previous 18 years (Figure 4.1). The trend in total acres burned in the USA follows a similar pattern (i.e. 76,578,801 for 2004 – 2014 and 70,234,744 for 1985 – 2003; Figure 4.1).

Figure 4.1. Federal Firefighting Suppression Costs, USA years 1985-2014[20]

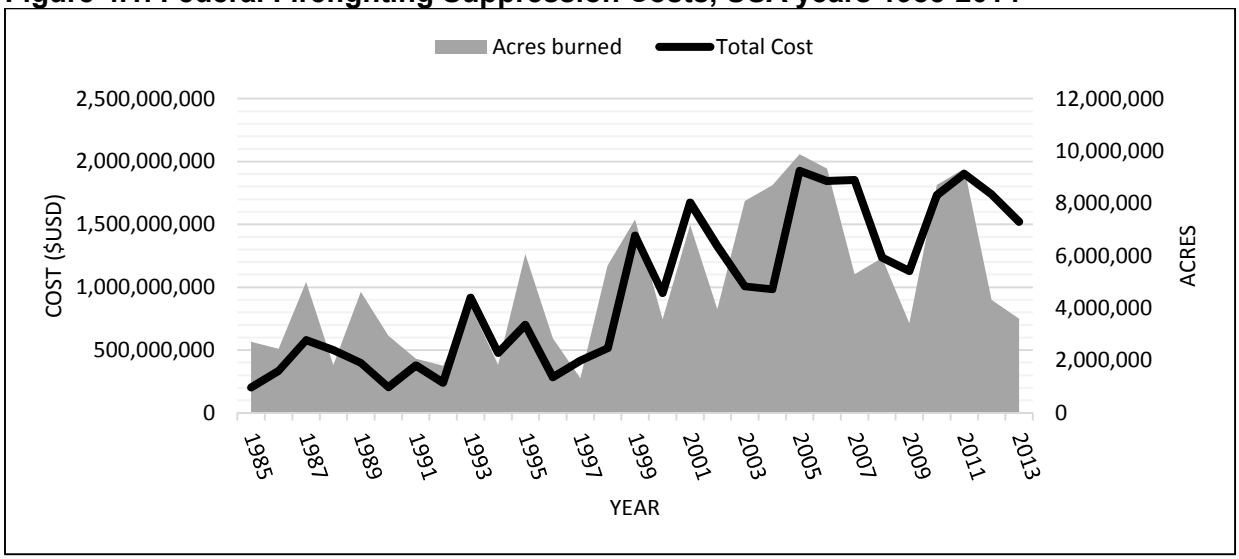

Increases in natural area use, development, and area distinguished as wildland-urban interface (WUI; Theobald and Romme, 2007)) are factors that will continue to alter area burned and cost of suppression for wildfires in the West; however, climatic conditions are also a driving force in large wildfires (Brown et al. 2004, Westerling et al. 2006, Littell et al. 2009, Liu et al. 2010, Trouet et al. 2010, Barbero et al. 2014, Dennison et al. 2014, Wing and Long 2015), and the climate can mute or amplify anthropogenic effects (Swetnam and Betancourt 2010). In some instances, these two factors may be coupled, such as alterations in fuel load quantity increasing forest sensitivity to climate variability (Westerling et al. 2006).

[20] *Acres include private, state, and Federal lands; cost does not include inflation. Created by A. West; data from National Interagency Fire Center; http://www.nifc.gov/fireInfo/fireInfo_statistics.html.*

The influence of climate on wildfire varies across spatial and temporal scales. After analyzing large wildfires (> 400 ha) in Oregon and Washington, USA, Wing and Long (2015) did not find a significant correlation between fire occurrence and size with monthly climate variables; however, they discovered evidence of correlation between fire severity and monthly climate. Dennison et al. (2014) used primarily seasonal climate variables including temperature, precipitation, and Palmer Drought Severity Index matched with year of fire in quantile regression to analyze trends in wildfire activity by ecoregion in the West from the years 1984-2001, and found ecoregions with the largest increases in fire activity trended toward hotter, dryer conditions relative to ecoregions not experiencing significant changes in these variables. Westerling et al. (2006) concluded that in mid-elevation ecosystems in the Northern Rockies, historical wildfires were strongly associated with increased spring and summer temperatures and an earlier spring snowmelt, but not land use.

Beginning with large scale industrialization in the mid-1800s, the human contribution to greenhouse gases in the atmosphere accelerated rapidly, trapping heat in the earth's atmosphere and altering the climate. Since the 1980s there have been significant snowpack declines along the entire Rocky Mountain range due to warmer spring temperatures (Pederson et al. 2013). Stewart et al. (2005) analyzed data from streamflow gauges throughout the West for the period 1948 – 2002, and the onset of snowmelt and streamflow occurred one to four weeks earlier at the end of the study period compared to the beginning. Average temperatures in some areas of the West increased as much as 1.1 ˚C between 2000 and 2006 (Hoerling and Eischeid, 2007). These rapid changes will certainly have implications wildfire season length. Westerling et al. (2006) reported the large wildfire (> 400 ha) season length (i.e. the time period between the first wildfire discovery date and the last wildfire control date) in the West increased by 78 days for the period 1987 to 2003 compared to 1970 to 1986.

Efforts are underway to forecast the likely effects of ongoing climate change on the frequency of wildfires, fire severity, and the total area burned in a given year. In one analysis, the relative probability for very large wildfires (i.e. > 20,234 ha) increases by at least 30% for the West across 14 different global circulation models (Stavros et al. 2014). Liu et al. (2010) projected fire potential will increase overall from low to moderate in the United States under future climates (i.e. 2070-2100). Although the current drought in the West has not extended over hundreds of years like the megadrought during the Medieval warming period, a business-as-usual future climate model (i.e. the Parallel Climate Model) indicated changing relative humidity and drying in the West through the year 2089 when compared to the 1975-1996 base period (Brown et al. 2004). Based on historical drought reconstruction, Cook et al. (2015) reported future drought risk will likely exceed the Medieval megadrought over the Central Plains and Southwest during the late 21st century based on two different Coupled Model Intercomparison Project Phase 5 (CMIP5) emissions scenarios from 17 Global Circulation Models (GCMs). This will have profound impacts on large wildfire occurrence, wildfire-drought feedbacks, vegetation community structure, wildlife habitat, natural resource management, biogeochemical cycling, hydrology, human life and property loss, and wildfire suppression costs. Additional tools are needed to evaluate areas most at risk for large wildfires in the future.

In this study, we evaluated the applicability of three niche modeling techniques to forecasting the likely extent and spatial distribution of wildfires in the West as climate change continues through the mid-21st century. Niche modeling (also referred to as species distribution modeling or habitat suitability modeling) relates the presence of a species to its environment in geographic space (Araújo and Peterson, 2012; Evangelista et al., 2013, 2008; Flory et al., 2012; Hijmans and Graham, 2006; Jarnevich and Stohlgren, 2008; Kumar et al., 2014; West et al., 2015). Similar to a species, a wildfire can be viewed as having a niche in environmental and geographic space. Although wildfires are typically ignited by lightning or anthropogenic sources,

suitable environmental conditions must also exist for fires to persist (Swetnam and Betancourt 2010). Therefore, methods such as MaxEnt (Phillips et al. 2006, Parisien and Moritz 2009, Parisien et al. 2012, Paritsis et al. 2013, Peters et al. 2013, Arnold et al. 2014, Arpaci et al. 2014), generalized linear models (GLM; (Syphard et al. 2008, Stan et al. 2014, Stavros et al. 2014, Bistinas et al. 2014)), and multivariate adaptive regression splines (MARS; (Balshi et al. 2009, Boulanger et al. 2014)) have been used to develop relationships between wildfire occurrence and environmental covariates. We compared these three methods for large wildfire environmental suitability models in Colorado and Wyoming, USA.

Our primary hypothesis was that the environmental suitability for large wildfires in these states can be forecasted using decadal climate averages in combination with topography. Our primary objective was to use the best environmental suitability model to forecast areas in Colorado and Wyoming most at risk for large wildfires given future potential climates.

Methods

Study Area

Our study area encompassed the states Colorado and Wyoming, USA, an area approximately 520,000 km^2 between 35º N to 45º N and 100º W to 115º W with elevation from 945 to 4,401 meters (Figure 4.2). The Continental Divide runs through both states.

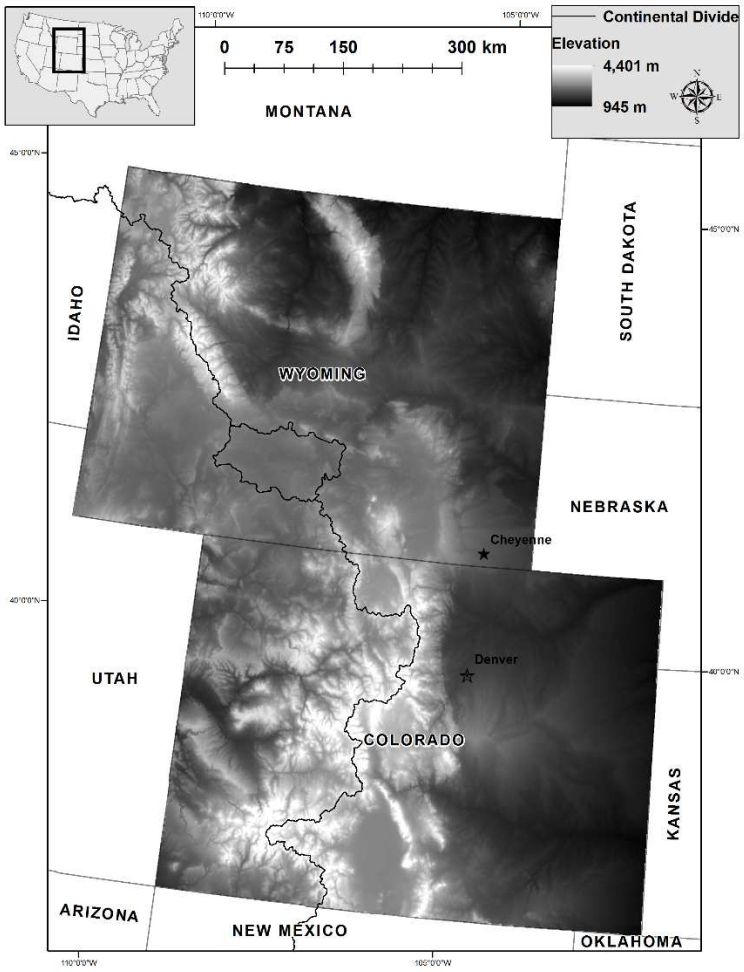

Figure 4.2. Study area including Colorado and Wyoming, USA.

The wide variation in elevation and topography across the study area makes it difficult to divide the states into homogenous climatological areas (Western Regional Climate Center; www.wrcc.dri.edu). The states are bisected by the Rocky Mountains running in a roughly north to south direction; therefore, air masses from the Pacific Ocean are largely blocked resulting in considerably more winter moisture on the western slopes. East of the Rocky Mountains, most precipitation comes in spring and summer. The landscape heterogeneity is well represented by the diversity of ecosystems in the study area; there are 35 and 39 level IV ecoregions in Colorado and Wyoming, respectively (Environmental Protection Agency; www.epa.gov/wed/pages/ecoregions). Examples of these ecoregions range from the alpine

zone along mountain peaks to lush subalpine forests, shrublands, volcanic plateaus, grasslands, and shale deserts.

Wildfire occurrence Data

Using burned area boundaries mapped from satellite remote sensing data (i.e. normalized difference burn ratio from Landsat imagery), we created polygons of wildfire occurrence for the years 1991-2000 and 2001-2010 for the study area (n = 149 and 240, respectively; data source: Monitoring Trends in Burn Severity [MTBS] website (http://www.mtbs.gov/) using ArcGIS v.10.2 [ESRI; Redlands, CA, USA]) These wildfires were greater than or equal to 400 ha and categorized as wildfire, wildland fire use, or unknown on both public and private lands in the MTBS query builder (i.e. we did not incorporate prescribed fire). In ArcMap, we generated random points within these polygons that were at least one kilometer apart, and then used the Optimized Hot Spot Analysis tool to remove points that were spatially autocorrelated with a statistical confidence level of 0.95. This resulted in n = 647 points for 1991-2000 and n = 951 points for 2001-2010.

We developed kernel density estimator (KDE) surfaces in ArcGIS v.10.2 to create a probability surface for model background point selection. Rather than using a presence-absence approach, we selected a presence-background (i.e. pseudo-absence) approach because fires with anthropogenic causes may have been present at background locations (Moritz et al. 2012). The KDE surface is a tool that can be used in SDMs built on presence-only data to prioritize background point selection within areas with greater confidence in species absence (Elith et al. 2011). We randomly selected 10,000 background points from each KDE surface during the MDS Builder in the Software for Assisted Habitat Modeling (SAHM; (Morisette et al. 2013)).

Climate Data

Using ClimateWNA v.5.10, we generated 166 unique climate variables at a 1 km^2 spatial resolution including directly calculated and derived yearly, seasonal, and monthly

averages for the two decades (i.e. 1991 – 2000 and 2001 – 2010) corresponding to the wildfire occurrence data (Appendix 2.1; (Wang et al. 2012)). Next, we downloaded the same variables for the 2020s (2010-2039) and 2050s (2040-2069) from two future climate ensembles (i.e. two representative concentration pathways; RCP 4.5 and RCP 8.5 with ensemble average projections from 15 global circulation models [GCMs]: CanESM2, ACCESS1.0, IPSL-CM5A-MR, MIROC5, MPI-ESM-LR, CCSM4, HadGEM2-ES, CNRM-CM5, CSIRO Mk 3.6, GFDL-CM3, INM-CM4, MRI-CGCM3, MIROC-ESM, CESM1-CAM5, and GISS-E2R). These GCMs were chosen to represent all major clusters of similar AOGCMs and had high validation stats in their CMIP3 equivalents (Knutti et al. 2013). The RCP 4.5 and RCP 8.5 were chosen to represent a moderate (i.e. radiative forcing level leading to 4.5 W/m^2 greenhouse gas levels or ~650 ppm CO_2 eq by year 2100) and high radiative forcing level (i.e. 8.5 W/m^2 or ~1370 ppm CO_2 eq by year 2100), respectively (van Vuuren et al. 2011). Raster layers were created from all climate data (n= 470,614 1km^2 cells for each raster) in ArcMap v.10.2.

Topographic data

A digital elevation model (DEM) with 1 km^2 spatial resolution to match the climate data was acquired from the Global Multi-resolution Terrain Elevation Data (GMTED 2010), a high-quality elevation dataset that incorporates global Digital Terrain Elevation Data (DTED®) from the Shuttle Radar Topography Mission (SRTM), Canadian elevation data, Spot 5 Reference3D data, and data from the Ice, Cloud, and land Elevation Satellite (ICESat). Using this digital elevation model, we developed 12 unique topographic raster layers in ArcGIS v. 10.2 (Appendix 2.2). We selected topographic indices as proxies for wind movement, wind speed, and surface water across the study area.

Modeling framework

We used the Software for Assisted Habitat Modeling (SAHM; Morisette et al., 2013) to develop three models; MaxEnt, MARS, and GLM. The SAHM program is an open source modeling

platform that expedites pre-processing and execution of species distribution models. First, we used the Project, Aggregate, Resample, and Clip (PARC) module within SAHM to ensure consistency between the rasters (n = 179 unique climatic and topographic predictors; Appendices 1 and 2). The Merged Dataset (MDS) builder was then incorporated to develop 10,000 random background points within the inverse KDE probability surface we created (see Wildfire Occurrence) and extract values from the 179 rasters at the presence (i.e. wildfire occurrence) and pseudo-absence (i.e. 10,000 random background) points. The Covariate Correlation and Model Selection module was then applied to evaluate cross-correlation among all 179 variables and address the issue of multicollinearity (Dormann et al. 2013). When two variables had a Pearson, Spearman, or Kendall correlation coefficient, $|r| \geq 0.70$, only one of the pair was selected for model development, based on percent deviances explained from a univariate generalized additive model (GAM) with the predictor and relative importance of each variable. As a result of this correlation analysis, we retained 10 variables; April relative humidity (rh04), June relative humidity (rh06), August relative humidity (rh08), August precipitation (ppt08), spring (i.e. March through May) precipitation (ppt_sp), mean summer (i.e. May through September) precipitation (msp), March climatic moisture deficit (cmd03), Winter (i.e. Dec-Mar) climatic moisture deficit (cmd_wt), June solar radiation (rad06), and topographic roughness. Using this subset of variables, we fit three models in SAHM; MaxEnt, MARS, and GLM. All models were trained using a 10-fold cross validation split for testing and a threshold that maximizes the sum of sensitivity and specificity divided by 2 (Freeman and Moisen 2008, Liu et al. 2013). The three models were tested with an independent dataset for large wildfire occurrence for the years 2001 – 2010.

MaxEnt is a widely used niche modeling algorithm developed by Phillips et al (Phillips et al. 2006). It is a machine-learning, non-parametic method that estimates the geographic distribution of a response variable (e.g. a species or in this case a wildfire) using the principle of maximum

entropy (i.e., exponential distribution given linear combination of features and equivalent to the Gibbs distribution). To optimize MaxEnt model settings, we used the ENMEval code in R statistical software (Appendix 4.1; Muscarella et al., 2014). The MARS is a non-parametric regression technique that automatically models non-linearity and interactions between variables (Friedman 1991, Friedman and Roosen 1995). The recursive partitioning of MARS makes it capable of fitting complex, non-linear relationships between a response variable and predictors. The GLM is a generalized linear regression approach that specifies a relationship between the mean of a random variable and a function of the linear combination of predictors (McCullagh and Nelder 1989).

We used AUC (area under the receiver operating characteristic curve), percent correctly classified, sensitivity, specificity, and true skill statistic to evaluate the models. The AUC is threshold-independent and is used to evaluate the ability of a model to discriminate presence from absence (or background). An AUC value of 0.5 indicates model predictions are not better than random; values less than 0.5 are worse than random; values between 0.5 and 0.70 indicate poor performance; and values increasing from 0.70 to 1.0 indicate progressively higher performance (Anderson et al. 2003). Sensitivity measures the percentage of presences correctly classified. Specificity measures the percentage of absences correctly classified. The true skill statistic (TSS = sensitivity + specificity – 1) places more weight on model sensitivity than specificity, with values ranging between -1 and 1 (Allouche et al. 2006). Values above zero indicate better model performance than chance alone. This accuracy measure is less sensitive to changes in prevalence (ratio of presence to absence data) within the model than other commonly used accuracy measures such as Cohen's Kappa (Allouche et al. 2006).

Results

The three historical environmental suitability models had area under the reciever operating characteristic curve (AUC_{CV}) values greater than 0.91 (Table 4.1).

Table 4.1. Model results

Model	AUC[21]	%Correctly Classified	Sensitivity	Specificity	True Skill Statistic
MaxEnt $_{CV}$	0.93 ± 0.007	85.86 ± 1.21	0.90 ± 0.02	0.84 ± 0.01	0.75 ± 0.03
MaxEnt $_{TEST}$	0.93	86.16	0.91	0.85	0.75
GLM $_{CV}$	0.91 ± 0.008	84.48 ± 1.19	0.89 ± 0.02	0.83 ± 0.01	0.72 ± 0.03
GLM $_{TEST}$	0.66	72.60	0.53	0.82	0.35
MARS $_{CV}$	0.94 ± 0.006	86.22 ± 0.64	0.88 ± 0.02	0.86 ± 0.01	0.73 ± 0.01
MARS $_{TEST}$	0.94	86.30	0.89	0.85	0.74

When applied to an independent dataset (i.e. large wildfire occurrence for the years 2001 – 2010 and climate averages for the same years), the MaxEnt and MARS models outperformed the GLM model, with AUC $_{TEST}$ values of 0.93 and 0.94, test sensitivity values of 0.91 and 0.89, and TSS values of 0.75 and 0.74, respectively. The GLM model performed poorly on the independent test dataset, with an AUC TEST value of 0.66, sensitvity of 0.53, and TSS value of 0.35. One possible reason the GLM model performed poorly is that this method does not include non-linear interactions between covariates. We selected the MaxEnt and MARS models to project into future potential climatic conditions based on the evaluation metrics.

For the three models, April relative humidity (rh04) had a greater relative contribution than the other nine variables. April relative humidity also had the greatest permutation importance (i.e. drop in training AUC resulting from random permutation of presence and background values) across these three models. For MaxEnt, March climatic moisture deficit (cmd03), August relative humidity (rh08), and spring precipitation (ppt_sp) also had high permutation importance (Appendix 4.2). For MARS, August precipitation (ppt08) and March climatic moisture deficit also had high permutation importance. The MaxEnt and MARS response curves for April relative

[21] *AUC s the average value for the test area under the reciever operating characteristic curve over ten model runs. CV is 10-fold cross validation; TEST is the AUC value for the independent test dataset).*

humidity indicated an increasing relative suitability for large wildfire occurrence with increasing April relative humidity values; conversely, the response curves for August relative humidity indicated an increasing relative suitability for large wildfire occurrence with decreasing August relative humidity values (Figures 4.3a. and 4.3b.).

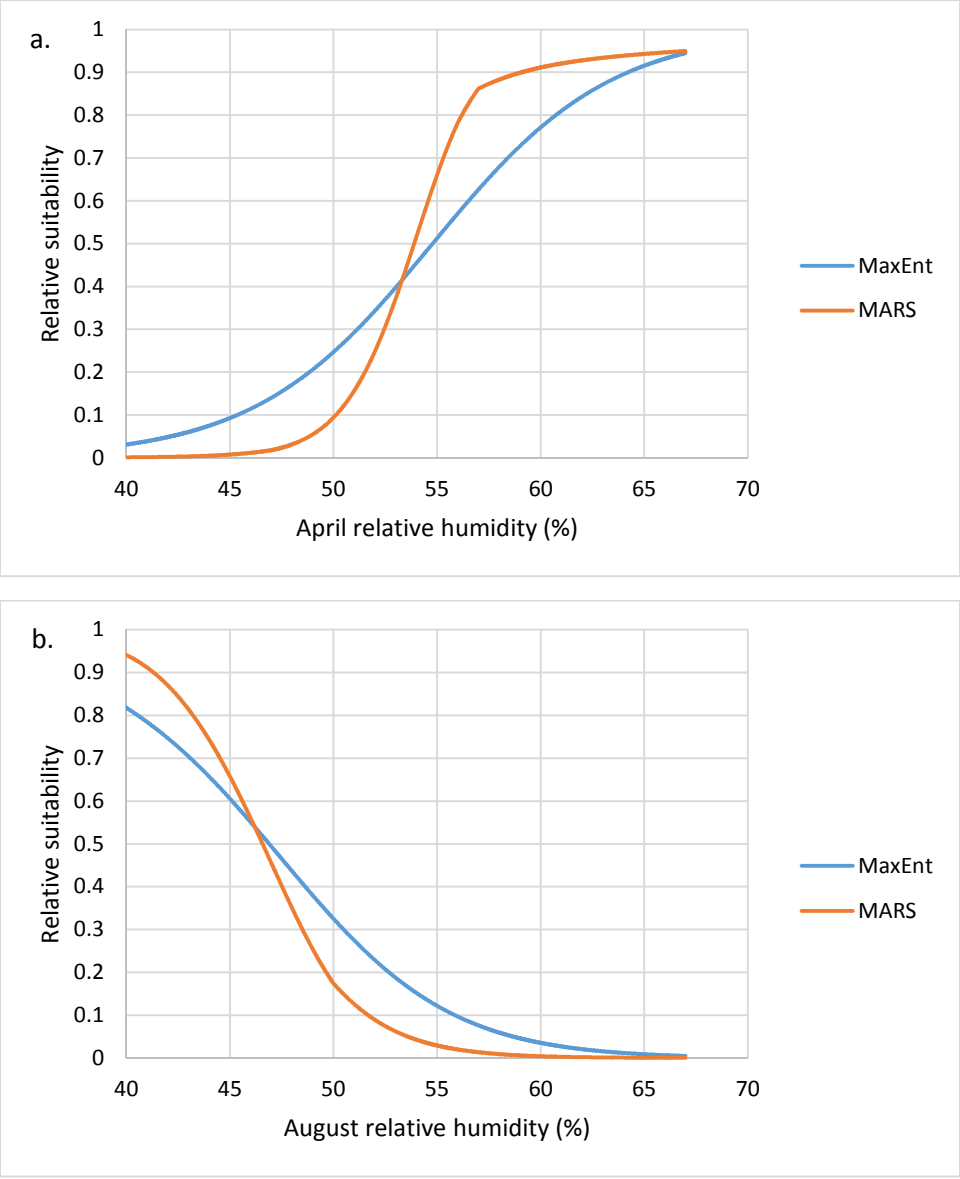

Figures 4.3a and 4.3b. Response curve for (a.) April relative humidity (decadal average; years 1991 – 2000) and (b.) August relative humidity (decadal average; years 1991 – 2000) based on the MaxEnt and MARS relative suitability models for large wildfires in Colorado and Wyoming.

We expected low relative humidity to be correlated with large wildfire occurrence and the response curve for August follows this hypothesis. Additionally, the number of large wildfires included in all models was greater in the month of August compared to the month of April (Figure 4.4).

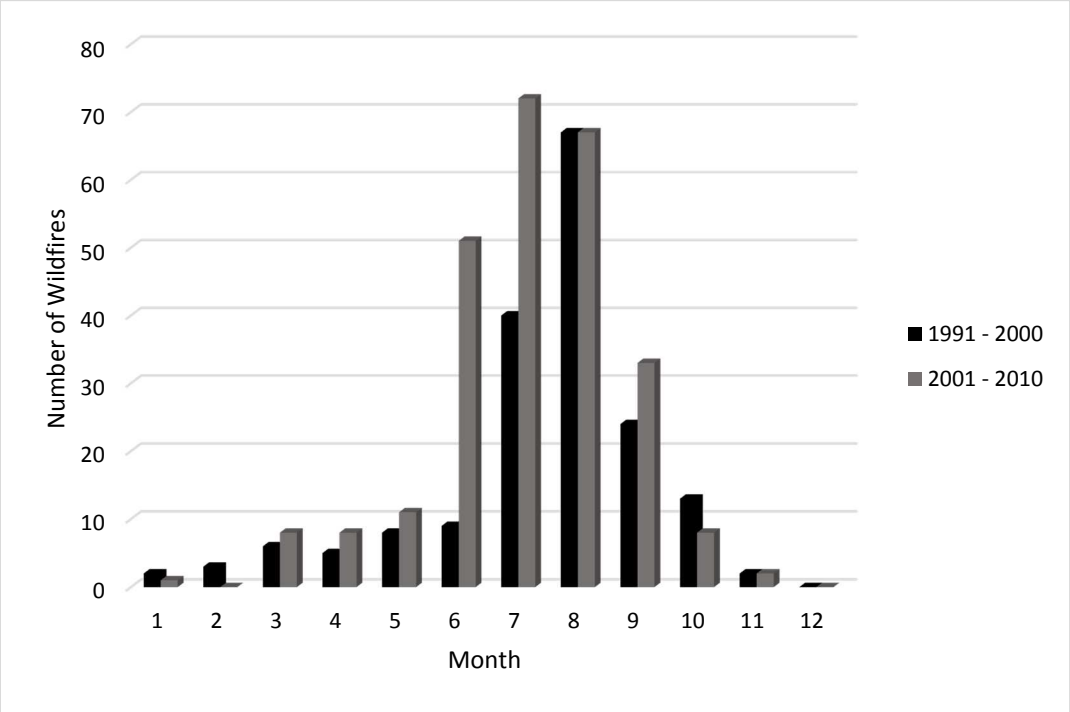

Figure 4.4. Number of wildfires per month in the two decadal time periods analyzed: 1991 – 2000 and 2001 – 2010.

MaxEnt transforms the exponential Gibbs distribution into a logistic output using a robust Bayes approach (for details see Elith et al., 2011; Phillips et al., 2006). MARS produces gridded values of the additive and second order ANOVA functions (Friedman 1991, Friedman and Roosen 1995, Elith and Leathwick 2007). We combined the MaxEnt and MARS model outputs in an ensemble to create relative rank-based maps for the current and future potential risk for large wildfire (Figures 4.5 a-e.).

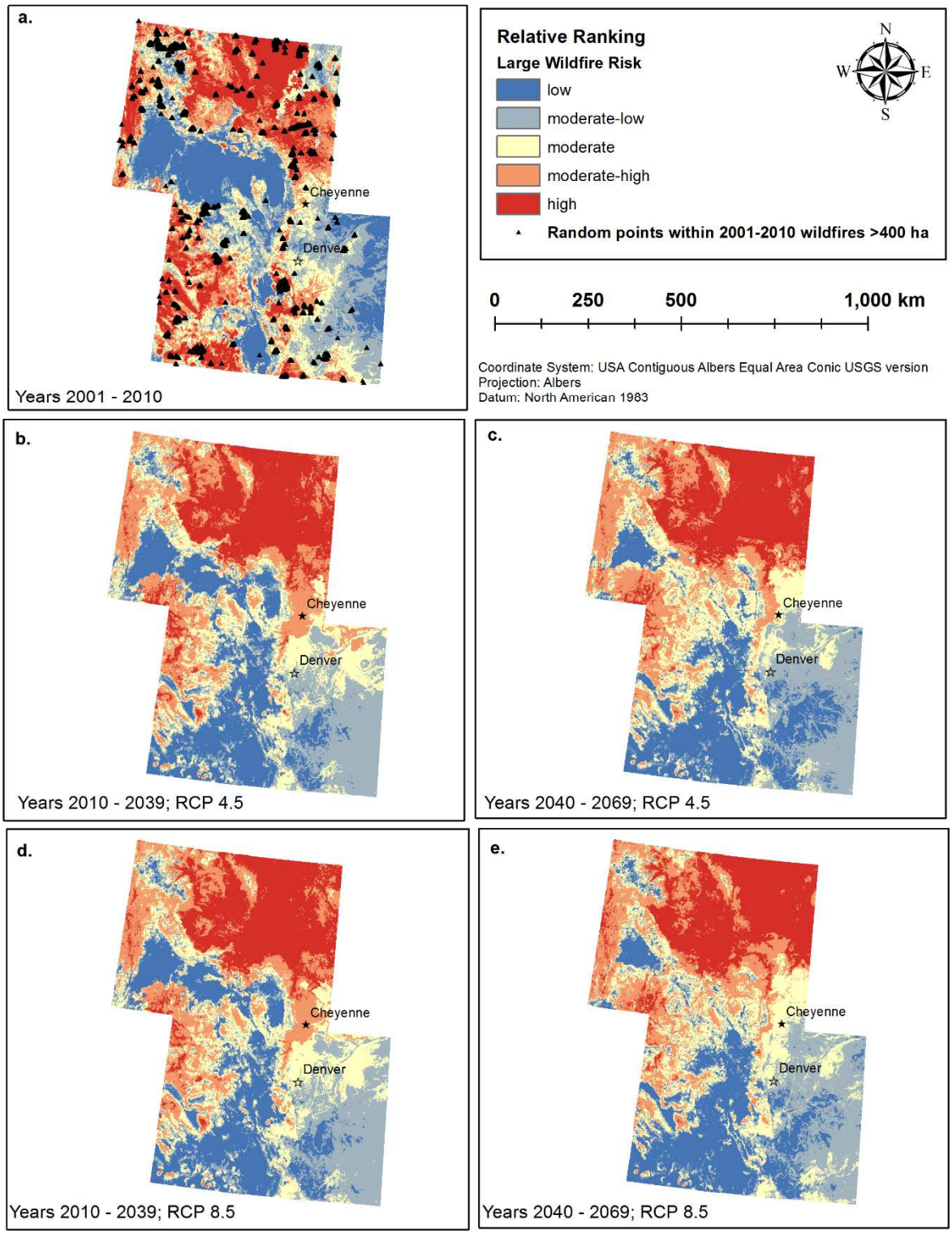

Figures 4.5 a-e. Relative ranking of large wildfire risk (i.e. > 400 ha) in Colorado and Wyoming, USA based on and ensemble of MaxEnt and MARS model results. At each 1km^2 cell, the ranking can be interpreted as the relative environmental suitability for large

wildfires. The years 2001 – 2010 model was produced from 1991 – 2000 large wildfire occurrence data and tested using the independent test dataset shown (i.e. random points within 2001 – 2010 wildfires > 400 ha).

Discussion

Our results indicate the area at high relative risk for large wildfires in Colorado and Wyoming may change in the near future based on an ensemble of average projections from 15 global circulation models. The RCP 4.5 and RCP 8.5 ensemble models show much agreement for the 2020s. These results are consistant with CMIP5 projections; the two RCPs do not significantly diverge until after the year 2050 (van Vuuren et al. 2011).The relative high risk for large wildfires increases most dramatically in northern Wyoming; these results agree with Westerling et al (2011). Many areas in southern Colorado decrease from high to relative risk to moderate, moderate-low, and even low relative risk for large wildfire across future models.

It is important to note that these estimates of relative risk are best examined as environmental suitability models for large wildfires; the total area at high risk will not necessarily burn. This study does not resolve the degree to which observed climate and future potential climate contribute to large wildfire occurrence relative to anthropogenic disturbance or management, decadal atmospheric cycles, lightning and other ignition sources, and fuel availability. However, proxies for some of these regimes are included in our models, including topographic roughness and decadal relative humidity and precipitation averages. Topographic roughness is a measure of the variability in landscape surface, and is linked to many abiotic components across ecological scales. Hansen and Sutera (1995) found evidence of topographic forcing in the low-frequency variability of a global circulation model. Topographic roughness has been cited as a proxy for variability in temperature, precipitation, vegetative propagation, and disturbance including wildfire return interval (Stambaugh and Guyette 2008).

We used decadal averages to project into potential climate space that was averaged over 30 years; therefore, it should also be noted that there is a temporal mismatch in the climate data.

We considered adding 1981 – 1990 wildfire occurrence and climate data to the historical model to correct for this, however MTBS data are only available post – 1984. Nonetheless, these models of relative suitability for future large wildfires in Colorado and Wyoming provide a starting point for evaluating areas most at risk given our current understanding of future climate change.

Model response curves for April relative humidity versus August relative humidity provided an interesting comparison; the former result was not expected. There are several possible explanations for this phenomenon. Across much of Colorado and Wyoming, moist, warm air frequently moves in from the south in the spring, particularly east of the Rocky Mountains (Western Regional Climate Center; www.wrcc.dri.edu). The decadal average we used may serve as a proxy for fuel load, as areas with higher spring relative humidity likely experience greater net primary productivity. Northerly slopes in the interior West have higher relative humidity, lower average temperatures, and less direct solar radiation which results in different forest community structure compared to southerly slopes; the former slopes typically have denser vegetation (Heyerdahl et al. 2001). Furthermore, both the MaxEnt and MARS models incorporate non-linear interactions between variables, and can capture complex relationships between climatic variables and topography (i.e. topographic roughness). Large wildfies occur more frequently in August in Colorado and Wyoming compared to other months of the year.

Previous research has evaluated the broad-scale effects of El Niño – Southern Oscillation (ENSO) and the Pacific Decadal Oscillation (PDO) on fire regimes (Westerling and Swetnam 2003, Schoennagel et al. 2005, Kitzberger et al. 2007, Kipfmueller et al. 2012). Westerling and Swetnam (2003) indicated that fire extent increases when the negative PDO phase coincides with La Niña in the southwestern USA and the southern Rockies (Arizona, Nevada, Utah, Colorado, and Wyoming) and during the positive PDO phases coinciding with El Niño events in the pacific northwest. Schoennagel et al. (2005) supported these results for negative PDO

phases in Colorado. However, in contrast to Westerling and Swetnam (2003), Schoennagel et al. (2005) discovered the occurrence of high-elevation fires in north-western Wyoming may actually increase during the positive PDO phase. The ENSO has a strong influence on wildfire in the Southwestern USA, but not in the Pacific Northwest, Northern California, or the Interior West (Trouet et al. 2010). However, other research provides evidence that PDO has little effect on wildfire occurrence and model results depend on choice of historical reconstruction of PDO (Kipfmueller et al. 2012).

Despite evidence for relationships between these oscillations and wildfire, the drivers of ENSO and PDO are still poorly understood and cannot be forecasted into future potential climates. Our models show that 10-year climate averages can be used to predict large wildfire occurrence at the same temporal scale. These data in combination with topography are appropriate for future large wildfire projections given the lack of our current ability to model future climate cycle events such as El Niño. Furthermore, these 10-year climate averages (particularly relative humidity) can capture at least some of the influence of these oscillations, as the ENSO and PDO operate at temporal scales of 2-7 years and 20-30 years, respectively.

After examining the raw data, we found the upper and lower value for April relative humidity is greater for the RCP 8.5 ensemble than the RCP 4.5 ensemble. Across GCMs, there is agreement in continued warming for these states; however, the percent change in precipitation is more uncertain, ranging from a five percent decrease to a six percent increase (Lukas et al. 2014). Nonetheless, the projected increase in temperatures will affect snowpack, snowmelt, and runoff, increasing the likelihood for depleted soil moisture. Finally, it must be recognized that one source of bias for modeling future climatic changes is the potential for change in the intrinsic covariance structure for future models compared to the observational data the GCMs were trained on, and the ground-level albedo effects of less snowpack and more snowmelt are one example of a complication in this covariance structure (Stavros et al. 2014).

Based on MTBS data, the actual area burned by large wildfires in Colorado and Wyoming increased almost 50% in the 2001 – 2010 decade compared to the 1991 – 2000 decade, from 368,900 ha to 526,400 ha. The continued increase in large wildfires has implications beyond state borders. Forests sequester 20 to 40% of carbon pools in the USA, and increasing wildfire frequency, extent, and season in the West may transition forests from carbon sinks to carbon sources (Pacala et al. 2001, Schimel and Braswell 2005, Kashian et al. 2006, Smithwick et al. 2009). Furthermore, emissions from wildfires add to the concentration of carbon in the atmosphere and are a source of atmospheric aerosol (Yue et al. 2013). These effects modify atmospheric circulation, degrade air quality, and feedback to climatic change. In turn, climate feedbacks to fire frequency and extent have the potential to reduce fire rotation and can lead to novel vegetation assemblages (Hurteau 2014). Abrupt changes in vegetation communities will inevitably have cascading ecosystem impacts; one example in the West is the cheatgrass invasion – wildfire feedback (D'Antonio and Vitousek 1992, Brooks et al. 2004, Freeman et al. 2007, Balch et al. 2013).

Conclusion

In conclusion, we find these modeling methods are an extremely useful tool in evaluating future large wildfire risk and can only enhance our preparedness for an uncertain future. Map output from our results can be used to enhance climate change vulnerability assessments. These models may be further refined at regional levels using land use and land cover data, as not all areas defined at risk based on climate and topography are necessarily suitable for large wildfires (e.g. some areas may be impervious surface or managed croplands). Notably, our results indicate that areas in northern Wyoming may need to be prioritized for large wildfire mitigation and monitoring in the coming decades.

Acknowledgements

The authors would like to thank William H. Romme for his insight and edits on an early draft of this manuscript.

Appendices

Appendix 4.1. Climate Variables Included in Initial Models[1].

Variable description and units of measurement
Annual Variables
Mean annual temperature (°C)
Mean warmest month temperature (°C)
Mean coldest month temperature (°C)
Continentality (°C; difference between MWMT and MCMT)
Mean annual precipitation (mm)
Mean summer (May to Sept.) precipitation (mm)
Annual heat: moisture index (MAT+10)/(MAP/1000)
Summer heat:moisture index ((MWMT)/(MSP/1000))
Number of frost-free days (FFP)
Frost-free period
Julian date on which FFP begins
Julian date on which FFP ends
Precipitation as snow (mm) between Aug and July
Extreme minimum temperature over 30 years
Extreme maximum temperature over 30 years
Hargreaves reference evaporation
Hargreaves climatic moisture deficit
Mean annual relative humidity (%)
Seasonal Variables
Winter (Dec.(prev. yr) - Feb.) mean temperature (°C)
Spring (Mar. - May) mean temperature (°C)
Summer (Jun. - Aug.) mean temperature (°C)
Autumn (Sep. - Nov.) mean temperature (°C)
Winter mean maximum temperature (°C)
Spring (Mar. - May) mean maximum temperature (°C)
Summer (Jun. - Aug.) mean maximum temperature (°C)
Autumn (Sep. - Nov.) mean maximum temperature (°C)
Winter (Dec.(prev. yr) - Feb.) mean minimum temperature (°C)
Spring (Mar. - May) mean minimum temperature (°C)
Summer (Jun. - Aug.) mean minimum temperature (°C)
Autumn (Sep. - Nov.) mean minimum temperature (°C)
Winter (Dec.(prev. yr) - Feb.) precipitation (mm)
Spring (Mar. - May) precipitation (mm)
Summer (Jun. - Aug.) precipitation (mm)
Autumn (Sep. - Nov.) precipitation (mm)
Winter (Dec.(prev. yr) - Feb.) number of frost-free days
Spring (Mar. - May) number of frost-free days
Summer (Jun. - Aug.) number of frost-free days

Autumn (Sep. - Nov.) number of frost-free days
Winter (Dec.(prev. yr) - Feb.) precipitation as snow
Spring (Mar. - May) precipitation as snow
Summer (Jun. - Aug.) precipitation as snow
Autumn (Sep. - Nov.) precipitation as snow
Winter (Dec.(prev. yr) - Feb.) Hargreaves reference evaporation
Spring (Mar. - May) Hargreaves reference evaporation
Summer (Jun. - Aug.) Hargreaves reference evaporation
Autumn (Sep. - Nov.) Hargreaves reference evaporation
Winter (Dec.(prev. yr) - Feb.) Hargreaves climatic moisture deficit
Spring (Mar. - May) Hargreaves climatic moisture deficit
Summer (Jun. - Aug.) Hargreaves climatic moisture deficit
Autumn (Sep. - Nov.) Hargreaves climatic moisture deficit
Winter (Dec.(prev. yr) - Feb.) solar radiation (MJ m^{-2} d^{-1})
Spring (Mar. – May) solar radiation (MJ m^{-2} d^{-1})
Summer (Jun. - Aug.) solar radiation (MJ m^{-2} d^{-1})
Autumn (Sep. - Nov.) solar radiation (MJ m^{-2} d^{-1})
Winter (Dec.(prev. yr) - Feb.) relative humidity (%)
Spring (Mar. - May) relative humidity (%)
Summer (Jun. - Aug.) relative humidity (%)
Autumn (Sep. - Nov.) relative humidity (%)
Monthly Variables
January – December mean temperatures (°C)
January – December maximum mean temperatures (°C)
January – December minimum mean temperatures (°C)
January – December precipitation (mm)
January – December precipitation as snow (mm)
January – December solar radiation (MJ m^{-2} d^{-1})
January – December Hargreaves reference evaporation (mm)
January – December Hargreaves climatic moisture deficit (mm)
January – December relative humidity (%)

[1]*Source: ClimateWNA v.5.10; (Wang et al. 2012)*

Appendix 4.2. Topographic variables included in initial models

Elevation[1]
Mean Slope[2]
Aspect[2]
Topographic roughness[2]
Cosine transformation of aspect[3]
Sine transformation of aspect[3]
Heat load index[2]
Integrated moisture index[2]
Flow accumulation[2]
Flow direction[2]

[1] Source of digital elevation model (DEM): Global Multi-resolution Terrain Elevation Data (GMTED2010; http://topotools.cr.usgs.gov/gmted_viewer/).
[2] Derived from DEM using ArcGIS v.10.2 system tools.
[3] Derived from DEM using Geomorphology and Gradient Metrics Toolbox for ArcGIS (Evans et al. 2014).

Appendix 4.3. Output from ENMEval (modified from Muscarella et al 2014) used to parameterize the MaxEnt models[1].

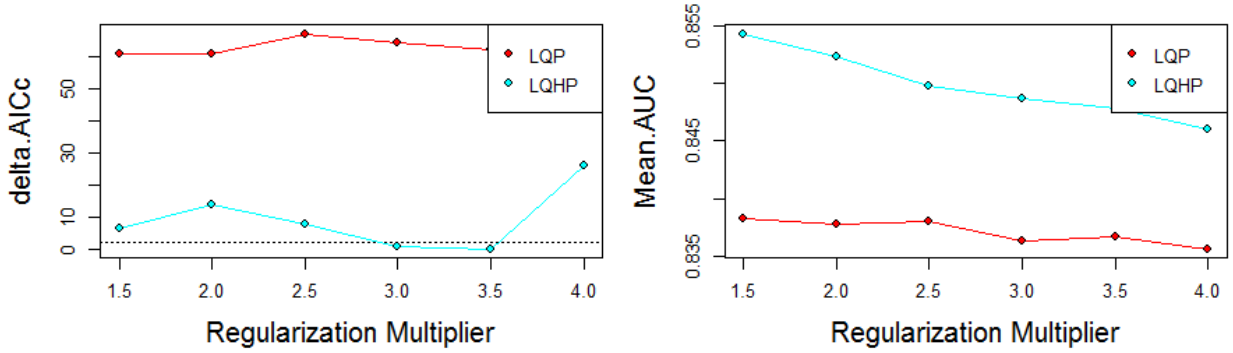

[1]LQP is a MaxEnt model fit with linear, quadratic, and product features; LQPH is a MaxEnt model fit with LQP features and hinge features; delta.AICc is change in corrected Akaike's information criterion (Hurvich et al. 1998); mean.AUC is mean area under the receiver operating curve value.

Appendix 4.4. Variable permuation importance in training (Train) and 10-fold cross validation test (CV) splits of the final MaxEnt model[1].

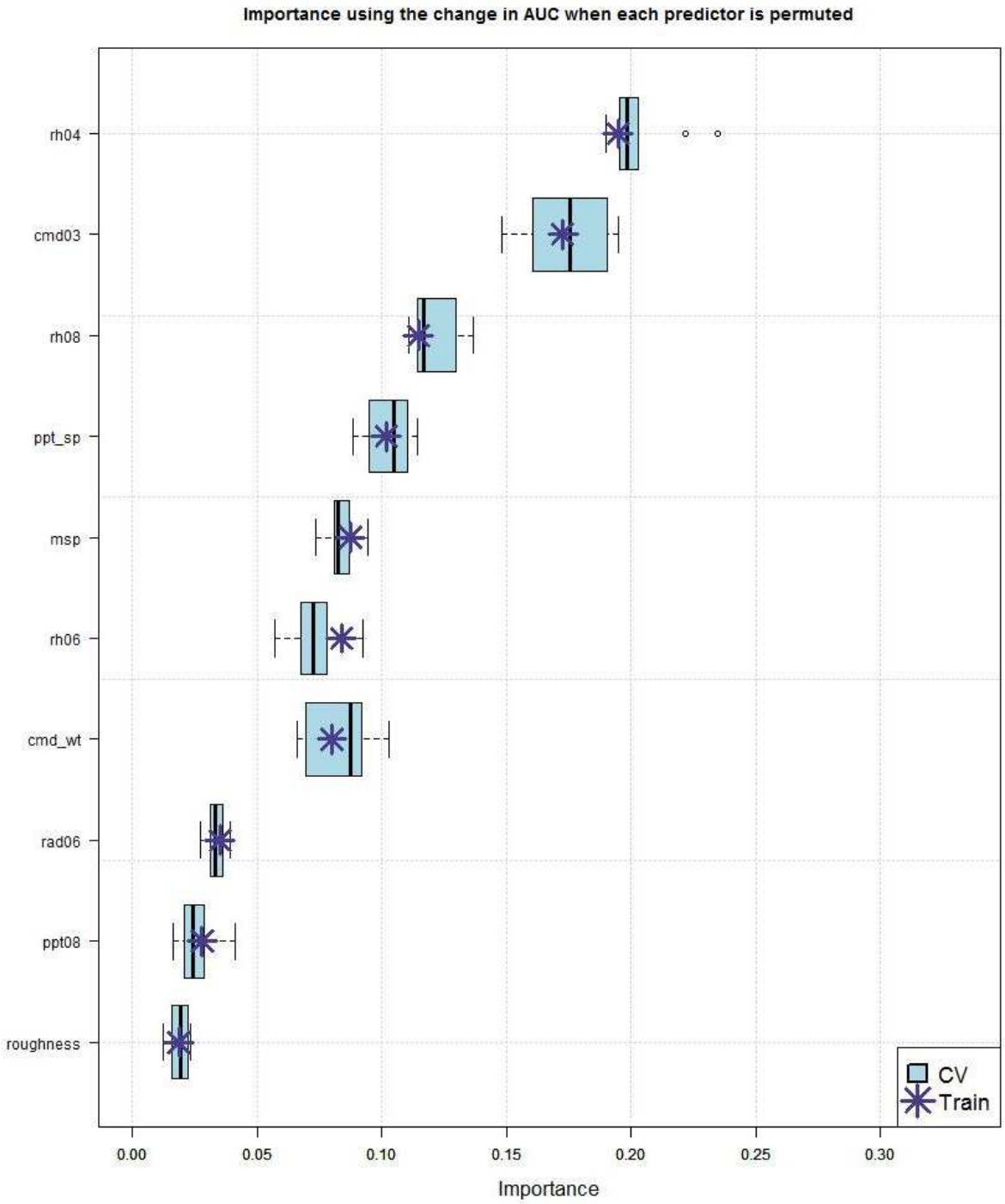

[1]*The variables listed are April relative humidity (rh04), June relative humidity (rh06), August relative humidity (rh08), August precipitation (ppt08), spring (i.e. March through May) precipitation (ppt_sp), mean summer (i.e. May through September) precipitation (msp), March climatic moisture deficit (cmd03), Winter (i.e. Dec-Mar) climatic moisture deficit (cmd_wt), June solar radiation (rad06), and topographic roughness (roughness).*

Appendix 4.5. Variable permuation importance in training (Train) and 10-fold cross validation test (CV) splits of the final MARS model[1].

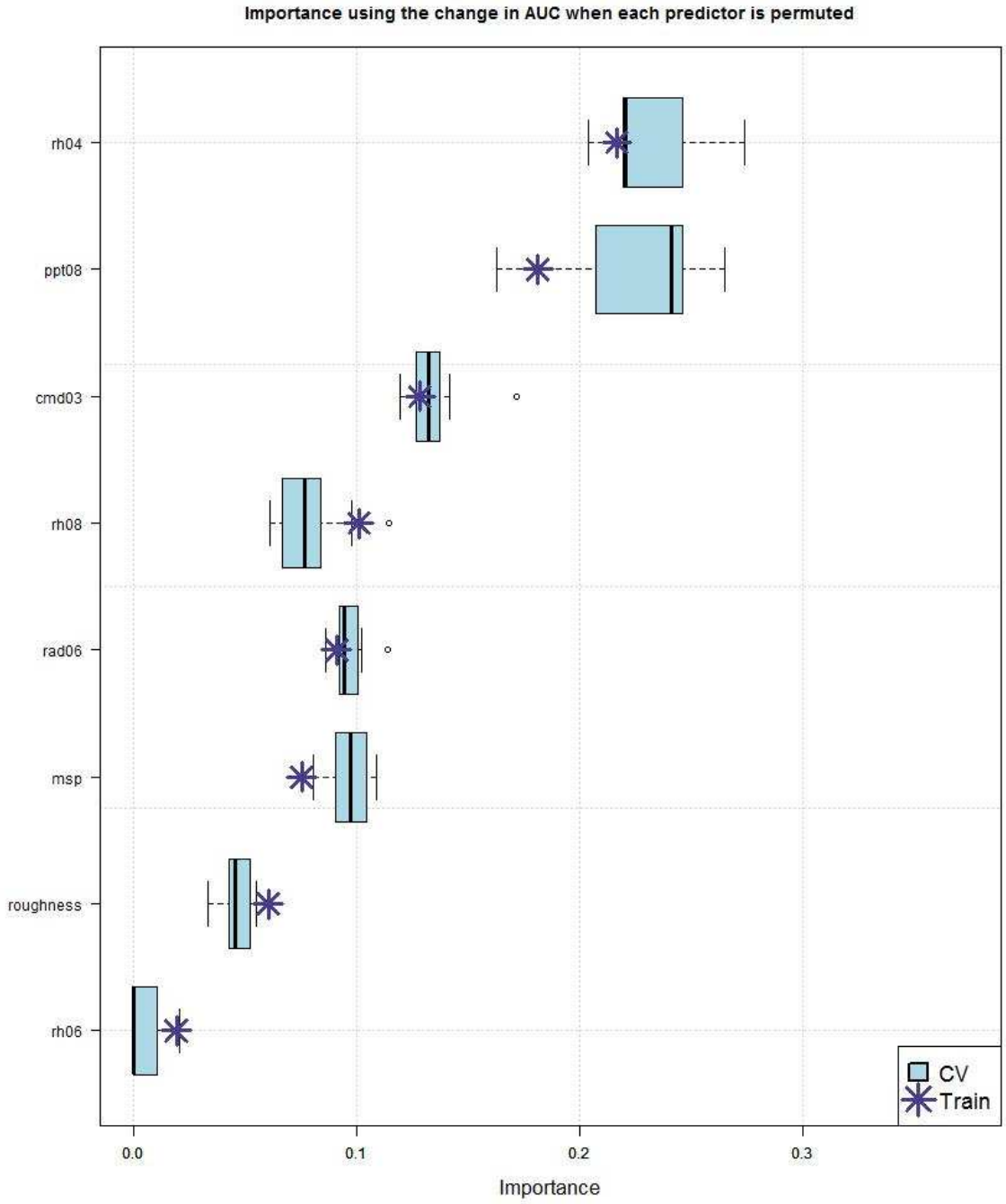

[1]The variables listed are April relative humidity (rh04), August precipitation (ppt08), March climatic moisture deficit (cmd03), August relative humidity (rh08), June solar radiation (rad06), mean summer (i.e. May through September) precipitation (msp), topographic roughness (roughness), and June relative humidity (rh06).

CHAPTER 5. SYNTHESIS

In an era of rapid environmental change, land managers need the best tools available to examine how the distribution of ecological phenomena are also changing. The results of this dissertation research indicate species distribution models and habitat suitability models can meet this challenge when parameterized based on the region of concern. In each of these studies we found selection of the appropriate scale (i.e. spatial and temporal) and relevant environmental covariates are crucial decisions that affect model outcome and efficacy.

In the second chapter five uncorrelated variables captured the current bioclimatic niche of the alien invasive *Bromus tectorum* in Rocky Mountain National Park, Colorado: mean annual temperature, continentality, beginning of frost-free period, mean summer precipitation, and spring heating degree days. These variables were selected after a detailed literature review of *B. tectorum* biology, covariate correlation analysis, and Akaike's Information Criterion calculations. Distance to roads and trails was also important in the model and served as a surrogate for propagule pressure. These variables were projected into the year 2050 using future potential climate data from six global circulation models (GCMs) and an ensemble of model outputs revealed an additional 14.9% of the Park will be suitable habitat for *B. tectorum*. This result must be taken with caution; we are assuming bioclimatic niche conservatism for *B. tectorum* over time. However, this methodology provides a useful tool that can be adopted to generate high resolution species distribution maps under current and future climate scenarios for other invasive species in National Parks. Land managers can incorporate the maps created from these models into integrated pest management regimes, and further tailor them based on what is already known about an area, keeping in mind that the models are not precise probabilities of species occurrence but rather ranking of suitable habitat. These maps may also

be displayed to the visiting public to increase awareness of climate change implications in National Parks.

In the third chapter, eleven distinct vegetation indices derived from Landsat 8 remotely sensed imagery were used by a Random Forest model to determine the current distribution of *B. tectorum* in a post-wildfire disturbance area of Medicine Bow National Forest, Wyoming. This study highlighted the importance of temporal matching of species phenology and using multiple unique spectral indices when employing remotely sensed data in species distribution models. It also supported the use of an iterative approach in which a threshold for vegetation cover should be established to increase accuracy of these models. The georeferenced *B. tectorum* distribution map will be used by land managers with the U.S. Forest Service in targeted invasive species control efforts with the goal of restoring native vegetation in areas deemed critical winter habitat for mule deer (*Odocoileus hemionus*) and elk (*Cervus canadensis*). Wealso incorporated this model in a habitat suitability assessment using topographic covariates and seed dispersal limitations to determine the total area at risk for future invasion of *B. tectorum* within the disturbed area.

The fourth chapter used decadal climate averages corresponding to the temporal resolution of wildfire occurrence and topographic covariates to produce pyrogeographic models for large wildfires in Colorado and Wyoming following a similar methodology to chapter one. April relative humidity, March climatic moisture deficit, and August relative humidity were the three most important covariates in the best model (i.e. MaxEnt). This is the first regional model for Colorado and Wyoming to forecast future potential wildfire extent, and our novel methodology provides a tool that can be modified for other regions of North America.

The methods outlined in this dissertation can be used as starting points for developing distribution models for other ecological phenomena, however we emphasize that approaching

each new study as an iterative process is crucial; careful scrutiny and refinement of the models result in the most robust maps. Results from these studies provide foundations on which further hypotheses can be tested and evaluated. As an example of extending these results, we superimposed a model for current suitable *B. tectorum* habitat in Colorado and Wyoming on the wildfire model for the same time period in geographic space (Figure 5.1). From this map, we can begin to ask questions about the areas that could be at high risk in the future for invasion-wildfire feedback.

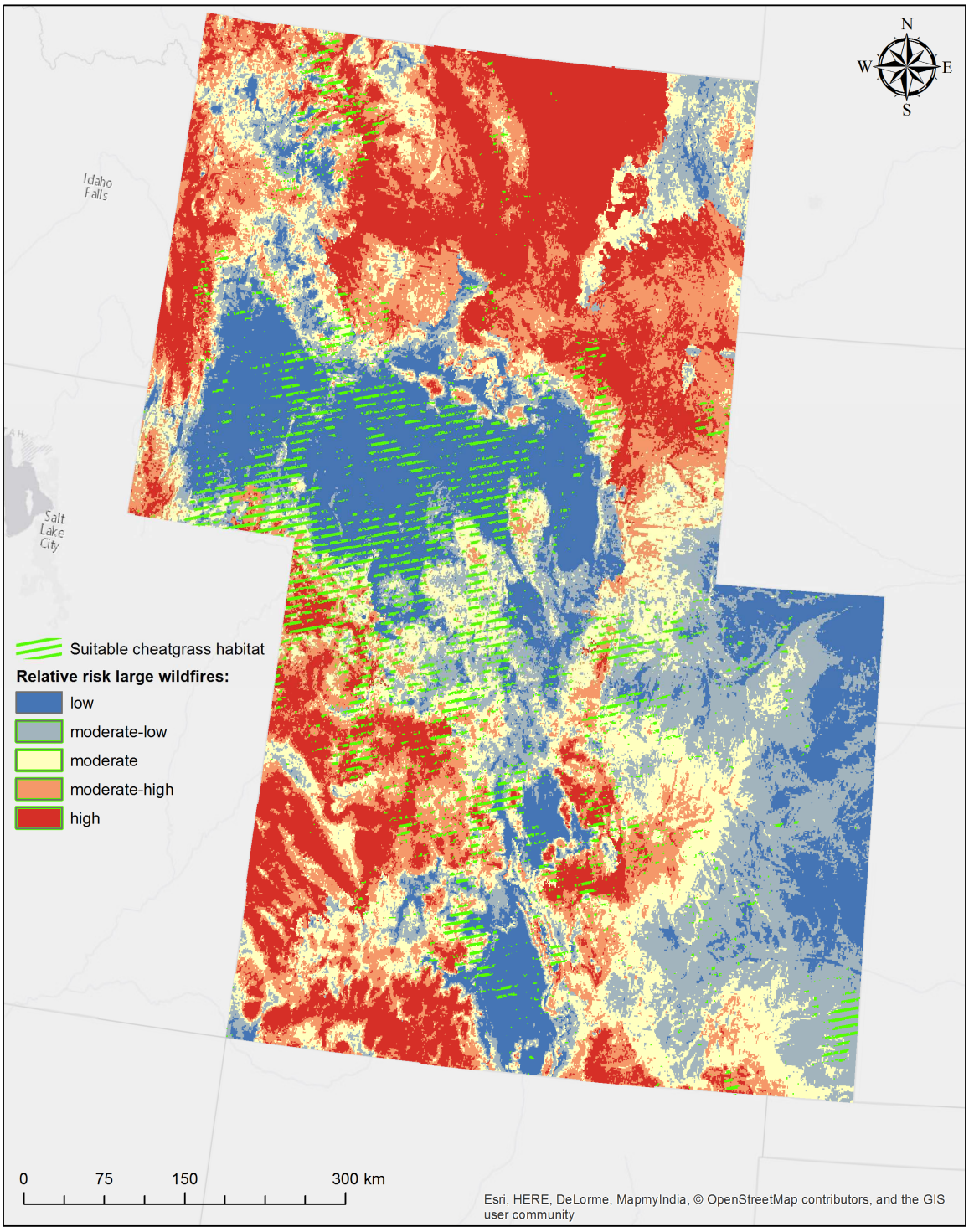

Figure 5.1. Preliminary analysis of wildfire model from Chapter 3 overlaid with a *Bromus tectorum* habitat suitability model (*B. tectorum* model used with permission from C. Jarnevich 2015; *In Prep*).

REFERENCES

Allouche, O., A. Tsoar, and R. Kadmon. 2006. Assessing the accuracy of species distribution models: prevalence, kappa and the true skill statistic (TSS). Journal of Applied Ecology 43:1223–1232.

Anderson, D., and K. Burnham. 2002. Avoiding pitfalls when using information-theoretic methods. The Journal of Wildlife Management 66:912–918.

Anderson, R., D. Lew, and A. Townsend Peterson. 2003. Evaluating predictive models of species' distributions: criteria for selecting optimal models. Ecological modelling 162:211–232.

Araújo, M. B., and M. New. 2007. Ensemble forecasting of species distributions. Trends in ecology & evolution 22:42–7.

Araújo, M. B., and A. T. Peterson. 2012. Uses and misuses of bioclimatic envelope modeling. Ecology 93:1527–1539.

Arnold, J. D., S. C. Brewer, and P. E. Dennison. 2014. Modeling climate-fire connections within the Great Basin and Upper Colorado River Basin, Western United States. Fire Ecology 10:64–75.

Arpaci, A., B. Malowerschnig, O. Sass, and H. Vacik. 2014. Using multi variate data mining techniques for estimating fire susceptibility of Tyrolean forests. Applied Geography 53:258–270.

Ashcroft, M. B., L. A. Chisholm, and K. O. French. 2009. Climate change at the landscape scale: predicting fine-grained spatial heterogeneity in warming and potential refugia for vegetation. Global Change Biology 15:656–667.

Austin, M. P., and K. P. Van Niel. 2011. Improving species distribution models for climate change studies: variable selection and scale. Journal of Biogeography 38:1–8.

Balch, J. K., B. A. Bradley, C. M. D'Antonio, and J. Gómez-Dans. 2013. Introduced annual grass increases regional fire activity across the arid western USA (1980-2009). Global Change Biology 19:173–83.

Ball, D. A., S. M. Frost, and A. I. Gitelman. 2004. Predicting timing of downy brome (Bromus tectorum) seed production using growing degree days. Weed Science 52:518–524.

Balshi, M. S., A. McGuire, D. Duffy, P. Flannigan, M. Walsh, and J. Melillo. 2009. Assessing the response of area burned to changing climate in western boreal North America using a Multivariate Adaptive Regression Splines (MARS) approach. Global Change Biology 15:578–600.

Banks, E. R., and W. L. Baker. 2011. Scale and pattern of cheatgrass (Bromus tectorum) invasion in Rocky Mountain National Park. Natural Areas Journal 31:377–390.

Barbero, R., J. T. Abatzoglou, and E. a Steel. 2014. Modeling very large-fire occurrences over the continental United States from weather and climate forcing. Environmental Research Letters 9:124009.

Bistinas, I., S. P. Harrison, I. C. Prentice, and J. M. C. Pereira. 2014. Causal relationships versus emergent patterns in the global controls of fire frequency. Biogeosciences 11:5087–5101.

Boulanger, Y., S. Gauthier, and P. J. Burton. 2014. A refinement of models projecting future Canadian fire regimes using homogeneous fire regime zones. Canadian Journal of Forest Research 44:345–376.

Bradford, J. B., and W. K. Lauenroth. 2006. Controls over invasion of Bromus tectorum: The importance of climate, soil, disturbance and seed availability. Journal of Vegetation Science 17:693–704.

Bradley, B. A. 2009. Regional analysis of the impacts of climate change on cheatgrass invasion shows potential risk and opportunity. Global Change Biology 15:196–208.

Bradley, B. A. 2013. Remote detection of invasive plants: a review of spectral, textural and phenological approaches. Biological Invasions 16:1411–1425.

Bradley, B., and J. F. Mustard. 2006. Characterizing the landscape dynamics of an invasive plant and risk of invasion using remote sensing. Ecological Applications 16:1132–1147.

Breiman, L. 2001. Random forests. Machine Learning:1–35.

Bremond, L., A. Boom, and C. Favier. 2012. Neotropical C3/C4 grass distributions - present, past and future. Global Change Biology 18:2324–2334.

Broennimann, O., M. C. Fitzpatrick, P. B. Pearman, B. Petitpierre, L. Pellissier, N. G. Yoccoz, W. Thuiller, M.-J. Fortin, C. Randin, N. E. Zimmermann, C. H. Graham, and A. Guisan. 2012. Measuring ecological niche overlap from occurrence and spatial environmental data. Global Ecology and Biogeography 21:481–497.

Bromberg, J. E., S. Kumar, C. S. Brown, and T. J. Stohlgren. 2011. Distributional changes and range predictions of downy brome (Bromus tectorum) in Rocky Mountain National Park. Invasive Plant Science and Management 4:173–182.

Brooks, M., C. D'Antonio, D. Richardson, J. Grace, Keeley JE, J. DiTomaso, R. Hobbs, Pellant M, and D. Pyke. 2004. Effects of invasive alien plants on fire regimes. BioScience 54:677–688.

Brown, C. S., and H. Rowe. 2004. The Unwelcome Arrival of Bromus tectorum to high elevations. Proceedings of the High Altitude Revegetation Workshop No. 16 Fort Collins, CO:1–12.

Brown, J. H. 2007. On the Relationship between abundance and distribution of species. The American Naturalist 124:255–279.

Brown, P. M., and W. D. Shepperd. 2001. Fire history and fire climatology along a 5 degree gradient in latitude in Colorado and Wyoming, USA. Palaeobotanist 50:133–140.

Brown, T. J., B. L. Hall, and A. L. Westerling. 2004. The impact of twenty-first century climate change on wildland fire danger in the Western United States: an applications perspective. Climatic Change 62:365–388.

Certini, G. 2005. Effects of fire on properties of forest soils: a review. Oecologia 143:1–10.

CGIAR_CSI Geoportal. (n.d.). . http://srtm.csi.cgiar.org/.

Chambers, J., and B. Roundy. 2007. What makes Great Basin sagebrush ecosystems invasible by Bromus tectorum? Ecological Monographs 77:117–145.

Clements, D. R., and A. Ditommaso. 2011. Climate change and weed adaptation: can evolution of invasive plants lead to greater range expansion than forecasted? Weed Research 51:227–240.

Compagnoni, A., and P. Adler. 2014. Warming, competition, and Bromus tectorum population growth across an elevation gradient. Ecosphere 5.

Cook, B. I., T. R. Ault, and J. E. Smerdon. 2015. Unprecedented 21st century drought risk in the American Southwest and Central Plains. Sci. Adv.:1–7.

Cook, E. R., C. a Woodhouse, C. M. Eakin, D. M. Meko, and D. W. Stahle. 2004. Long-term aridity changes in the western United States. Science 306:1015–1018.

Crall, A. W., C. S. Jarnevich, B. Panke, N. Young, M. Renz, and J. Morisette. 2013. Using habitat suitability models to target invasive plant species surveys. Ecological applications : a publication of the Ecological Society of America 23:60–72.

Crist, E. P., and R. C. Cicone. 1984. A physically-based transformation of Thematic Mapper Data---The TM Tasseled Cap. IEEE Transactions on Geoscience and Remote Sensing GE-22:256–263.

D'Antonio, C., and P. Vitousek. 1992. Biological invasions by exotic grasses, the grass/fire cycle, and global change. Annual Review of Ecology Systematics 23:63–87.

Davis, M. B., and R. G. Shaw. 2001. Range shifts and adaptive responses to Quaternary climate change. Science (New York, N.Y.) 292:673–9.

De'ath, G. 2007. Boosted trees for ecological modeling and prediction. Ecology 88:243–51.

De'ath, G., K. Fabricius, and T. E. Studies. 2000. Classification and regression trees: a powerful yet simple technique for ecological data analysis. Ecology 81:3178–3192.

Delong, C. 2010. Corroboration of biogeoclimatic ecosystem classification climate zonation by spatially modelled climate data. BC Journal of Ecosystems and Management 10:49–64.

Dennison, P. E., S. C. Brewer, J. D. Arnold, and M. A. Moritz. 2014. Large wildfire trends in the western United States, 1984-2011. Geophysical Research Letters 41:2928–2933.

Dormann, C. F., J. Elith, S. Bacher, C. Buchmann, G. Carl, G. Carré, J. R. G. Marquéz, B. Gruber, B. Lafourcade, P. J. Leitão, T. Münkemüller, C. McClean, P. E. Osborne, B. Reineking, B. Schröder, A. K. Skidmore, D. Zurell, and S. Lautenbach. 2013. Collinearity: a review of methods to deal with it and a simulation study evaluating their performance. Ecography 36:27–46.

Dormann, C. F., S. J. Schymanski, J. Cabral, I. Chuine, C. Graham, F. Hartig, M. Kearney, X. Morin, C. Römermann, B. Schröder, and A. Singer. 2012. Correlation and process in species distribution models: bridging a dichotomy. Journal of Biogeography 39:2119–2131.

Duncan, C. A., J. J. Jachetta, M. L. Brown, F. Carrithers, J. K. Clark, J. M. DiTomaso, R. G. Lym, C. Kirk, M. J. Renz, and P. M. Rice. 2004. Assessing the economic, environmental, and societal losses from invasive plants on rangeland and wildlands. Weed Technology.

Elith, J., and C. H. Graham. 2009. Do they? How do they? WHY do they differ? On finding reasons for differing performances of species distribution models. Ecography 32:66–77.

Elith, J., C. H. Graham, R. P. Anderson, M. Dudik, S. Ferrier, A. Guisan, R. J. Hijmans, F. Huettmann, J. R. Leathwick, A. Lehmann, J. Li, L. G. Lohmann, B. A. Loiselle, G. Manion, C. Moritz, M. Nakamura, and E. Al. 2006. Novel methods improve prediction of species' distributions from occurrence data. Ecography 29:129–151.

Elith, J., and J. Leathwick. 2007. Predicting species distributions from museum and herbarium records using multiresponse models fitted with multivariate adaptive regression splines. Diversity and Distributions 13:265–275.

Elith, J., and J. R. Leathwick. 2008. Boosted regression trees - a new technique for modelling ecological data. Journal of Animal Ecology.

Elith, J., and J. R. Leathwick. 2009. Species distribution models: ecological explanation and prediction across space and time. Annual Review of Ecology, Evolution, and Systematics 40:677–697.

Elith, J., J. R. Leathwick, and T. Hastie. 2008. A working guide to boosted regression trees. The Journal of Animal Ecology 77:802–13.

Elith, J., S. J. Phillips, T. Hastie, M. Dudík, Y. E. Chee, and C. J. Yates. 2011. A statistical explanation of MaxEnt for ecologists. Diversity and Distributions 17:43–57.

Ellstrand, N. C., and K. A. Schierenbeck. 2006. Hybridization as a stimulus for the evolution of invasiveness in plants? Euphytica 148:35–46.

Elton, C. 1927. Animal Ecology. University of Chicago Press, Chicago, USA.

Evangelista, P. H., S. Kumar, T. J. Stohlgren, C. S. Jarnevich, A. W. Crall, J. B. Norman III, and D. T. Barnett. 2008a. Modelling invasion for a habitat generalist and a specialist plant species. Diversity and Distributions 14:808–817.

Evangelista, P. H., J. Norman, L. Berhanu, S. Kumar, and N. Alley. 2008b. Predicting habitat suitability for the endemic mountain nyala (Tragelaphus buxtoni) in Ethiopia. Wildlife Research 35:409.

Evangelista, P., N. Young, and J. Burnett. 2013. How will climate change spatially affect agriculture production in Ethiopia? Case studies of important cereal crops. Climatic Change 119:855–873.

Evans, J. S., J. Oakleaf, S. A. Cushman, and D. Theobald. 2014. An ArcGIS Toolbox for Surface Gradient and Geomorphometric Modeling, v. 2.0. http://evansmurphy.wix.com/evansspatial.

Fielding, A. H., and J. F. Bell. 1997. A review of methods for the assessment of prediction errors in conservation presence/absence models. Environmental Conservation 24:38–49.

Flory, A. R., S. Kumar, T. J. Stohlgren, and P. M. Cryan. 2012. Environmental conditions associated with bat white-nose syndrome mortality in the north-eastern United States. Journal of Applied Ecology 49:680–689.

Franklin, J. 2009. Mapping species distributions: spatial inference and prediction. Cambridge University Press, New York, NY.

Franklin, J., F. W. Davis, M. Ikegami, A. D. Syphard, L. E. Flint, A. L. Flint, and L. Hannah. 2013. Modeling plant species distributions under future climates: how fine scale do climate projections need to be? Global Change Biology 19:473–83.

Freeman, E. A., and G. Moisen. 2008. PresenceAbsence: An R Package for Presence Absence Analysis. Journal of Statistical Software 23:1–31.

Freeman, J. P., T. J. Stohlgren, M. E. Hunter, P. N. Omi, E. J. Martinson, G. W. Chong, and C. S. Brown. 2007. Rapid assessment of postfire plant invasions in coniferous forests of the western United States. Ecological Applications 17:1656–65.

Friedman, J. 1991. Multivariate adaptive regression splines. The Annals of Statistics 19:1–67.

Friedman, J. H., and C. B. Roosen. 1995. An introduction to multivariate adaptive regression splines. Statistical Methods in Medical Research 4:197–217.

Gallien, L., R. Douzet, S. Pratte, N. E. Zimmermann, and W. Thuiller. 2012. Invasive species distribution models - how violating the equilibrium assumption can create new insights. Global Ecology and Biogeography 21:1126–1136.

Gates, D. M., H. J. Keegan, J. C. Schleter, and V. R. Weidner. 1965. Spectral properties of plants. Applied Optics 4:11.

Gausman, H., W. Allen, and R. Cardenas. 1969. Reflectance of cotton leaves and their structure. Remote Sensing of Environment 1:19–22.

Gessler, P. E., I. D. Moore, N. J. McKenzie, and P. J. Ryan. 1995. Soil-landscape modelling and spatial prediction of soil attributes. International Journal of Geographical Information Systems 9:421–432.

Gillingham, P. K., B. Huntley, W. E. Kunin, and C. D. Thomas. 2012a. The effect of spatial resolution on projected responses to climate warming. Diversity and Distributions:1–11.

Gillingham, P. K., S. C. F. Palmer, B. Huntley, W. E. Kunin, J. D. Chipperfield, and C. D. Thomas. 2012b. The relative importance of climate and habitat in determining the distributions of species at different spatial scales: a case study with ground beetles in Great Britain. Ecography 35:831–838.

Guisan, A., and W. Thuiller. 2005. Predicting species distribution: offering more than simple habitat models. Ecology Letters 8:993–1009.

Guisan, A., R. Tingley, J. B. Baumgartner, I. Naujokaitis-Lewis, P. R. Sutcliffe, A. I. T. Tulloch, T. J. Regan, L. Brotons, E. McDonald-Madden, C. Mantyka-Pringle, T. G. Martin, J. R. Rhodes, R. Maggini, S. a Setterfield, J. Elith, M. W. Schwartz, B. a Wintle, O. Broennimann, M. Austin, S. Ferrier, M. R. Kearney, H. P. Possingham, and Y. M. Buckley. 2013. Predicting species distributions for conservation decisions. Ecology letters.

Hamann, A., and T. Wang. 2006. Potential effects of climate change on ecosystem and tree species distribution in British Columbia. Ecology 87:2773–2786.

Hansen, A. R., and A. Sutera. 1995. The role of topography in the low-frequency variability of the large-scle midlatitude circulation. Journal of the Atmospheric Sciences 52:2498–2508.

Heffernan, J. B., P. a Soranno, M. J. Angilletta, L. B. Buckley, D. S. Gruner, T. H. Keitt, J. R. Kellner, J. S. Kominoski, A. V Rocha, J. Xiao, T. K. Harms, S. J. Goring, L. E. Koenig, W. H. McDowell, H. Powell, A. D. Richardson, C. a Stow, R. Vargas, and K. C. Weathers. 2014. Macrosystems ecology: understanding ecological patterns and processes at continental scales. Frontiers in Ecology and the Environment 12:5–14.

Hernandez, P., C. Graham, L. Master, and D. Albert. 2006. The effect of sample size and species characteristics on performance of different species distribution modeling methods. Ecography 29:773–785.

Heyerdahl, E., L. Brubaker, and J. Agee. 2001. Spatial controls of historical fire regimes: a multiscale example from the Interior West, USA. Ecology 82:660–678.

Higuera, P. E., C. E. Briles, and C. Whitlock. 2014. Fire-regime complacency and sensitivity to centennial-through millennial-scale climate change in Rocky Mountain subalpine forests, Colorado, USA. Journal of Ecology 102:1429–1441.

Hijmans, R. J., and J. Elith. 2013. Species distribution modeling with R. R CRAN Project.

Hijmans, R. J., and C. H. Graham. 2006. The ability of climate envelope models to predict the effect of climate change on species distributions. Global Change Biology 12:2272–2281.

Hirzel, A., and A. Guisan. 2002. Which is the optimal sampling strategy for habitat suitability modelling. Ecological Modelling 157:331–341.

Hirzel, A. H., and G. Le Lay. 2008. Habitat suitability modelling and niche theory. Journal of Applied Ecology 45:1372–1381.

Hoerling, M., and J. Eischeid. 2007. Past peak water in the Southwest. Southwest Hydrology 6:18–19.

Hurteau, M. 2014. Projected effects of climate and development on California wildfire emissions through 2100. Environmental Science & Technology 48:2298–2304.

Hutchinson GE. 1957. Concluding remarks. Cold Spring Harbor Symp Quant Biol. Pages 22:415–427.

IPCC. 2013. Climate Change 2013. The Physical Science Basis. Contribution of Working Group I to the Fifth Assessment Report of the Intergovernmental Panel on Climate Change (eds T.F. Stocker, D. Qin, G.K. Plattner, M. Tig- nor, S.K. Allen, J. Boschung, A.).

Jarnevich, C. S., and T. J. Stohlgren. 2008. Near term climate projections for invasive species distributions. Biological Invasions 11:1373–1379.

Jiménez-Valverde, A., A. T. Peterson, J. Soberón, J. M. Overton, P. Aragón, and J. M. Lobo. 2011. Use of niche models in invasive species risk assessments. Biological Invasions 13:2785–2797.

Johnson, B. G., D. W. Johnson, J. C. Chambers, and R. R. Blank. 2010. Fire effects on the mobilization and uptake of nitrogen by cheatgrass (Bromus tectorum L.). Plant and Soil 341:437–445.

Kashian, D. M., W. H. Romme, D. B. Tinker, M. G. Turner, and M. G. Ryan. 2006. Carbon storage on landscapes with stand-replacing fires. BioScience 56:598–606.

Kaufmann, M. R., D. Binkley, P. Z. Fulé, M. Johnson, S. L. Stephens, and T. W. Swetnam. 2007. Defining old growth for fire-adapted forests of the western United States. Ecology and Society 12:15.

Kearney, M. R., B. A. Wintle, and W. P. Porter. 2010. Correlative and mechanistic models of species distribution provide congruent forecasts under climate change. Conservation Letters 3:203–213.

Key, C. H., and N. C. Benson. 2005. Landscape assessment: remote sensing of severity, the Normalized Burn Ratio. In: D.C. Lutes et al. (Editors), FIREMON: Fire Effects Monitoring and Inventory System , Ogden, UT: USDA Forest Service, Rocky Mountain Research Station, General Technical Report.

Kipfmueller, K. F., E. R. Larson, and S. S. George. 2012. Does proxy uncertainty affect the relations inferred between the Pacific Decadal Oscillation and wildfire activity in the western United States? Geophysical Research Letters 39:1–5.

Kitzberger, T., P. M. Brown, E. K. Heyerdahl, T. W. Swetnam, and T. T. Veblen. 2007. Contingent Pacific-Atlantic Ocean influence on multicentury wildfire synchrony over western North America. Proceedings of the National Academy of Sciences of the United States of America 104:543–548.

Knapp, P. A. 1996. Cheatgrass (Bromus tectorum L) dominance in the Great Basin Desert. Global Environmental Change 6:37–52.

Knutti, R., D. Masson, and A. Gettelman. 2013. Climate model genealogy: Generation CMIP5 and how we got there. Geophysical Research Letters 40:1194–1199.

Kohl, M. T., M. Hebblewhite, S. M. Cleveland, and R. M. Callaway. 2012. Forage value of invasive species to the diet of rocky mountain elk. Rangelands 34:24–28.

Kriticos, D. J., B. L. Webber, A. Leriche, N. Ota, I. Macadam, J. Bathols, and J. K. Scott. 2012. CliMond: global high-resolution historical and future scenario climate surfaces for bioclimatic modelling. Methods in Ecology and Evolution 3:53–64.

Kumar, S., J. Graham, A. M. West, and P. H. Evangelista. 2014a. Using district-level occurrences in MaxEnt for predicting the invasion potential of an exotic insect pest in India. Computers and Electronics in Agriculture 103:55–62.

Kumar, S., L. Neven, and W. Yee. 2014b. Evaluating correlative and mechanistic niche models for assessing the risk of pest establishment. Ecological Applications 5.

Kumar, S., S. A. Spaulding, T. J. Stohlgren, K. A. Hermann, T. S. Schmidt, and L. L. Bahls. 2009. Potential habitat distribution for the freshwater diatom Didymosphenia geminata in the continental US. Frontiers in Ecology and the Environment 7:415–420.

Kumar, S., and T. Stohlgren. 2009. Maxent modeling for predicting suitable habitat for threatened and endangered tree Canacomyrica monticola in New Caledonia. Journal of Ecology and Natural Environment 1:94–98.

Leger, E. A., E. K. Espeland, K. R. Merrill, and S. E. Meyer. 2009. Genetic variation and local adaptation at a cheatgrass (Bromus tectorum) invasion edge in western Nevada. Molecular Ecology 18:4366–4379.

Lenoir, J., J. C. Gégout, P. A. Marquet, P. de Ruffray, and H. Brisse. 2008. A significant upward shift in plant species optimum elevation during the 20th century. Science (New York, N.Y.) 320:1768–71.

Levy, O., B. a Ball, B. Bond-Lamberty, K. S. Cheruvelil, A. O. Finley, N. R. Lottig, S. W. Punyasena, J. Xiao, J. Zhou, L. B. Buckley, C. T. Filstrup, T. H. Keitt, J. R. Kellner, A. K. Knapp, A. D. Richardson, D. Tcheng, M. Toomey, R. Vargas, J. W. Voordeckers, T.

Wagner, and J. W. Williams. 2014. Approaches to advance scientific understanding of macrosystems ecology. Frontiers in Ecology and the Environment 12:15–23.

Lillesand, T. M., R. W. Kiefer, and J. W. Chipman. 2008. Remote Sensing and Image Interpretation: Sixth Edition. Hoboken, NJ: John Wiley & Sons.

Littell, J. S., D. Mckenzie, D. L. Peterson, and A. L. Westerling. 2009. Climate and wildfire area burned in western U.S. ecoprovinces, 1916-2003. Ecological Applications 19:1003–1021.

Liu, C., M. White, and G. Newell. 2013. Selecting thresholds for the prediction of species occurrence with presence-only data. Journal of Biogeography 40:778–789.

Liu, Y. 2005. Enhancement of the 1988 northern U.S. drought due to wildfires. Geophysical Research Letters 32:1–4.

Liu, Y., J. Stanturf, and S. Goodrick. 2010. Trends in global wildfire potential in a changing climate. Forest Ecology and Management 259:685–697.

Lukas, J., J. Barsugli, N. Doesken, I. Rangwala, and K. Wolter. 2014. Climate Change in Colorado: A Synthesis to Support Water Resources Management and Adaptation. A Report for the Colorado Water Conservation Board. University of Colorado, Boulder, CO. Available online at: http://wwa.colorado.edu/climate/co2014report/.

Mack, R. N. 1981. Invasion of Bromus tectorum L. into western North America: an ecological chronicle. Agro-Ecosystems 7:145–165.

Mack, R. N., and D. Pyke. 1983. The demography of Bromus tectorum: variation in time and space. Journal of Ecology 71:69–93.

McCullagh, P., and J. A. Nelder. 1989. Generalized Linear Models. Chapman and Hall.

Mealor, B. A., R. D. Mealor, W. K. Kelley, D. L. Bergman, S. A. Burnett, T. W. Decker, B. Fowers, M. E. Herget, C. E. Noseworthy, J. L. Richards, C. S. Brown, K. G. Beck, and M. Fernandez-Gimenez. 2013. Cheatgrass Management Handbook: Managing and Invasive Annual Grass in the Rocky Mountain Region. University of Wyoming, Laramie Wyoming and Colorado State University, Fort Collins, Colorado.

Merow, C., M. J. Smith, and J. A. Silander. 2013. A practical guide to MaxEnt for modeling species' distributions: what it does, and why inputs and settings matter. Ecography 36:001–012.

Miller, M. E., J. Belnap, S. W. Beatty, and R. L. Reynolds. 2006. Performance of Bromus tectorum L. in relation to soil properties, water additions, and chemical amendments in calcareous soils of southeastern Utah, USA. Plant and Soil 288:1–18.

Monty, A., C. S. Brown, and D. B. Johnston. 2013. Fire promotes downy brome (Bromus tectorum L.) seed dispersal. Biological Invasions 15:1113–1123.

Moore, I. D., P. E. Gessler, G. A. Nielson, and G. A. Peterson. 1993. Soil attribute prediction using terrain analysis. Soil Science Society of America Journal.

Morisette, J. T., C. S. Jarnevich, T. R. Holcombe, C. B. Talbert, D. Ignizio, M. K. Talbert, C. Silva, D. Koop, A. Swanson, and N. E. Young. 2013. VisTrails SAHM: visualization and workflow management for species habitat modeling. Ecography 36:129–135.

Moritz, M. A., M.-A. Parisien, E. Batllori, M. A. Krawchuk, J. Van Dorn, D. J. Ganz, and K. Hayhoe. 2012. Climate change and disruptions to global fire activity.

Muscarella, R., P. J. Galante, M. Soley-Guardia, R. a. Boria, J. M. Kass, M. Uriarte, and R. P. Anderson. 2014. ENMeval: An R package for conducting spatially independent evaluations and estimating optimal model complexity for Maxent ecological niche models. Methods in Ecology and Evolution.

Myers, V. I., and W. A. Allen. 1968. Electrooptical remote sensing methods as nondestructive testing and measuring techniques in agriculture. Applied optics 7:1819–38.

Novak, S., R. Mack, and P. Soltis. 1993. Genetic variation in Bromus tectorum (Poaceae): introduction dynamics in North America. Canadian Journal of Botany 71:1441–1448.

Odum, E. P., and G. W. Barrett. 2005. Fundamentals of Ecology. Thomson Brooks/Cole, CA, USA.

Pacala, S. W., G. C. Hurtt, D. Baker, and P. Peylin. 2001. Consistent land- and atmosphere-based U.S. carbon sink estimates. Science 292:2316–2320.

Parisien, M., and M. Moritz. 2009. Environmental controls on the distribution of wildfire at multiple spatial scales. Ecological Monographs 79:127–154.

Parisien, M.-A., S. Snetsinger, J. a. Greenberg, C. R. Nelson, T. Schoennagel, S. Z. Dobrowski, and M. a. Moritz. 2012. Spatial variability in wildfire probability across the western United States. International Journal of Wildland Fire 21:313.

Paritsis, J., a Holz, T. Veblen, and T. Kitzberger. 2013. Habitat distribution modeling reveals vegetation flammability and land use as drivers of wildfire in SW Patagonia. Ecosphere 4:1–20.

Paruelo, J. M., and W. K. Lauenroth. 1996. Relative abundance of plant functional types in grasslands and shrublands of North America. Ecological applications 6:1212–1224.

Pearman, P. B., A. Guisan, O. Broennimann, and C. F. Randin. 2008. Niche dynamics in space and time. Trends in ecology & evolution 23:149–58.

Pearson, R. G. 2007. Species' Distribution Modeling for Conservation Educators and Practitioners. Synthesis. American Museum of Natural History.

Pechony, O., and D. T. Shindell. 2010. Driving forces of global wildfires over the past millennium and the forthcoming century. Proceedings of the National Academy of Sciences of the United States of America 107:19167–19170.

Pederson, G. T., J. L. Betancourt, and G. J. McCabe. 2013. Regional patterns and proximal causes of the recent snowpack decline in the Rocky Mountains, U.S. Geophysical Research Letters 40:1811–1816.

Peters, M. P., L. R. Iverson, S. N. Matthews, and A. M. Prasad. 2013. Wildfire hazard mapping: exploring site conditions in eastern US wildland-urban interfaces. International Journal of Wildland Fire 22:567–578.

Peterson, A. T., M. Papeş, and J. Soberón. 2008. Rethinking receiver operating characteristic analysis applications in ecological niche modeling. Ecological Modelling 213:63–72.

Peterson, A. T., R. G. Soberon, R. P. Pearson, E. Anderson, M. Martinez-Meyer, Nakamura, and M. B. Araujo. 2011. Ecological Niches and Geographic Distributions. Princeton University Press, Princeton, New Jersey, USA.

Peterson, E. 2005. Estimating cover of an invasive grass (Bromus tectorum) using tobit regression and phenology derived from two dates of Landsat ETM+ data. International Journal of Remote Sensing 26:37–41.

Phillips, S. J., R. P. Anderson, and R. E. Schapire. 2006. Maximum entropy modeling of species geographic distributions. Ecological Modelling 190:231–259.

Phillips, S. J., and M. Dudík. 2008. Modeling of species distributions with Maxent : new extensions and a comprehensive evaluation. Ecography 31:161–175.

Pyke, D. 2011. In Greater Sage Grouse: Ecology and Conservation of Landscape Species and Its Habitats. (J. W. Knick, S.T. & Connelly, Ed.). University of California Press.

Randin, C. F., R. Engler, S. Normand, M. Zappa, N. E. Zimmermann, P. B. Pearman, P. Vittoz, W. Thuiller, and A. Guisan. 2009. Climate change and plant distribution: local models predict high-elevation persistence. Global Change Biology 15:1557–1569.

Raupach, M. R., G. Marland, P. Ciais, C. Le Quéré, J. G. Canadell, G. Klepper, and C. B. Field. 2007. Global and regional drivers of accelerating CO2 emissions. Proceedings of the National Academy of Sciences of the United States of America 104:10288–93.

Rejmánek, M., and M. J. Pitcairn. 2002. When is eradication of exotic pest plans a realistic goal? Pages 249–253 *in* C. R. Veitch and M. N. Clout, editors. Turning the Tide: the Eradication of Invasive Species. IUCN SSC Invasive Species Specialist Group, IUCN, Gland, Switzerland and Cambridge, UK.

Rosenberg, N. J. 1983. Microclimate: The Biological Environment. 2nd edition. John Wiley & Sons, New York, NY.

Rouse, J. W. J., R. H. Haas, J. A. Schell, and D. W. Deering. 1974. Monitoring Vegetation Systems in the Great Plains with Erts. Page 1994 *in* S. C. Freden, E. P. Mercanti, and M. A. Becker, editors. Third Earth Resources Technology Satellite-1 Symposium- Volume I: Technical Presentations. NASA SP-351. NASA, Washington, D.C.

Sakai, A., F. Allendorf, J. Holt, D. Lodge, J. Molofsky, K. With, S. Baughman, R. Cabin, J. E. Cohen, N. Ellstrand, D. McCauley, P. O'Neil, I. Parker, J. Thompson, and S. Weller. 2001. The population biology of invasive species. Annu. Rev. Ecol. Syst. 32:305–332.

Schimel, D., and B. H. Braswell. 2005. The role of mid-latitude mountains in the carbon cycle: global perspective and a western U.S. case study. Pages 449–456 *in* U. M. Huber, H. K. M. Bugmann, and M. A. Reasoner, editors. in Global Change and Mountain Regions: An Overview of Current Knowledge. Springer, Dordrecht, Netherlands.

Schoennagel, T., T. T. Veblen, and W. H. Romme. 2004. The interaction of fire, fuels, and climate across Rocky Mountain forests. BioScience 54:661.

Schoennagel, T., T. T. Veblen, W. H. Romme, J. S. Sibold, and E. R. Cook. 2005. ENSO and PDO variability affect drought-induced fire occurrence in Rocky Mountain subalpine forests. Ecological Applications 15:2000–2014.

Shabani, F., L. Kumar, and A. Esmaeili. 2014. Future distributions of Fusarium oxysporum f. spp. in European, Middle Eastern and North African agricultural regions under climate change. Agriculture, Ecosystems & Environment 197:96–105.

Shabani, F., L. Kumar, and S. Taylor. 2012. Climate change impacts on the future distribution of date palms: a modeling exercise using CLIMEX. PloS ONE 7:e48021.

Sheppard, C. S. 2013. How does selection of climate variables affect predictions of species distributions? A case study of three new weeds in New Zealand. Weed Research 53:259–268.

Sherrill, K. R., and W. H. Romme. 2012. Spatial variation in postfire cheatgrass: Dinosaur National Monument, USA. Fire Ecology 8:38–56.

Singh, N., and N. F. Glenn. 2009. Multitemporal spectral analysis for cheatgrass (Bromus tectorum) classification. International Journal of Remote Sensing 30:3441–3462.

Smithwick, E. a H., M. G. Ryan, D. M. Kashian, W. H. Romme, D. B. Tinker, and M. G. Turner. 2009. Modeling the effects of fire and climate change on carbon and nitrogen storage in lodgepole pine (Pinus contorta) stands. Global Change Biology 15:535–548.

Stage, A. R. 1976. Notes: An expression for the effect of aspect, slope, and habitat type on tree growth. Forest Science 22.

Stambaugh, M. C., and R. P. Guyette. 2008. Predicting spatio-temporal variability in fire return intervals using a topographic roughness index. Forest Ecology and Management 254:463–473.

Stan, A. B., P. Z. Fulé, K. B. Ireland, and J. S. Sanderlin. 2014. Modern fire regime resembles historical fire regime in a ponderosa pine forest on Native American lands. International Journal of Wildland Fire 23:686–697.

Stanton, J. C., R. G. Pearson, N. Horning, P. Ersts, and H. Reşit Akçakaya. 2012. Combining static and dynamic variables in species distribution models under climate change. Methods in Ecology and Evolution 3:349–357.

Stavros, E. N., J. T. Abatzoglou, D. Mckenzie, and N. K. Larkin. 2014. Regional projections of the likelihood of very large wildland fires under a changing climate in the contiguous Western United States. Climatic Change 126:455–468.

Stephens, S. L. 2005. Forest fire causes and extent on United States Forest Service lands. International Journal of Wildland Fire 14:213–222.

Stewart, G., and A. Hull. 1949. Cheatgrass (Bromus tectorum L.)--an ecologic intruder in southern Idaho. Ecology 30:58–74.

Stewart, I. T., D. R. Cayan, and M. D. Dettinger. 2005. Changes toward earlier streamflow timing across western North America. Journal of Climate 18:1136–1155.

Stohlgren, T., D. Barnett, and S. Simonson. 2010a. Beyond North American Weed Management Association Standards.

Stohlgren, T., and D. Binkley. 1999. Exotic plant species invade hot spots of native plant diversity. Ecological Monographs 69:25–46.

Stohlgren, T. J., M. Falkner, and L. D. Schell. 1995. A Modified-Whittiker nested vegetation sampling method. Vegetatio 117:121–133.

Stohlgren, T. J., P. Ma, S. Kumar, M. Rocca, J. T. Morisette, C. S. Jarnevich, and N. Benson. 2010b. Ensemble habitat mapping of invasive plant species. Risk analysis : an official publication of the Society for Risk Analysis 30:224–35.

Swetnam, T. W., and J. L. Betancourt. 2010. Mesoscale Disturbance and Ecological Response to Decadal Climatic Variability in the American Southwest. Pages 329–359 *in* M. et al Stoffel, editor. Tree Rings and Natural Hazards: A State-of-the-Art. Springer.

Swets, J. A. 1988. Measuring the accuracy of diagnostic systems. Science 240:1285–1293.

Syphard, A. D., V. C. Radeloff, N. S. Keuler, R. S. Taylor, T. J. Hawbaker, S. I. Stewart, and M. K. Clayton. 2008. Predicting spatial patterns of fire on a southern California landscape. International Journal of Wildland Fire 17:602.

Taylor, S., L. Kumar, N. Reid, and D. J. Kriticos. 2012. Climate change and the potential distribution of an invasive shrub, Lantana camara L. PloS ONE 7:e35565.

The National Park Service Rocky Mountain National Park Website. (n.d.). . http://www.nps.gov/romo/naturescience/exotic_plants.htm.

Theobald, D. M., and W. H. Romme. 2007. Expansion of the US wildland-urban interface. Landscape and Urban Planning 83:340–354.

Trouet, V., A. H. Taylor, E. R. Wahl, C. N. Skinner, and S. L. Stephens. 2010. Fire-climate interactions in the American West since 1400 CE. Geophysical Research Letters 37:1–5.

UNFAO (Food and Agriculture Organization of the United Nations. 2010. Global Forest Resources Assessment 2010. Forestry Paper.

United States Department of Agriculture PLANTS database. 2014. . http://plants.usda.gov/.

Upadhyaya. 1986. Biology of Bromus tectorum. Canadian Journal of Plant Science 66:689–709.

Uresk, D. W., J. F. Cline, and W. H. Rickard. 1979. Growth Rates of a Cheatgrass Community and Some Associated Factors. Journal of Range Management 32:168.

Van Vuuren, D. P., J. Edmonds, M. Kainuma, K. Riahi, A. Thomson, K. Hibbard, G. C. Hurtt, T. Kram, V. Krey, J. F. Lamarque, T. Masui, M. Meinshausen, N. Nakicenovic, S. J. Smith, and S. K. Rose. 2011. The representative concentration pathways: An overview. Climatic Change 109:5–31.

Wang, T., A. Hamann, D. L. Spittlehouse, and T. Q. Murdock. 2012. ClimateWNA—High-Resolution Spatial Climate Data for Western North America. Journal of Applied Meteorology and Climatology 51:16–29.

Warren, D. L., R. E. Glor, and M. Turelli. 2010. ENMTools: a toolbox for comparative studies of environmental niche models. Ecography 1:607–611.

West, A. M., S. Kumar, T. Wakie, C. Brown, T. Stohlgren, M. Laituri, and J. Bromberg. 2015. Using high-resolution future climate scenarios to forecast Bromus tectorum invasion in Rocky Mountain National Park. PloS ONE 10.

Westerling, a L., H. G. Hidalgo, D. R. Cayan, and T. W. Swetnam. 2006. Warming and earlier spring increase western U.S. forest wildfire activity. Science (New York, N.Y.) 313:940–3.

Westerling, A. L., and T. W. Swetnam. 2003. Interannual to decadal drought and wildfire in the western United States. Eos, Transactions American Geophysical Union 84:545.

Westerling, A. L., M. G. Turner, E. a H. Smithwick, W. H. Romme, and M. G. Ryan. 2011. Continued warming could transform Greater Yellowstone fire regimes by mid-21st century. Proceedings of the National Academy of Sciences of the United States of America 108:13165–70.

Western Regional Climate Center. (n.d.). . www.wrcc.dri.edu/.

Wing, M. G., and J. Long. 2015. A 25-Year History of Spatial and Temporal Trends in Wildfire Activity in Oregon and Washington, U.S.A. Modern Applied Science 9:117–132.

Wisz, M. S., R. J. Hijmans, J. Li, A. T. Peterson, C. H. Graham, and A. Guisan. 2008. Effects of sample size on the performance of species distribution models. Diversity and Distributions 14:763–773.

Xu, H. 2006. Modification of normalised difference water index (NDWI) to enhance open water features in remotely sensed imagery. International Journal of Remote Sensing 27:3025–3033.

Yang, X., G. A. Chapman, G. A. Young, and J. M. Gray. 2006. Using Compound Topographic Index to delineate soil landscape facets from Digital Elevation Models for comprehensive coastal assessment. MODSIM 2005 International Congress on Modelling and Simulation. Modelling and Simulation Society of Australia and New Zealand:7.

Yue, X., L. J. Mickley, J. a Logan, and J. O. Kaplan. 2013. Ensemble projections of wildfire activity and carbonaceous aerosol concentrations over the western United States in the mid-21st century. Atmospheric Environment 77:767–780.

Zelikova, T. J., R. A. Hufbauer, S. C. Reed, T. Wertin, C. Fettig, and J. Belnap. 2013. Eco-evolutionary responses of Bromus tectorum to climate change: implications for biological invasions. Ecology and Evolution 3:1374–1387.

Zouhar, K., J. Smith, S. Southerland, and M. Brooks. 2008. Wildland fire in ecosystems: fire and nonnative invasive plants. Gen Tech. Rep. RMRS-GTR-42. Ogden, UT.